Supplementary Information for

Immunosuppressive polyketides from the mantis-associated *Daldinia eschscholzii*

Ying L. Zhang,[†,§,#] Jie Zhang,[†,#] Nan Jiang,[‡] Yan H. Lu,[‖] Lu Wang,[†] Su H. Xu,[†] Wei Wang,[†] Gao F. Zhang,[†] Qiang Xu,[†] Hui M. Ge,[†] Jing Ma,[‡] Yong C. Song,[†] and Ren X. Tan*[,†]

[†]Institute of Functional Biomolecules, State Key Laboratory of Pharmaceutical Biotechnology, Nanjing University, Nanjing 210093, P. R. China

[‡]Institute of Theoretical and Computational Chemistry, Lab of Mesoscopic Chemistry, Nanjing University, Nanjing 210093, P. R. China

[‖]State Key Laboratory of Bioreactor Engineering, East China University of Science & Technology, Shanghai 200237, P. R. China

[§]College of Chemistry and Life Sciences, Zhejiang Normal University, Jinhua 321004, P. R. China

[#]These authors contributed equally.

Correspondence should be addressed to R.X.T. (rxtan@nju.edu.cn)

Contents:

Supplementary References

Complete reference 16

Supplementary Materials and Methods

Isolation and identification of metabolites

The filtrate of the culture broth was extracted exhaustively with ethyl acetate. Evaporation of solvent *in vacuo* from the ethyl acetate extract gave a brown oily residue (140 g), which was subjected to column chromatography over silica gel eluted with $CHCl_3$-MeOH mixtures (gradient v/v 100:0 to 100:32) to afford seven fractions (F_1-F_7). F_1 was purified subsequently by silica gel chromatography eluted with petroleum ether-ethyl acetate system (gradient v/v 100:10 to 100:80) to give four subfractions (F_{1A}-F_{1D}). F_{1A}, F_{1B} and F_{1C} were further subjected to size-exclusion chromatography on Sephadex LH-20 with $CHCl_3$:MeOH mixture (v/v 1:1) and recrystallization in MeOH to yield **14** (53 mg), **29** (30 mg), **21** (28 mg) and dalesconol A (300 mg), respectively. The second fraction F_2 was separated on a silica gel column eluted with $CHCl_3$-MeOH mixtures (gradient v/v 200:0 to 200:4) to give five subfractions (F_{2A}-F_{2E}). F_{2A} was then chromatographed using a petroleum ether-acetone system (gradient v/v 100:10 to 100:80) to afford **3** (16 mg), **19** (1.8 g) and **20** (2.2 g). Gel filtration of F_{2B} over a Sephadex LH-20 column with MeOH and then recrystallized from MeOH at room temperature to yield **5** (150 mg), **22** (25 mg) and dalesconol B (290 mg). Compounds **1** (143 mg), **8** (15 mg) and **12** (3.2 g) were obtained from subfraction F_{2C} by silica gel column eluted with petroleum ether-acetone gradient system. F_{2D} was purified on Sephadex LH-20 column with MeOH to give **4** (148 mg) and **9** (17 mg). The third fraction F_3 was chromatographed on a silica gel column eluted with $CHCl_3$-MeOH mixtures (gradient v/v 100:1 to 100:4) to afford four subfractions (F_{3A}-F_{3D}). F_{3A} was further subjected to silica gel chromatography using petroleum ether-acetone system (gradient v/v 100:20 to 100:80), followed by gel filtration over Sephadex LH-20 with MeOH to yield **2** (15 mg), **10** (27 mg) and **27** (18 mg). Compounds **28** (28 mg) and **25** (19 mg) were obtained on a Sephadex LH-20 column with MeOH from subfractions F_{3B} and F_{3C}, respectively. F_{3D} was isolated by a Sephadex LH-20 column (MeOH), followed recrystallization in MeOH, to give compounds **13** (48 mg) and **17** (425 mg). The fraction F_4 was purified on a silica gel column eluted with $CHCl_3$-MeOH mixtures (gradient v/v 100:2 to 100:8) to give three subfractions (F_{4A}-F_{4C}). The fraction F_{4A} and F_{4B} was rechromatographed on a silica gel column and subsequent gel filtration over Sephadex LH-20 with MeOH and then recrystallization in MeOH to give **23** (53 mg), **24** (45 mg) and **26** (107 mg). The fraction F_{4C} was separated on a reversed-phase column to afford **7** (27 mg) and a mixture that was isolated by a Sephadex LH-20 column to give **6** (23 mg) and **18** (21 mg). Finally, the fraction F_5 was subjected to reversed-phase column chromatography eluted with MeOH-H_2O mixtures (gradient v/v 40:60 to 60:40) to give three fractions (F_{5A}-F_{5C}).

F_{5A}, F_{5B} and F_{5C} were then separated on a Sephadex LH-20 column eluted with MeOH to give **11** (4.4 g), **15** (150 mg) and **16** (15 mg), respectively.

The structure determination of new compounds **5**-**6**, **10**, **15**-**16**,, **22**-**23**, **27** and **29** were mentioned in the text. Identified by comparison of their spectral data with those in literature were dalesconols A and B,[1] 2,6-dihyroxyacetophenone (**1**),[2] 2,4,6-trihydroxy-acetophenone (**2**),[3] 2,4-dihydroxyphenylethanone (**3**),[4] (-)-6-hydroxymellein (**4**),[5] sphaerolone(**7**),[6] dihydrosphaerolone(**8**),[6] daldinone C (**9**),[7] 4-hydroxyscytalone (**11**),[8] 3,4-dihydro-3,4,8-trihydroxy-1(2H)-naphthalenone (**12**),[9] 4,6,8-trihydroxy-3,4-dihydronaphthalen-1(2*H*)-one (**13**),[10] (-)-isosclerone(**14**),[11] 2,3-dihydro-5-hydroxy-2-methylchromen-4-one (**17**),[12] 5-hydroxy-2-methyl-4H-chromen-4-one (**18**),[12] 1-(2,6-dihydroxyphenyl)butan-1-one (**19**),[12] 3-hydroxy-1-(2,6-dihydroxyphenyl)-butan-1-one (**20**),[12] nodulisporin F (**21**),[13] 6,8-dihydroxy-3-(2-oxopropyl)-1H-isochromen-1-one (**24**),[14] diaporthin (**25**),[15] (+)-orthosporin (**26**),[16] and nodulone (**28**).[17]

Supplementary Tables

Table S1. Analytic conditions of **5**, **6**, **15**, **16**, **22** and **23** by chiral HPLC.

Compounds	Column type	Column size	Column temperature (°C)	Mobile phase (v/v/v)
5	Chiralpak IA	0.46×15 cm	35	Hexane/Ethyl Alcohol/TFA=60/40/0.1
6	Chiralpak AD-H	0.46×15 cm	35	Hexane//Isopropanol/TFA=80/20/0.1
15	Chiralpak OD-H	0.46×15 cm	35	Hexane/IPA/EDA=80/20/0.1
16	Chiralpak IC	0.46×15 cm	35	Hexane/EtOH/TFA=85/15/0.3
22	Chiralpak IA	0.46×25 cm	35	MtBE/MeOH/TFA=65/35/0.1
23	Chiralpak IC	0.46×25 cm	35	MeOH/TFA=100/0.1

Table S2. ^{1}H, ^{13}C, and HMBC NMR Data for **6** in acetone-d_6.

position	δ_C	δ_H (mult., *J*, Hz)	^{1}H-^{13}C HMBC	position	δ_C	δ_H (mult., *J*, Hz)	^{1}H-^{13}C HMBC
1	207.3			17	128.7		
2	119.0			18	147.2		
3	163.2			19	64.7		
4	120.0	6.92 (d, 8.0)	2, 6	20	144.2		
5	136.3	7.57 (d, 8.0)	3, 7	21	107.1	5.51 (s)	22, 23, 25
6	125.6	7.11 (d, 8.0)	2, 8	22	165.2		
7	136.7			23	102.2	6.04 (s)	21, 24, 25
8	163.7			24	165.5		
9	132.9			25	112.2		
10	134.4	7.90 (d, 9.8)	12, 18	26	200.7		
11	133.2	6.67 (d, 9.8)	9, 13	27	42.3	2.73 (dd, 16.7, 3.8)	1, 19
						3.75 (dd, 16.7, 6.9)	26, 28, 29
12	188.3			28	35.9	3.25 (m)	
13	108.3			29	51.7	3.45 (dd, 13.2, 6.8)	1, 27, 28
						2.82 (dd, 13.2, 2.2)	1, 19
14	162.2			3–OH		12.69 (s)	
15	102.4	6.37 (s)	13, 14, 16, 17	14-OH		10.98 (s)	
16	158.0			24–OH		12.26 (s)	

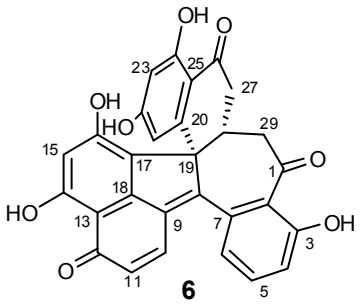

6

Table S3. ^{1}H, ^{13}C, and HMBC NMR Data for **10** in acetone-d_6.

position	δ_C	δ_H (mult., *J*, Hz)	^{1}H-^{13}C HMBC	position	δ_C	δ_H (mult., *J*, Hz)	^{1}H-^{13}C HMBC
1	125.4			12	125.4	8.64 (d, 7.0)	10, 14, 20
2	155.1			13	127.9	7.79 (dd, 8.0, 7.0)	11, 15
3	108.3	6.96 (dd, 7.5, 0.8)	1, 2, 5	14	122.7	8.25 (d, 8.0)	12, 16, 20
4	128.6	7.50 (dd, 8.5, 7.5)	2, 6	15	122.9		
5	116.3	8.33 (dd, 8.5, 0.8)	1, 3, 10	16	156.9		
6	133.0 [a]			17	111.2	7.09 (d, 7.5)	15, 17, 19
7	123.4	8.38 (d, 8.6)	2, 6, 9	18	123.9	8.03 (d, 7.5)	9, 16, 20
8	119.0	8.10 (d, 8.6)	1, 10, 19	19	129.4		
9	139.3			20	134.1		
10	133.3 [a]			2-OH		9.57 (br s) [b]	
11	138.2			16-OH		9.12 (br s) [b]	

[a, b] Interchangeable assignments.

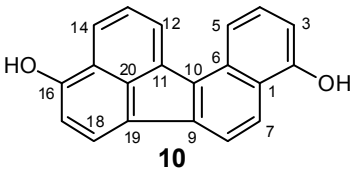

10

Table S4. ^{1}H, ^{13}C, and HMBC NMR Data for **27** in acetone-d_6 and **28** in DMSO-d_6.

	27			**28**		
position	δ_C	δ_H (mult., *J*, Hz)	^{1}H-^{13}C HMBC	δ_c	δ_H (mult., *J*, Hz)	^{1}H-^{13}C HMBC
1	203.8			203.7		
1a	115.3			114.5		
2	44.6	2.71 (dd, 17.2, 8.8) 3.03 (dd, 17.2, 4.2)	1, 3, 4, 1a	43.1	2.65 (dd, 17.2, 7.3) 2.99 (dd, 17.2, 3.5)	1, 3, 4, 1a
3	71.8	4.07~4.12 (m)	1, 4a	69.8	3.95~3.98 (m)	1, 4, 4a
4	73.5	4.66 (dd, 7.2, 5.1)	2, 3, 7, 1a, 4a	71.2	4.50 (d, 6.2)	2, 3, 5, 1a, 4a
4a	146.2			146.0		
5	117.0	7.16 (s)	4, 6, 7, 9, 1a	112.2	7.04 (s)	4, 7, 9, 1a
6	153.6			149.1		
7	114.2	6.86 (s)	5, 6, 8, 9, 1a	124.7		
8	163.3			155.4		
9	64.3	4.65 (d, 5.8)	5, 6, 7	73.4	5.05 (br s)	5, 6, 7, 10
10				70.4	4.99 (br s)	6, 7, 8, 9
3-OH		4.61 (d, 4.0)	2, 3, 4			
4-OH		4.90 (d, 5.1)	3, 4, 4a			
8-OH		12.38 (s)	7, 8, 1a		12.50 (s)	7, 8, 1a
9-OH		4.47 (t, 5.8)	6, 9			

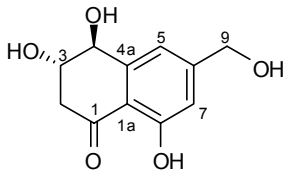

27

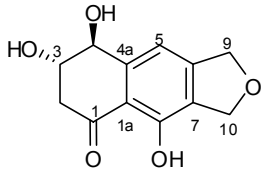

28

Table S5. ^{1}H, ^{13}C, and HMBC NMR Data for **29** in $CDCl_3$.

position	δ_C	δ_H (mult., *J*, Hz)	^{1}H-^{13}C HMBC	position	δ_C	δ_H (mult., *J*, Hz)	^{1}H-^{13}C HMBC
1	173.9			15	37.8	1.93~1.98 (m) 2.54 (dd, 24.2, 11.6)	13, 14, 16, 17, 22
2-NH		5.74 (br s)	3, 4, 9	16	39.0	2.85~2.93 (m)	14, 15, 18, 22
3	54.0	3.25~3.29 (m)	1, 4, 5, 1'	17	217.8		
4	48.4	2.96 (dd, 5.7, 2.9)	1, 3, 5, 6, 8, 9, 10, 11, 21	18	49.1 [a]	2.25~2.33 (m)	16, 17, 19, 20
5	34.9	2.34~2.40 (m)	3, 4	19	25.8	1.61~1.69 (m)	17, 18, 20, 21, 23
6	140.0			20	37.2	1.72~1.78 (m) 3.30~3.39 (m)	18, 19, 21
7	125.1	5.41 (br s)		21	210.6		
8	49.2 [a]	2.41~2.47 (m)	4, 14	22	20.2	1.04 (d, 6.8)	15, 17
9	68.8			23	16.9	1.16 (d, 6.9)	17, 18, 19
10	44.5	2.43 (dd, 13.4, 7.8) 2.73 (dd, 13.4, 4.7)	3, 4, 1', 2'/6'	1′	136.8		
11	13.3	1.14 (d, 7.2)	4, 5, 6	2′, 6′	129.6	7.07 (d, 7.8)	10, 4', 6'/2'
12	19.8	1.71 (s)	5, 6, 7	3′, 5′	128.7	7.23~7.31 (m)	1', 5'/3'
13	130.9	6.16 (ddd, 15.2, 10.2, 1.1)	7, 8, 15	4′	126.8	7.20~7.23 (m)	2'/6'
14	130.2	5.22 (ddd, 15.2, 11.2, 4.0)	8, 15, 16				

[a] Interchangeable assignments.

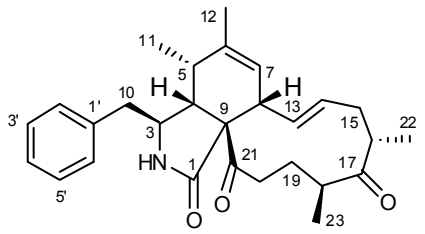

29

Table S6. TDDFT results for the optimized conformer of (*8R,19R,28R,29S*)-**5** (200nm<λ<400nm).

Transition	Excitation energy[a] (nm)	Rotatory Strength R^b (10^{-40} cgs)	Oscillator Strength f^b	Dominant Contributions	Weight
4	326.78	28.76	0.0193	130→133	0.30
				131→134	0.04
				132→136	0.05
5	322.24	27.00	0.0035	132→135	0.18
				132→136	0.50
6	318.66	–79.65	0.0813	130→134	0.06
				131→137	0.70
7	313.60	63.60	0.0617	130→133	0.18
				130→134	0.50
9	306.71	109.52	0.0493	124→133	0.12
				130→134	0.19
10	301.85	–45.39	0.1690	132→135	0.56
				132→136	0.20
11	291.09	27.46	0.0661	128→135	0.10
				132→137	0.72
12	289.43	–33.65	0.0058	139→133	0.26
				129→134	0.24
15	272.74	–33.87	0.0143	126→133	0.30
				127→133	0.16
				128→133	0.30
19	261.60	–40.06	0.0242	126→130	0.13
				126→131	0.29
24	255.05	34.88	0.0150	123→133	0.22
				125→133	0.29
				125→134	0.16
				127→134	0.14
26	247.03	–27.60	0.0329	124→134	0.24
				125→134	0.10
				132→139	0.34
29	240.85	46.93	0.1727	123→133	0.34
				124→133	0.18
31	237.24	–21.78	0.0162	123→134	0.12
				131→137	0.72
37	226.11	23.12	0.0081	130→138	0.22
				131→138	0.54
40	219.60	85.24	0.0254	123→136	0.10
				125→136	0.12
				132→140	0.09
45	215.97	–161.81	0.0715	130→138	0.36
				131→138	0.08
				131→139	0.24
46	214.61	128.19	0.1322	125→136	0.16
				128→135	0.12
				132→141	0.16
49	210.41	169.05	0.2468	123→136	0.09
				124→136	0.12
				125→136	0.09
				127→137	0.10
				128→135	0.09
51	209.21	–46.95	0.1078	127→137	0.48
				128→137	0.12
				129→137	0.08
56	203.82	–65.68	0.0250	129→138	0.09
				132→142	0.49
60	201.70	–36.25	0.0853	121→134	0.24
				123→135	0.28
				128→137	0.09

[a] Excited states with f < 0.1 and R < ± 20.0 were not presented.
[b] All the strengths were in the velocity representation.

Table S7. TDDFT results for the optimized conformer of (2*R*,3*S*)-**15** (200nm<λ<600nm).

Transition	Excitation energy[a] (nm)	Rotatory Strength R^b (10^{-40} cgs)	Oscillator Strength f^b	Dominant Contributions	Weight
1	464.23	-35.4623	0.2781	90 → 92	0.02
				91 → 92	0.41
2	384.73	21.7678	0.0629	89 → 92	0.19
				90 → 92	0.26
3	359.84	-10.6517	0.2181	89 → 92	0.25
				90 → 92	0.15
				91 → 93	0.02
4	339.62	-24.2959	0.0049	87 → 92	0.43
				87 → 93	0.02
				88 → 92	0.03
6	304.00	37.5579	0.1191	90 → 92	0.01
				91 → 93	0.43
8	268.12	-16.4585	0.0896	85 → 92	0.06
				90 → 93	0.31
				91 → 94	0.04
				91 → 95	0.05
10	255.43	-18.9357	0.1405	85 → 92	0.28
				89 → 93	0.11
				91 → 95	0.06
12	243.65	-35.1157	0.3252	84 → 92	0.08
				89 → 93	0.02
				90 → 93	0.04
				91 → 95	0.30
13	242.08	-36.7292	0.0168	84 → 92	0.07
				90 → 94	0.02
				91 → 94	0.03
				91 → 95	0.02
				91 → 96	0.31
15	233.68	4.7918	0.2048	84 → 92	0.16
				88 → 93	0.17
				90 → 93	0.02
				91 → 94	0.05
				91 → 96	0.02
18	223.42	–15.0645	0.0394	88 → 94	0.03
				89 → 94	0.20
				89 → 95	0.03
				90 → 94	0.15
				90 → 96	0.02
20	216.23	4.0129	0.1023	88 → 95	0.01
				89 → 94	0.12
				89 → 95	0.04
				89 → 96	0.04
				90 → 95	0.16
				90 → 96	0.08
21	213.66	-4.2623	0.1120	86 → 93	0.01
				88 → 94	0.02
				89 → 94	0.05
				89 → 96	0.14
				90 → 94	0.01
				90 → 95	0.12
				90 → 96	0.09
26	205.09	26.2361	0.0674	81 → 92	0.06
				88 → 94	0.02
				89 → 95	0.17
				89 → 96	0.05
				90 → 96	0.08

[a] Excited states with f < 0.1 and R < ± 16.0 were not presented.
[b] All the strengths were in the velocity representation.

Table S8. TDDFT results for the optimized conformer of (*2R,3R,2'R*)-**23** (200nm<λ<600nm).

Transition	Excitation energy[a] (nm)	Rotatory Strength R^b (10^{-40} cgs)	Oscillator Strength f^b	Dominant Contributions	Weight
1	497.63	11.1870	0.2313	145 → 146	0.42
2	402.92	8.7739	0.1692	143 → 146	0.42
4	383.32	−2.0654	0.1111	142 → 146 145 → 148	0.32 0.13
6	350.04	−3.9694	0.2549	145 → 148	0.30
16	289.09	22.2876	0.3985	143 → 148	0.31
19	275.2	24.1932	0.0111	137 → 146 139 → 148	0.13 0.26
21	269.50	16.5994	0.0465	136 → 146	0.35
22	267.43	−26.3659	0.0065	138 → 148	0.33
24	261.16	−16.3377	0.4265	140 → 147	0.39
26	255.18	13.4363	0.2854	141 → 148	0.33
27	252.62	−43.6832	0.0162	135 → 146	0.26
34	239.71	−18.4188	0.0097	134 → 146	0.41
35	236.45	18.0745	0.1038	133 → 146 145 → 151	0.14 0.12
36	235.55	22.1256	0.1344	133 → 146	0.14
42	219.45	25.8962	0.0585	142 → 150	0.28
45	215.99	8.5950	0.1229	145 → 153	0.10
50	213.19	34.7230	0.0292	130 → 146	0.32

[a] Excited states with f < 0.1 and R < ± 15.0 were not presented.
[b] All the strengths were in the velocity representation.

Table S9. Antioxidative activities of daeschols and dalesconol A as determined by DPPH radical Assay

Compound	DPPH radical IC_{50} (μM)
5	16.9
(+)-**5**	25.6
(–)-**5**	33.3
dalesconol A	>200
Butyl hydroxy anisol (BHA)[a]	17.6

[a] Co-assayed as a positve control.

Supplementary Figures

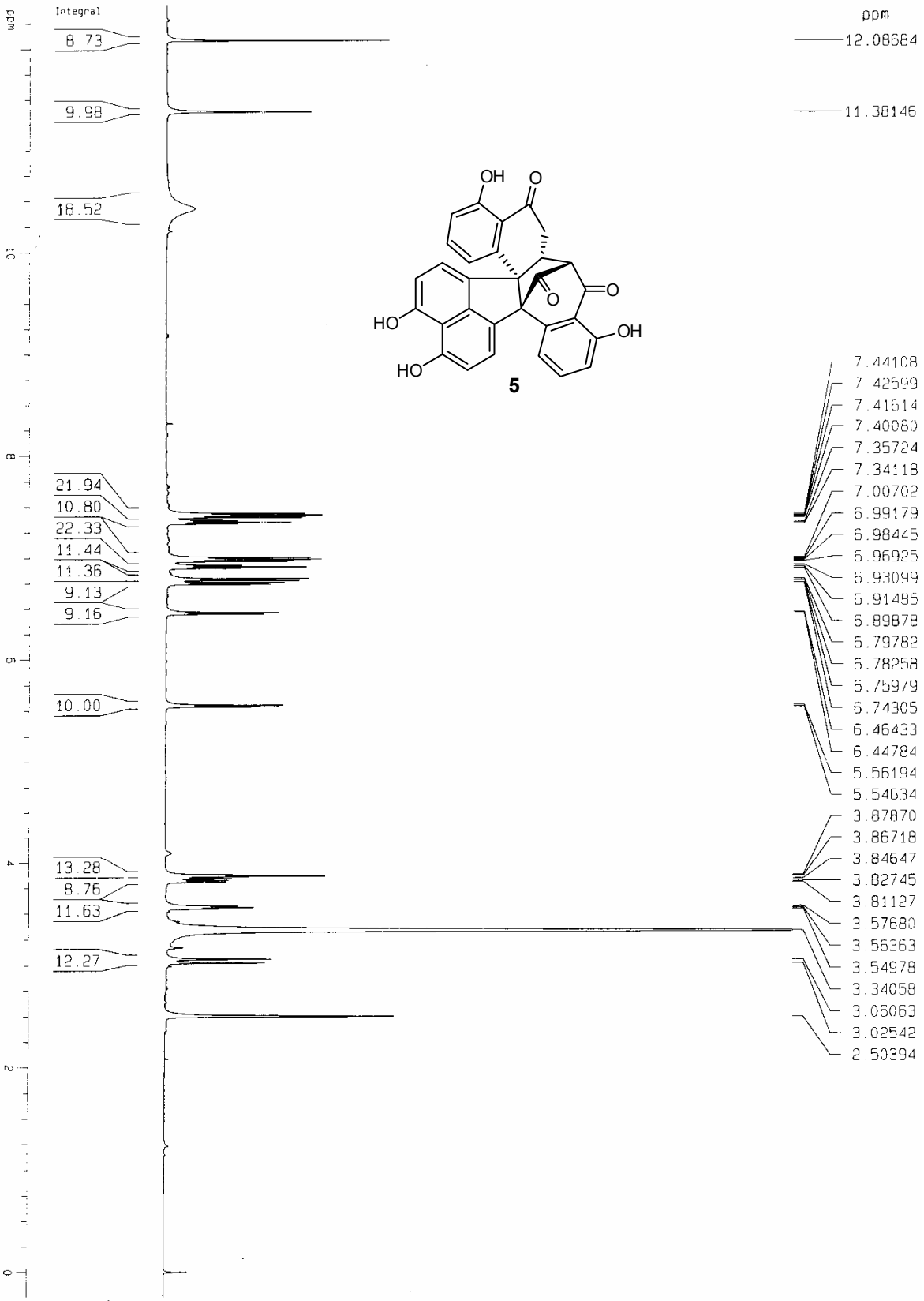

Figure S1. The ^{1}H NMR spectrum of **5** in DMSO-d_6 (500 MHz).

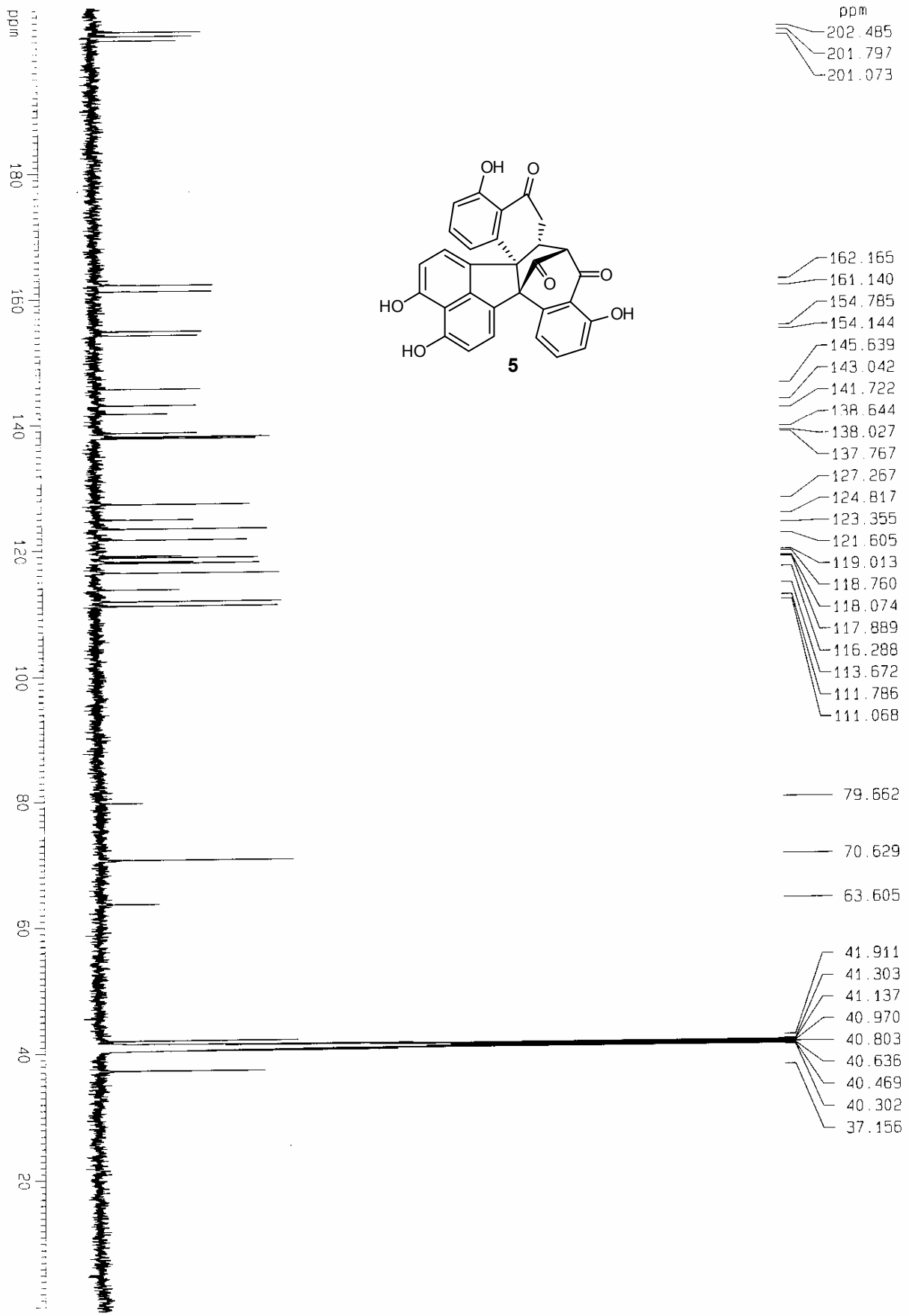

Figure S2. The ^{13}C NMR spectrum of **5** in DMSO-d_6 (125 MHz).

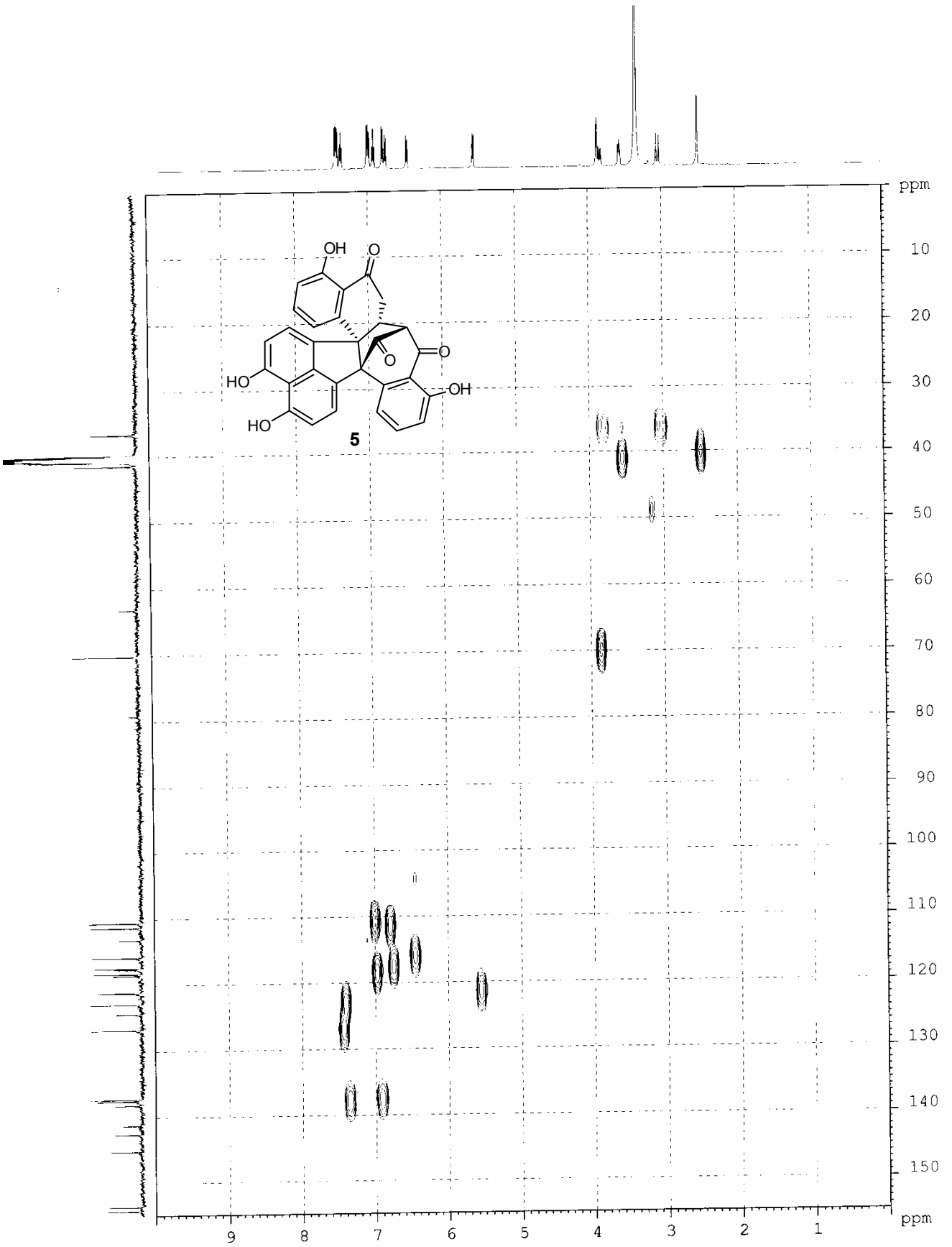

Figure S3. The HMQC spectrum of **5** in DMSO-d_6 (500 MHz).

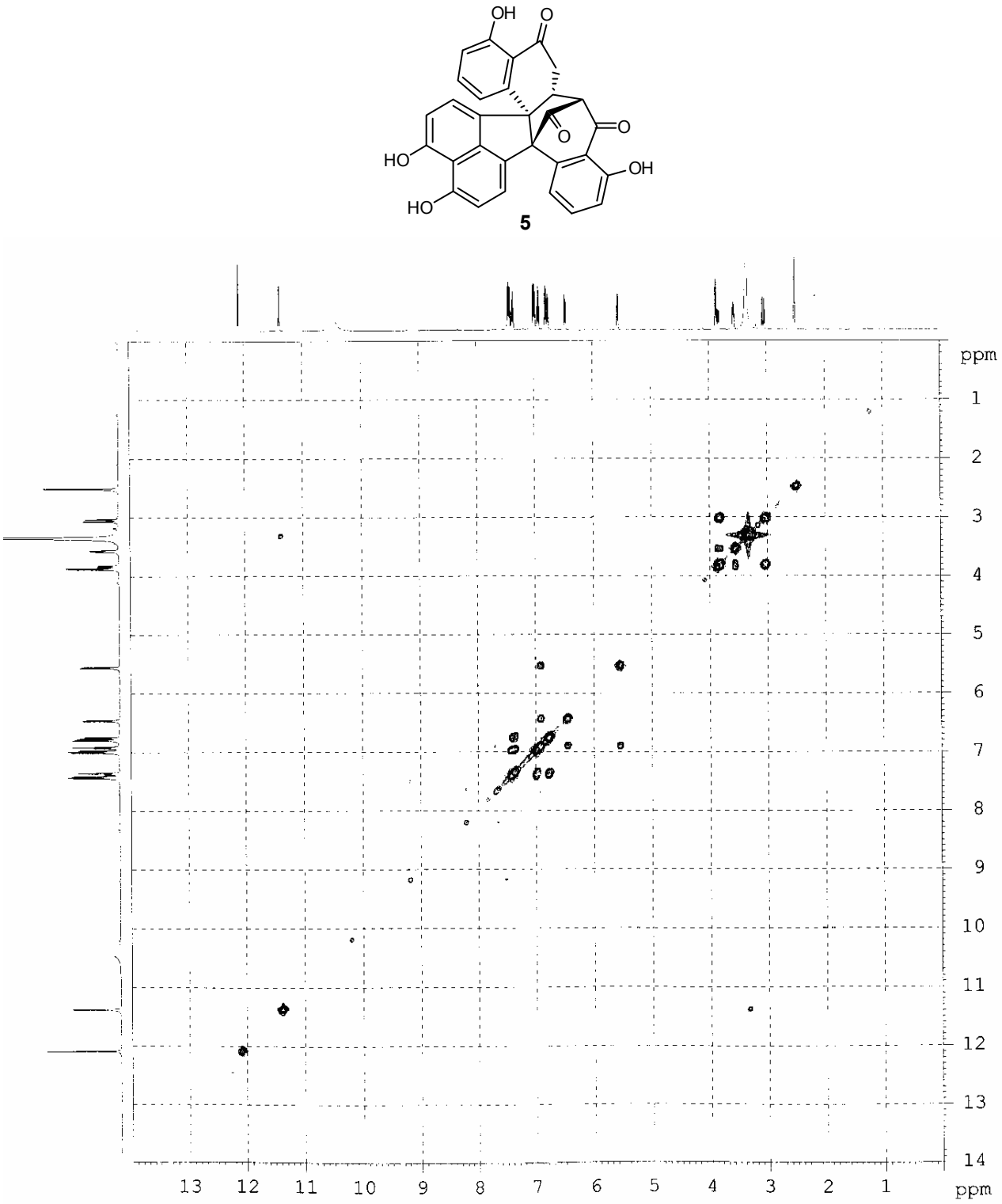

Figure S4. The ^{1}H-^{1}H COSY spectrum of **5** in DMSO-d_6 (500 MHz).

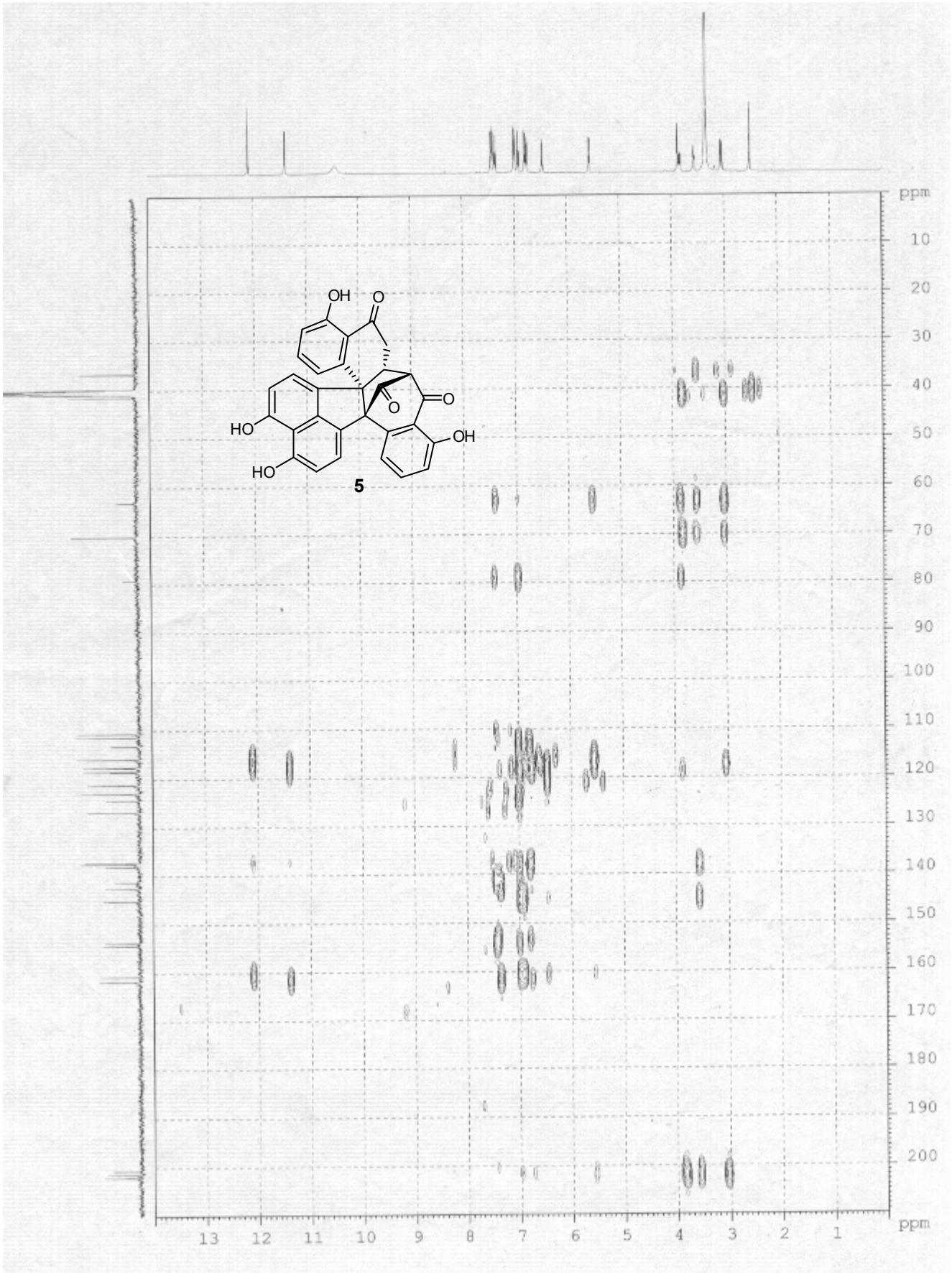

Figure S5. The HMBC spectrum of **5** in DMSO-d_6 (500 MHz).

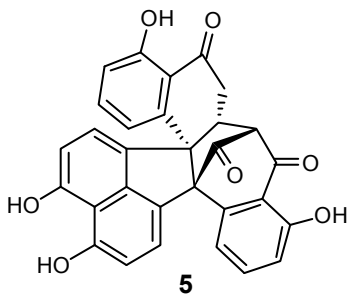

5

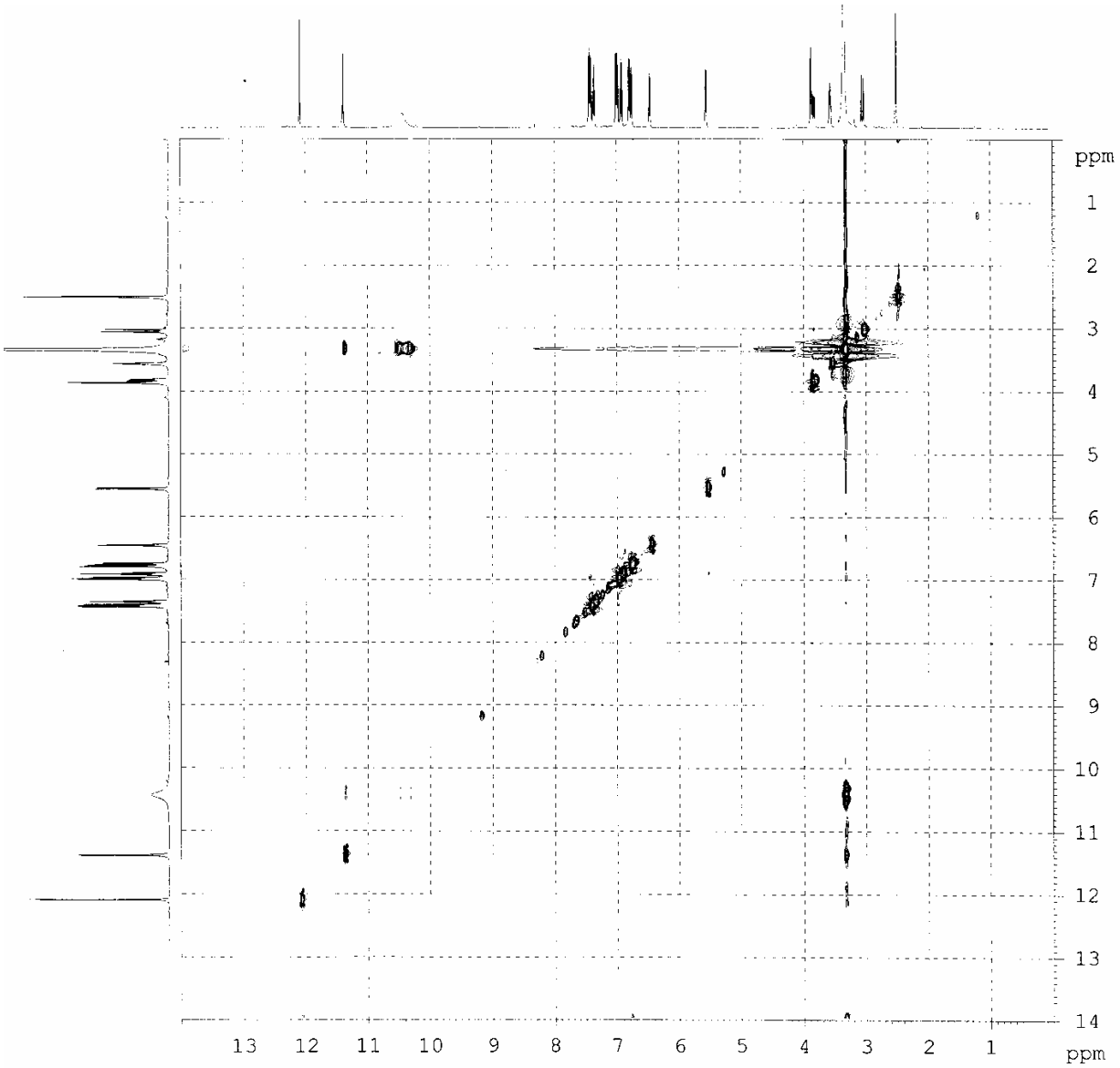

Figure S6. The NOESY spectrum of **5** in DMSO-d_6 (500 MHz).

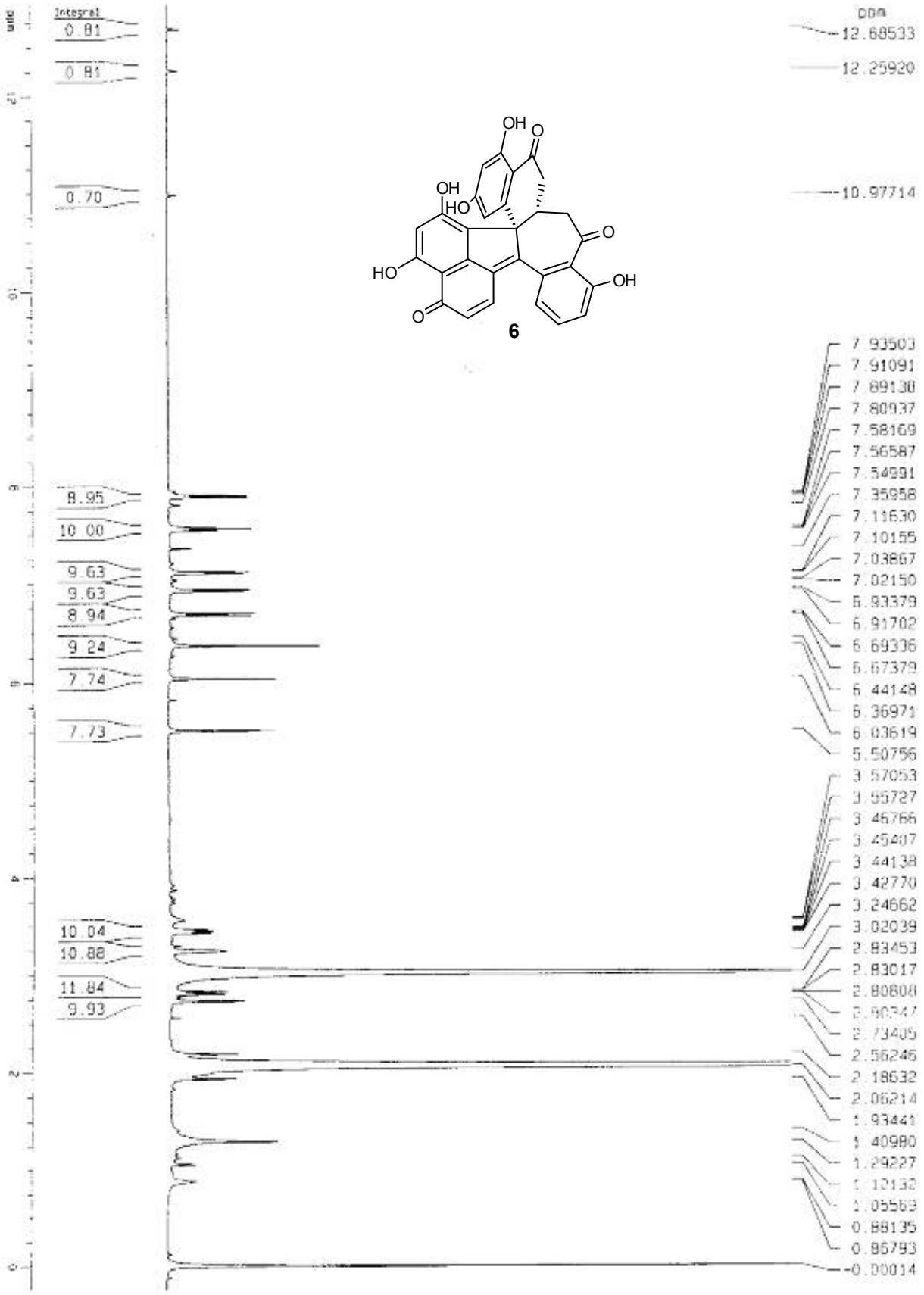

Figure S7. The ^{1}H NMR spectrum of **6** in acetone-d_6 (500 MHz).

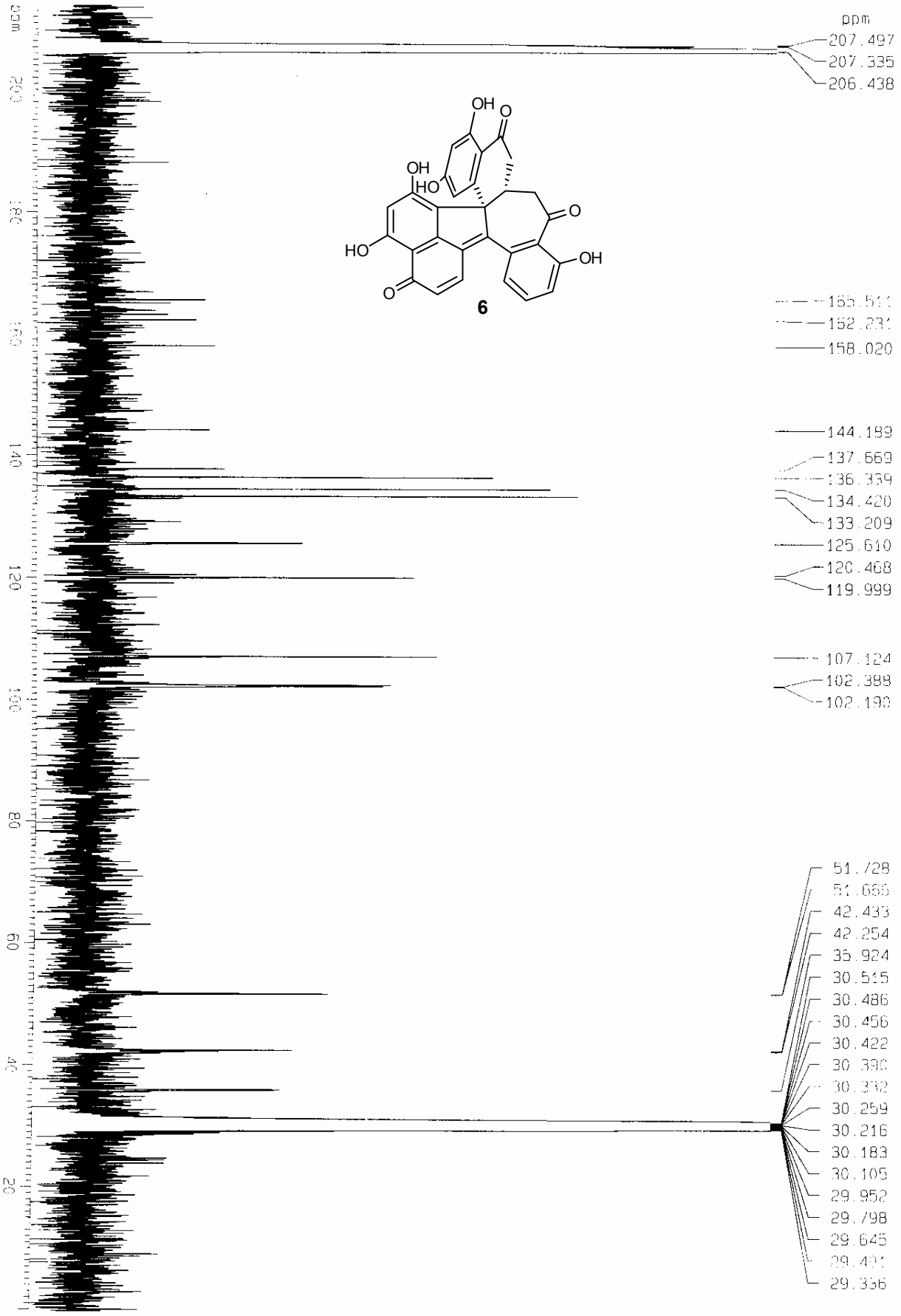

Figure S8. The ^{13}C NMR spectrum of **6** in acetone-d_6 (75 MHz).

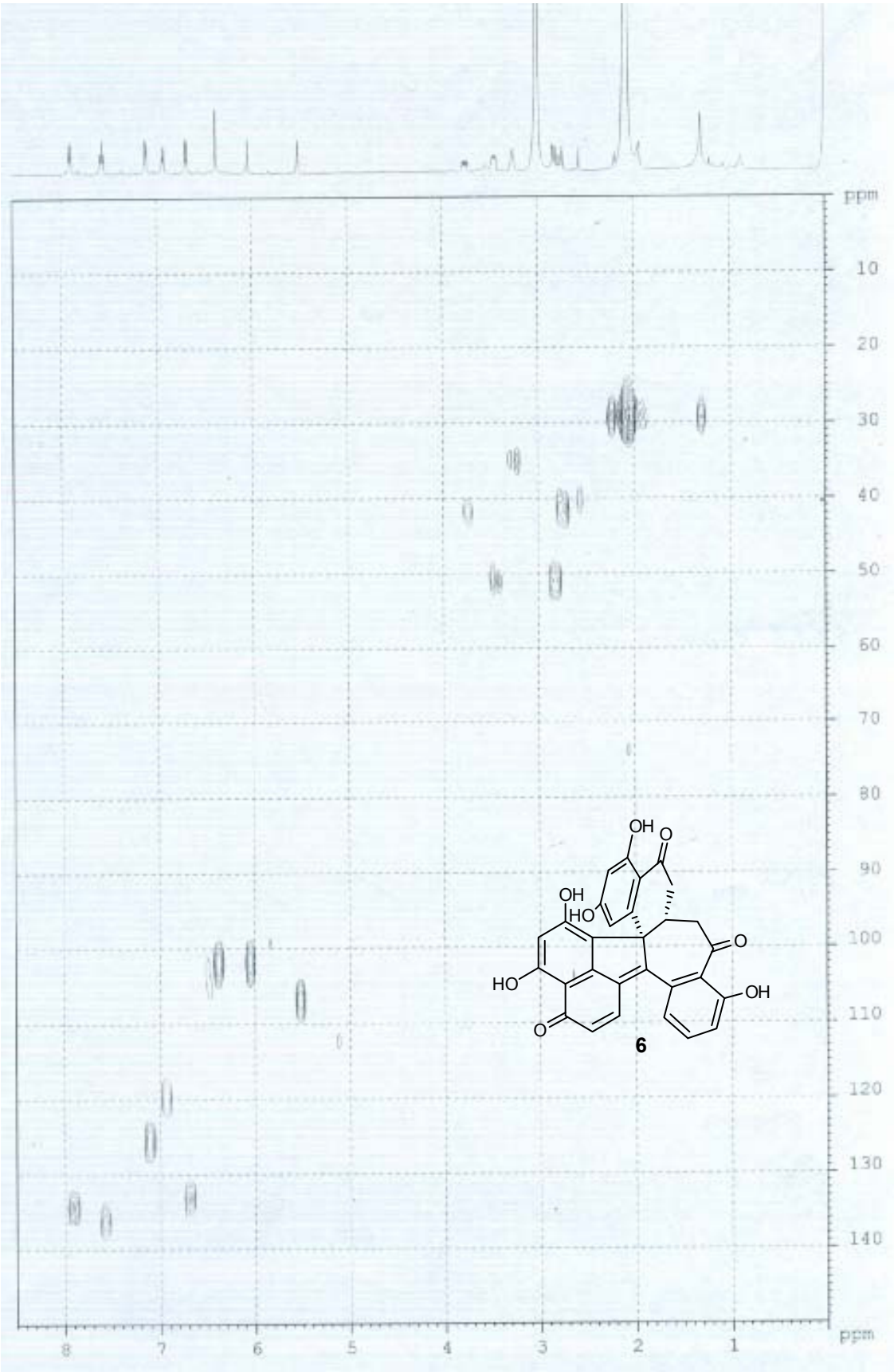

Figure S9. The HMQC spectrum of **6** in acetone-d_6 (500 MHz).

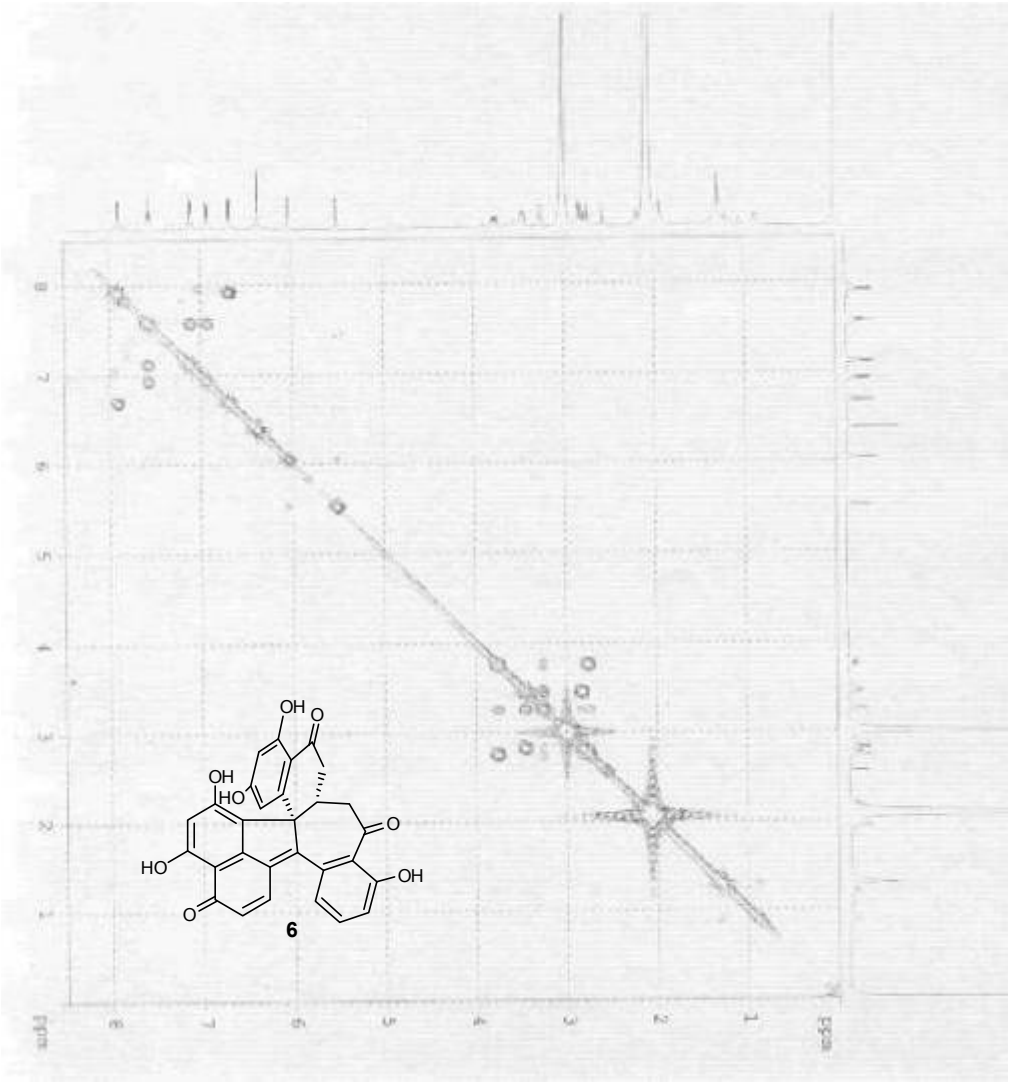

Figure S10. The ^{1}H-^{1}H COSY spectrum of **6** in acetone-d_6 (500 MHz).

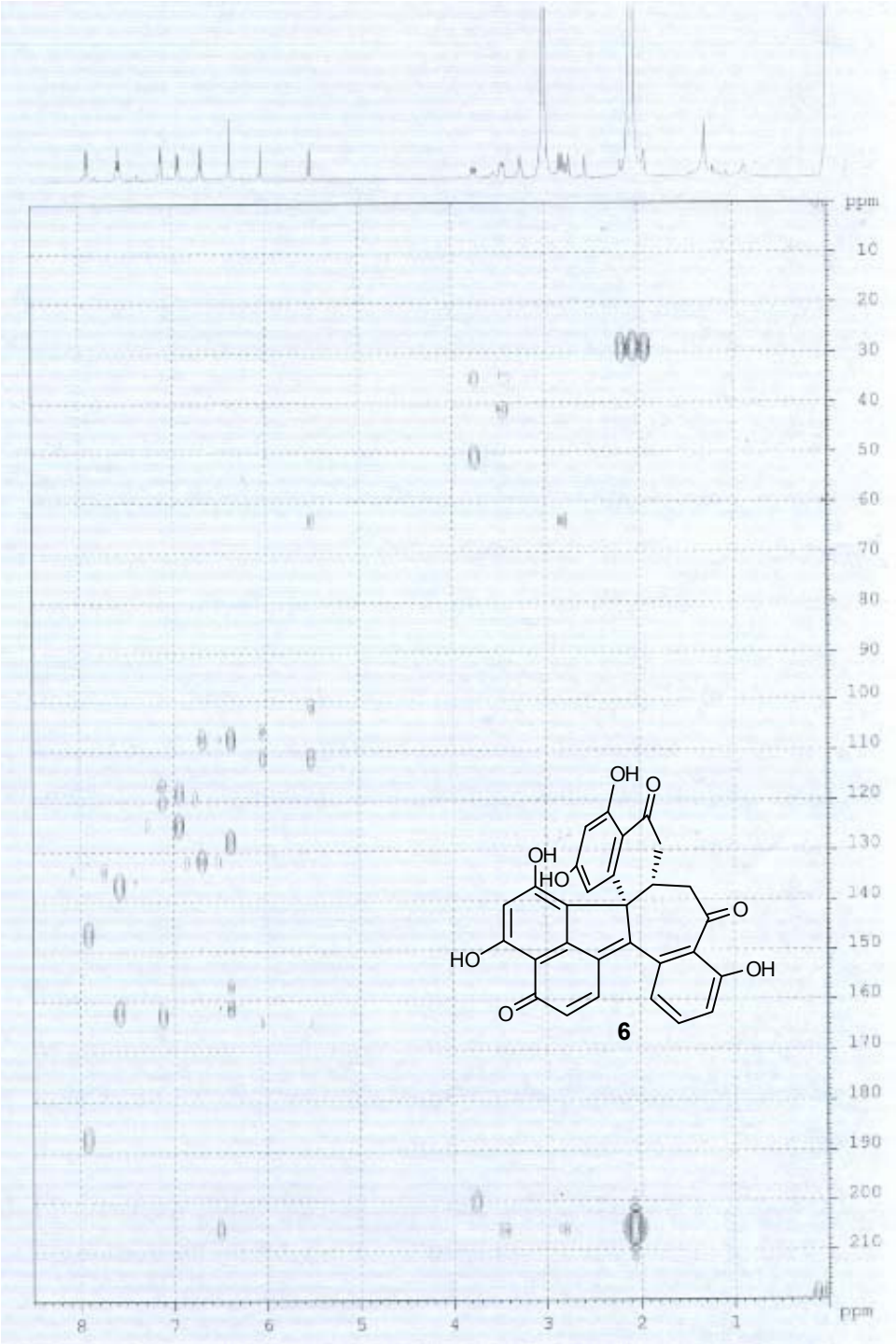

Figure S11. The HMBC spectrum of **6** in acetone-d_6 (500 MHz).

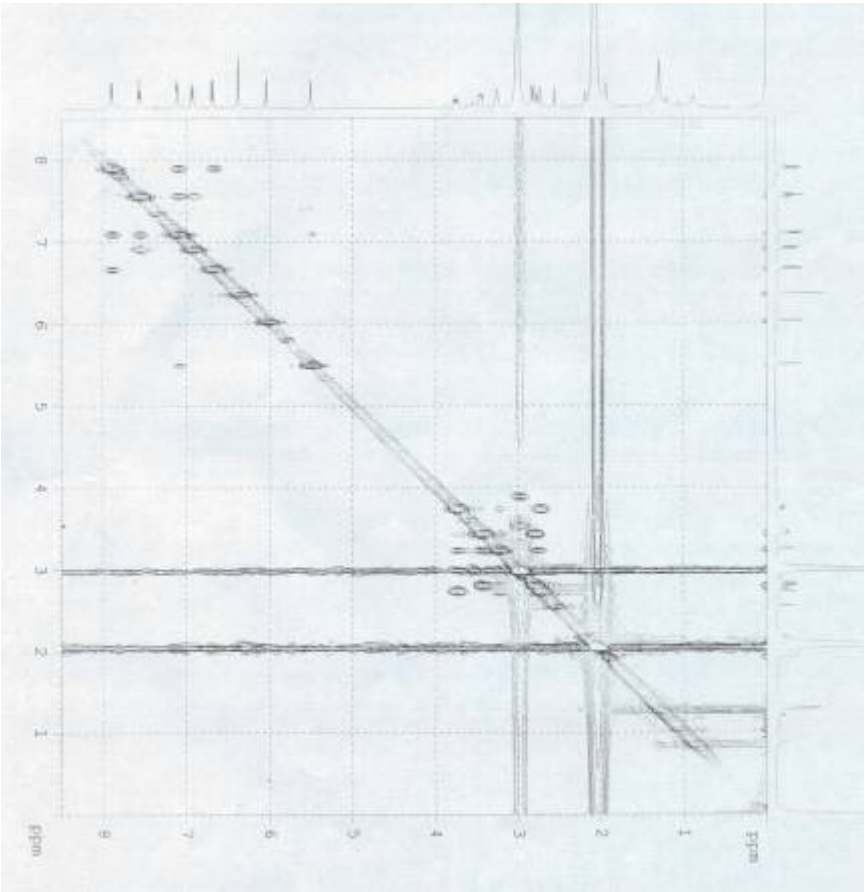

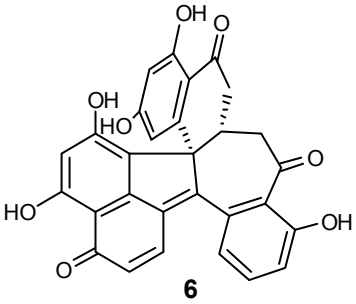

Figure S12. The NOESY spectrum of **6** in acetone-d_6 (500 MHz).

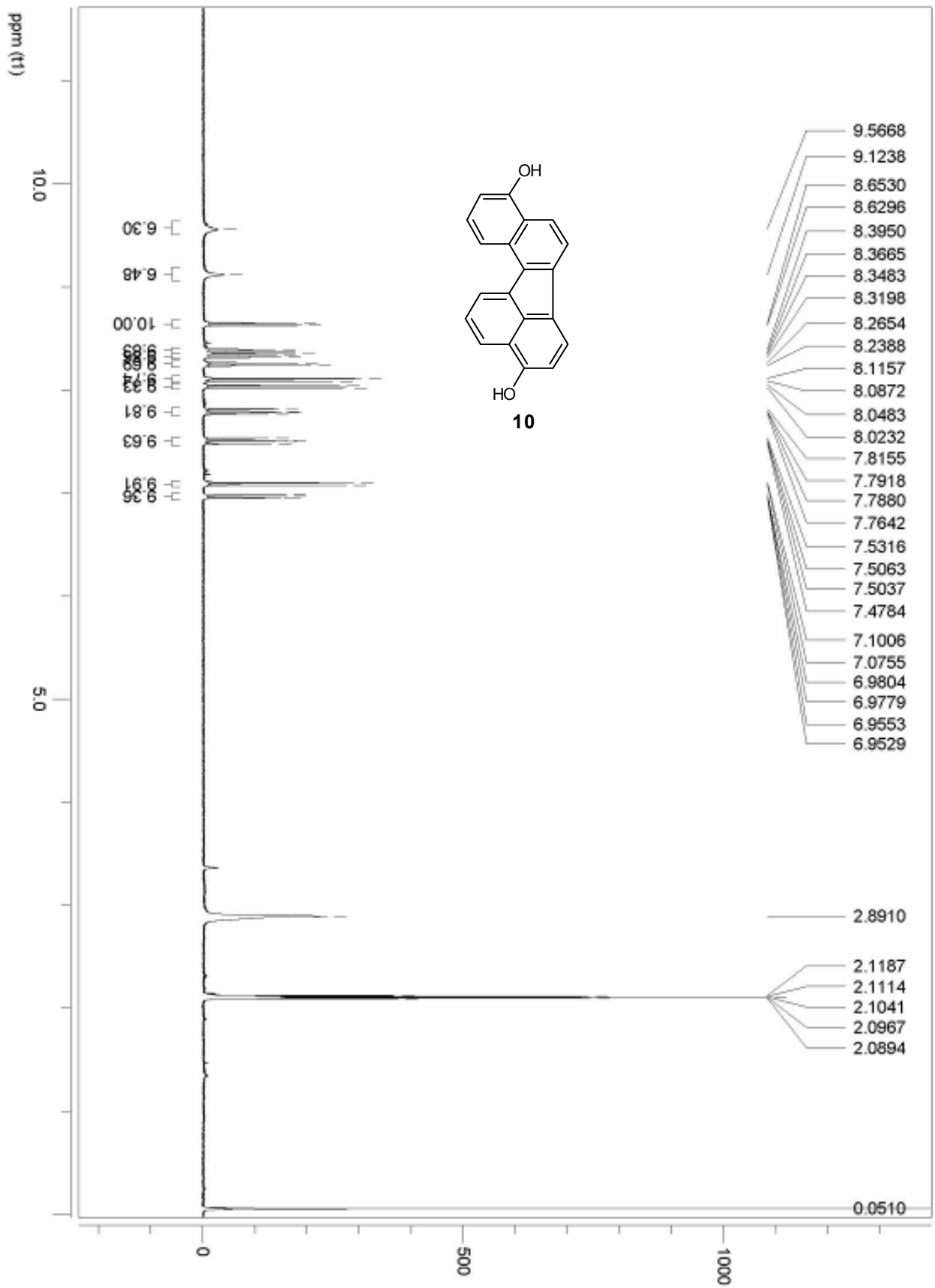

Figure S13. The ^{1}H NMR spectrum of **10** in acetone-d_6 (300 MHz).

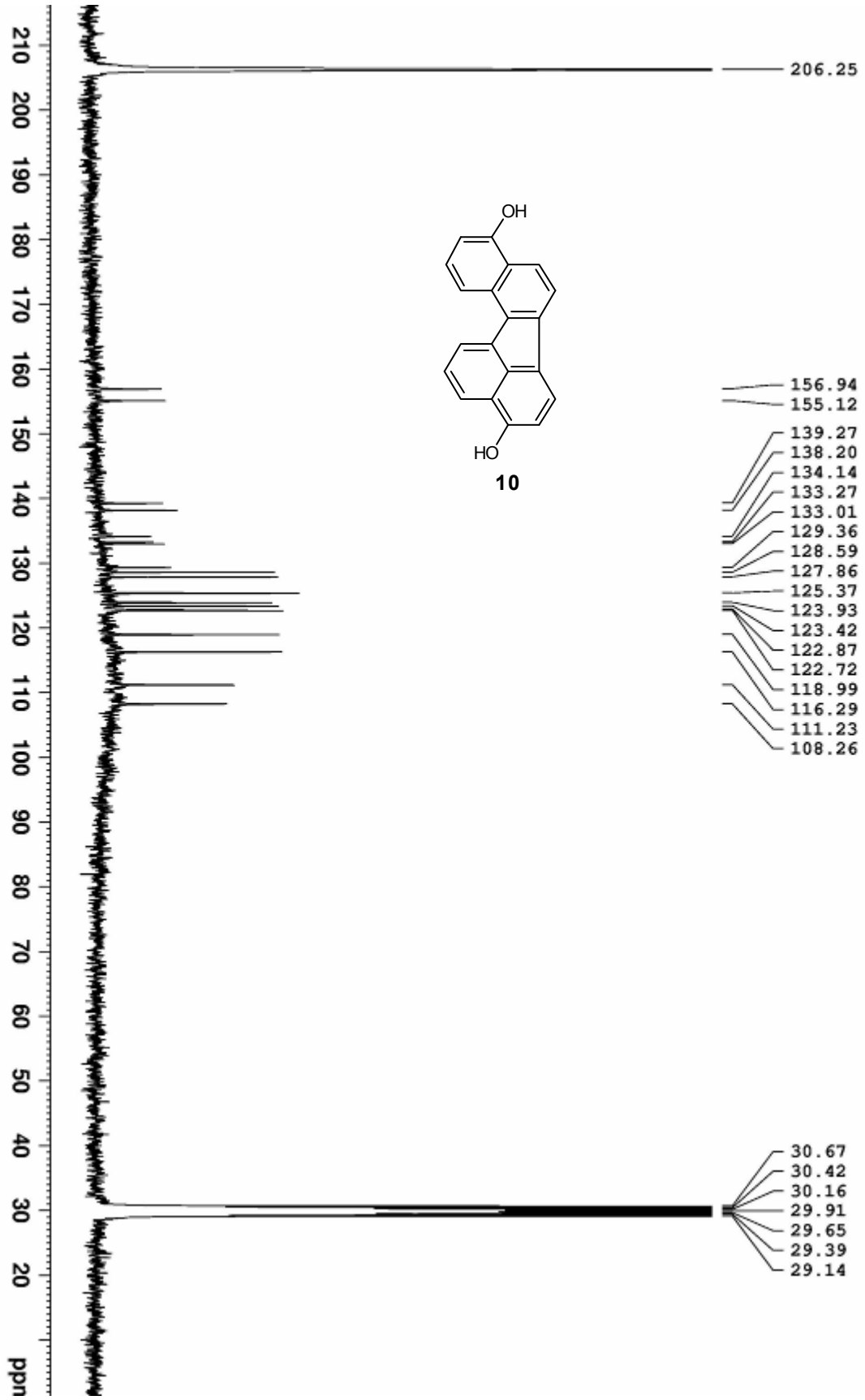

Figure S14. The ^{13}C NMR spectrum of **10** in acetone-d_6 (75 MHz).

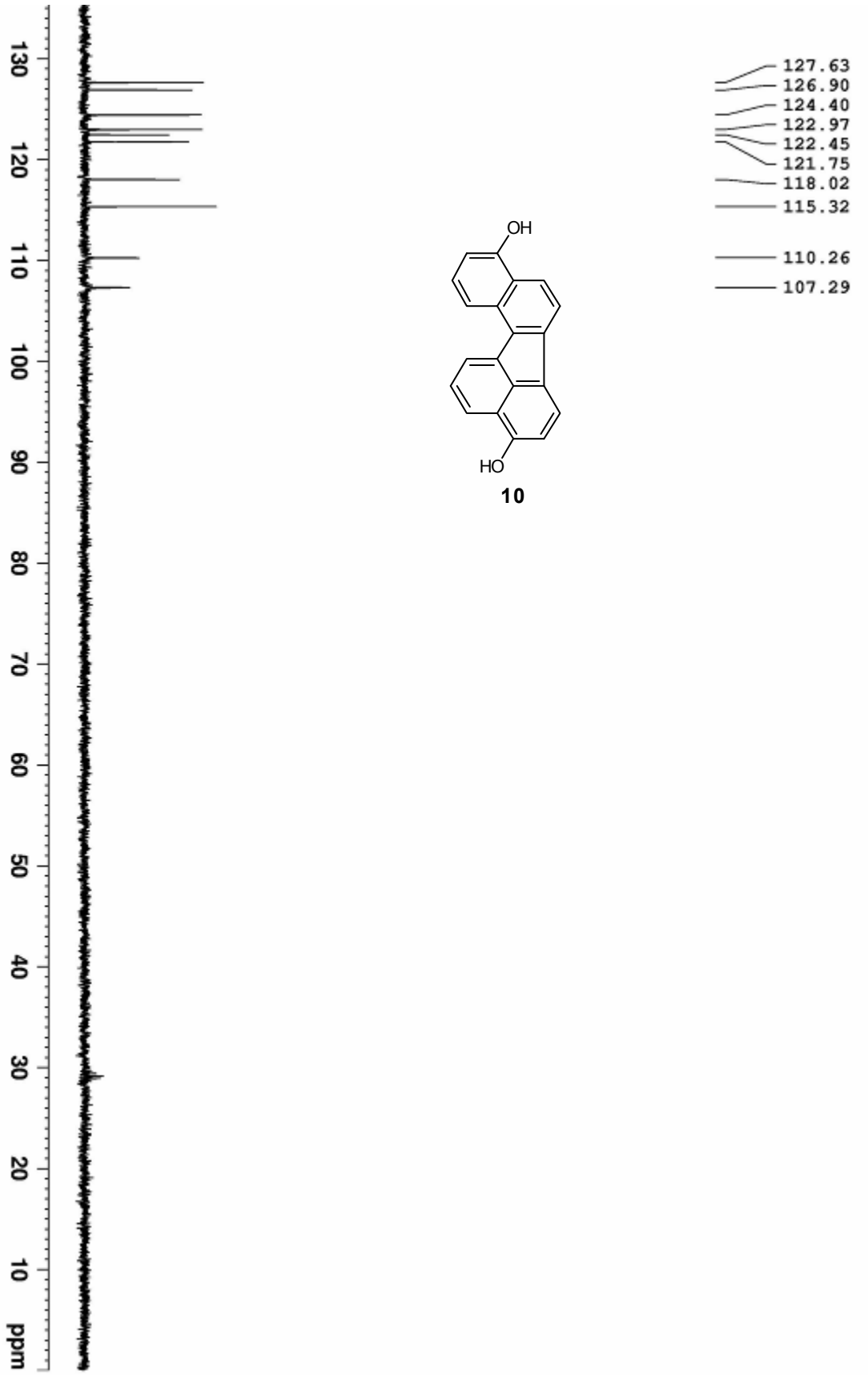

Figure S15. The DEPT135 spectrum of **10** in acetone-d_6 (75 MHz).

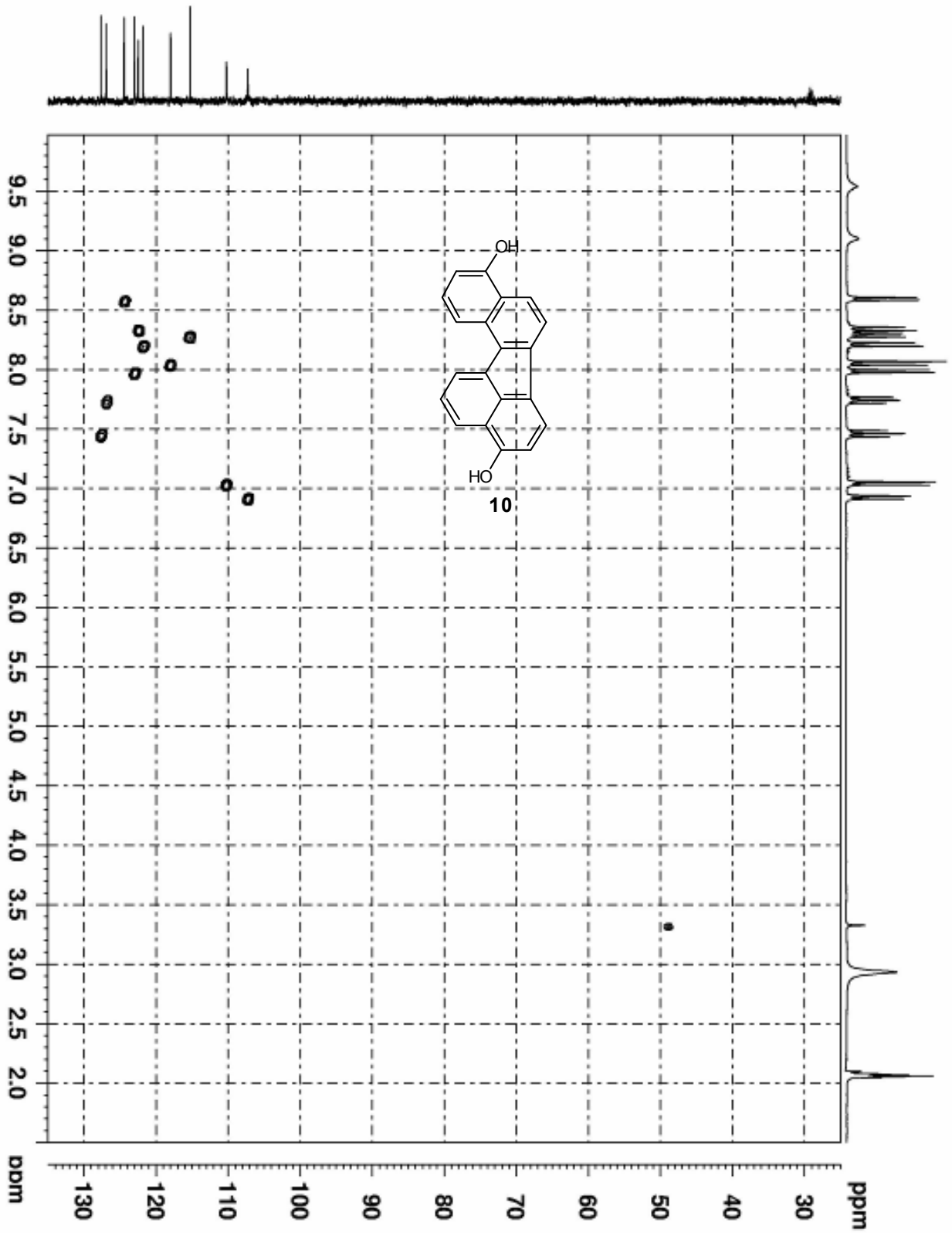

Figure S16. The HMQC spectrum of **10** in acetone-d_6 (300 MHz).

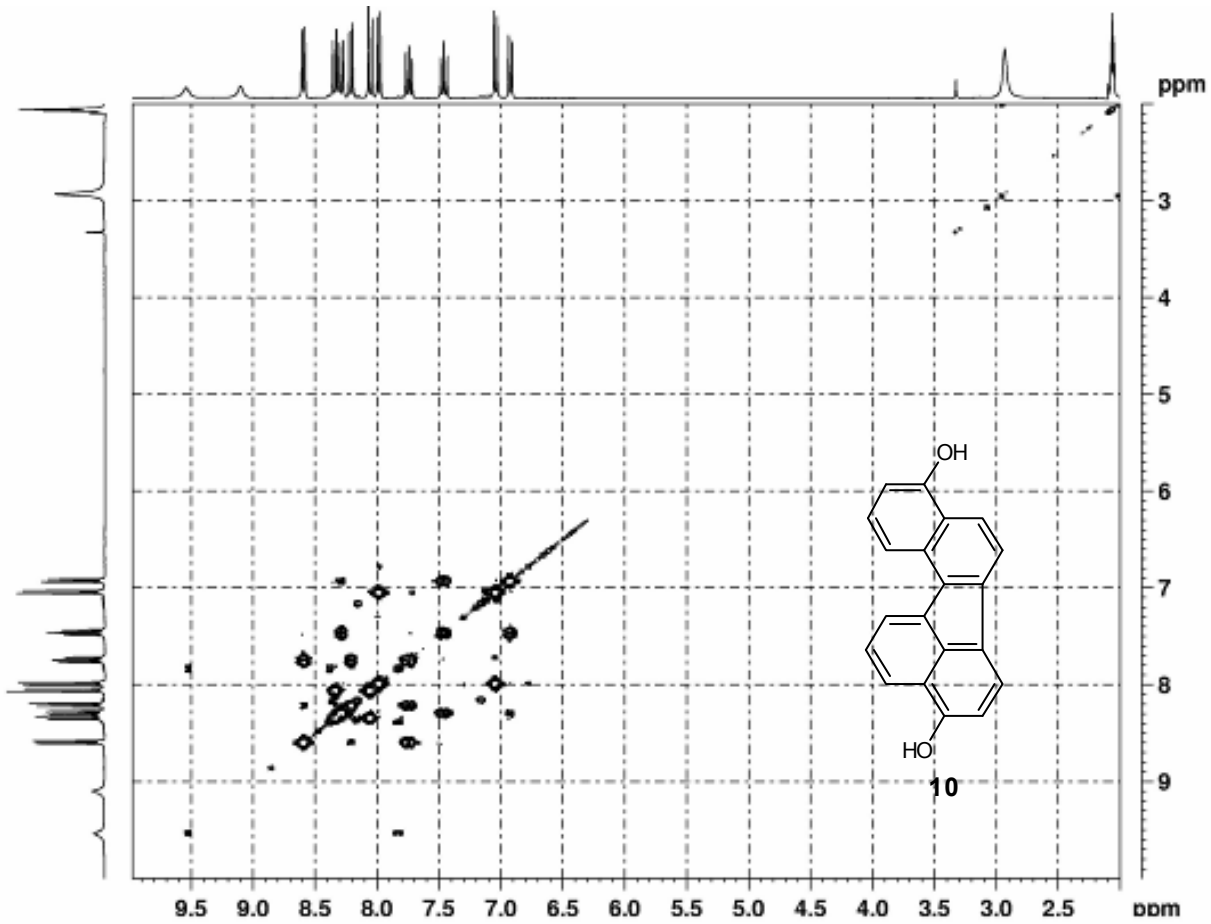

Figure S17. The ^{1}H-^{1}H COSY spectrum of **10** in acetone-d_6 (300 MHz).

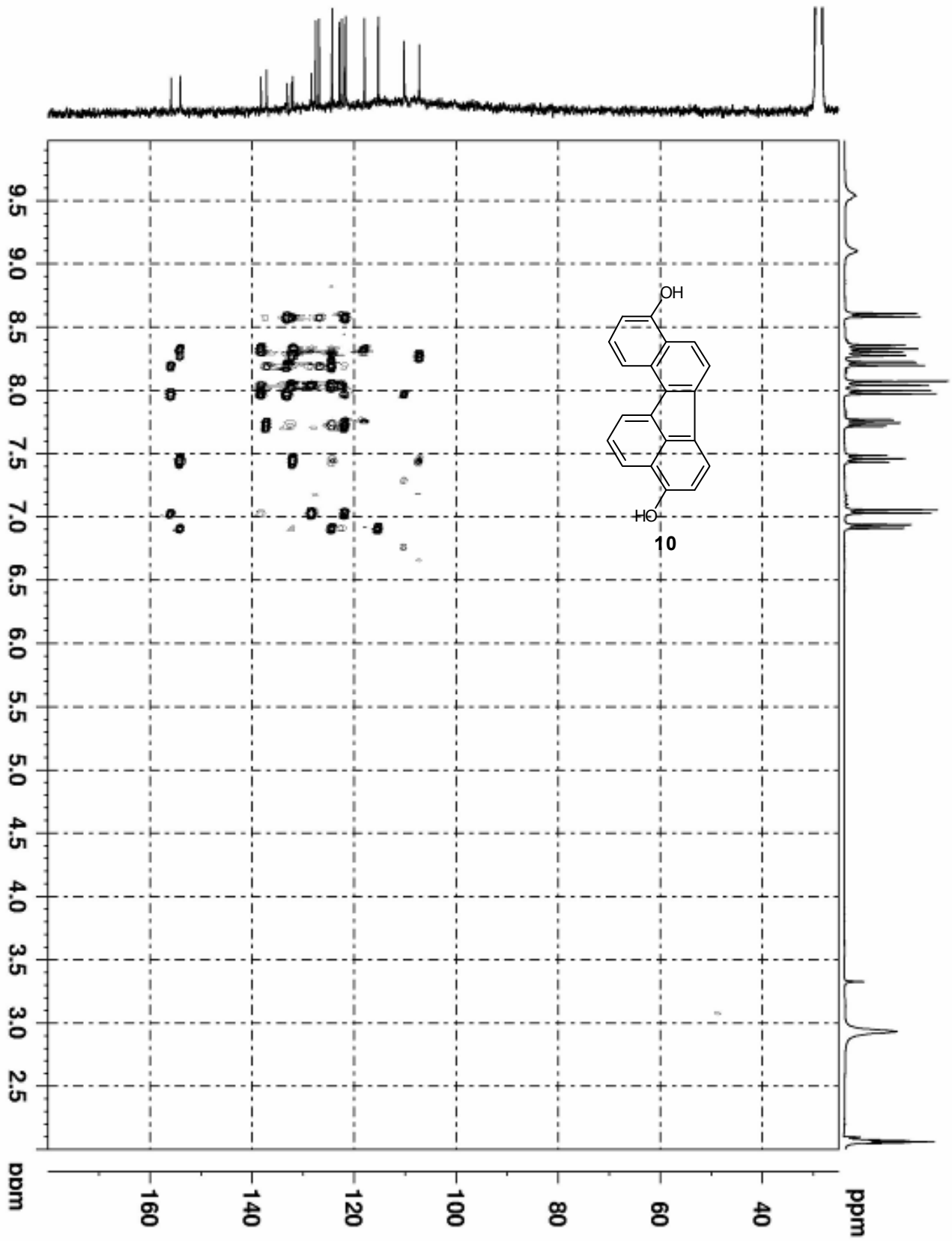

Figure S18. The HMBC spectrum of **10** in acetone-d_6 (300 MHz).

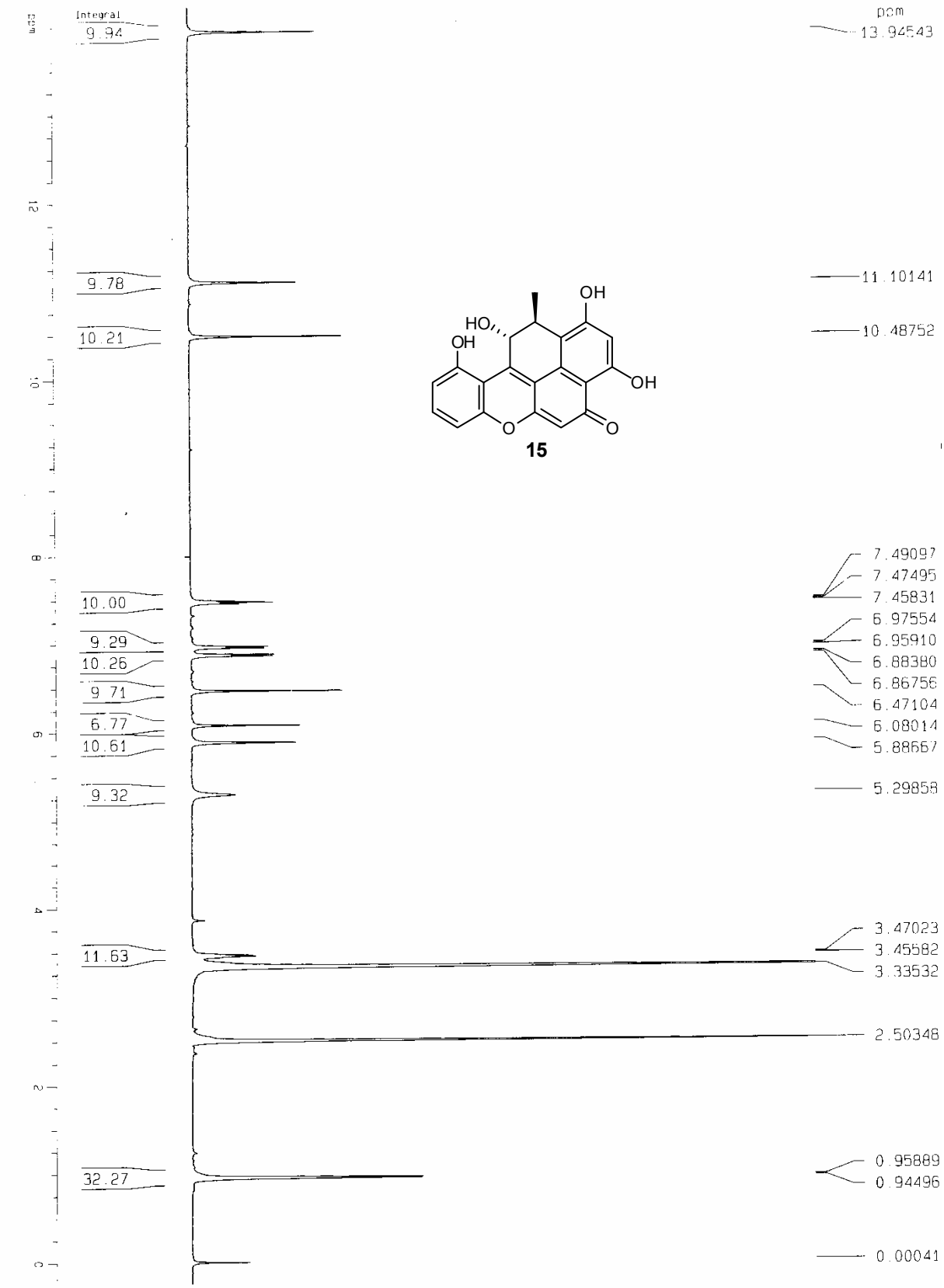

Figure S19. The ^{1}H NMR spectrum of **15** in DMSO-d_6 (500 MHz).

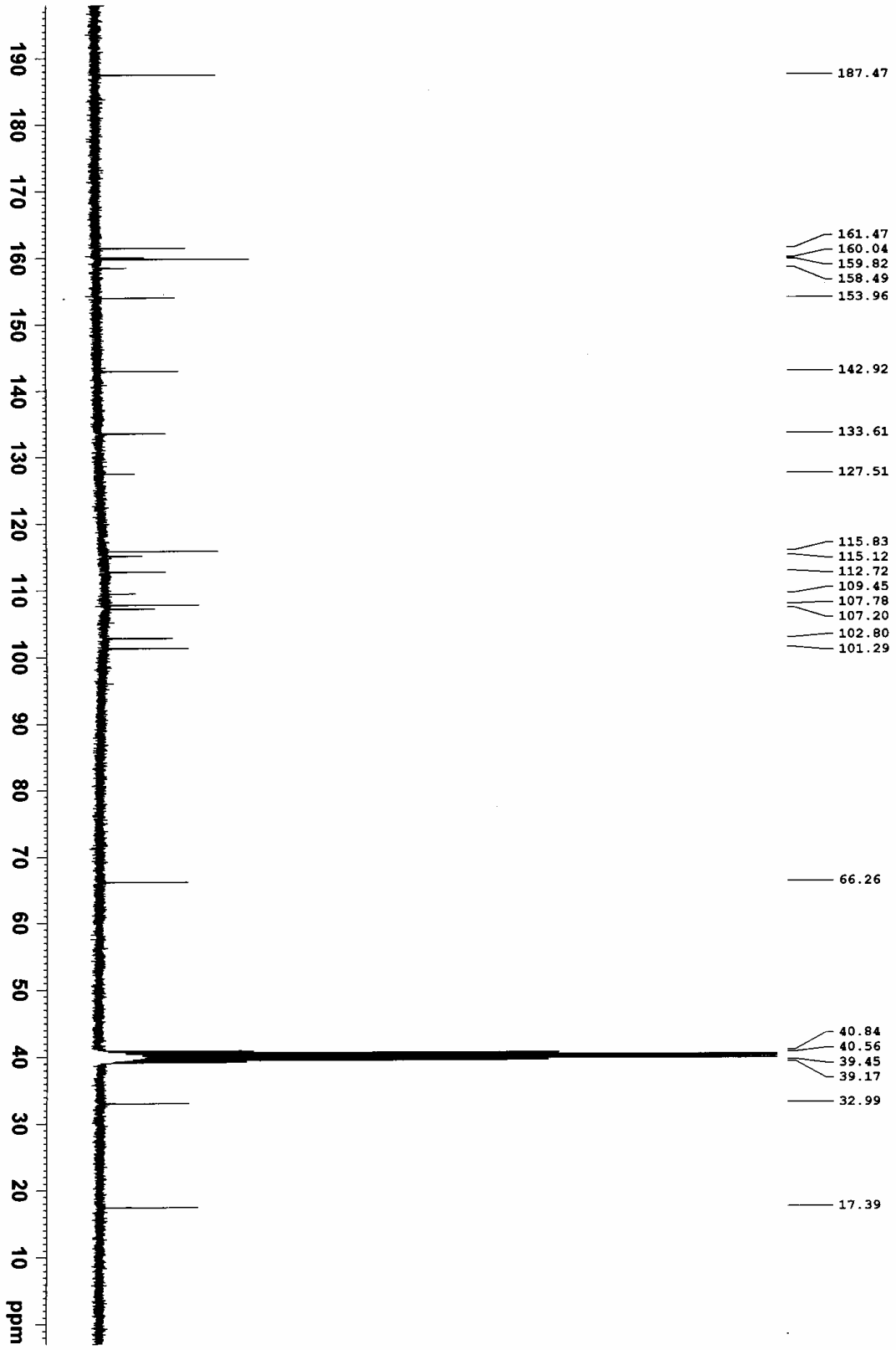

Figure S20. The ^{13}C NMR spectrum of **15** in DMSO-d_6 (75MHz).

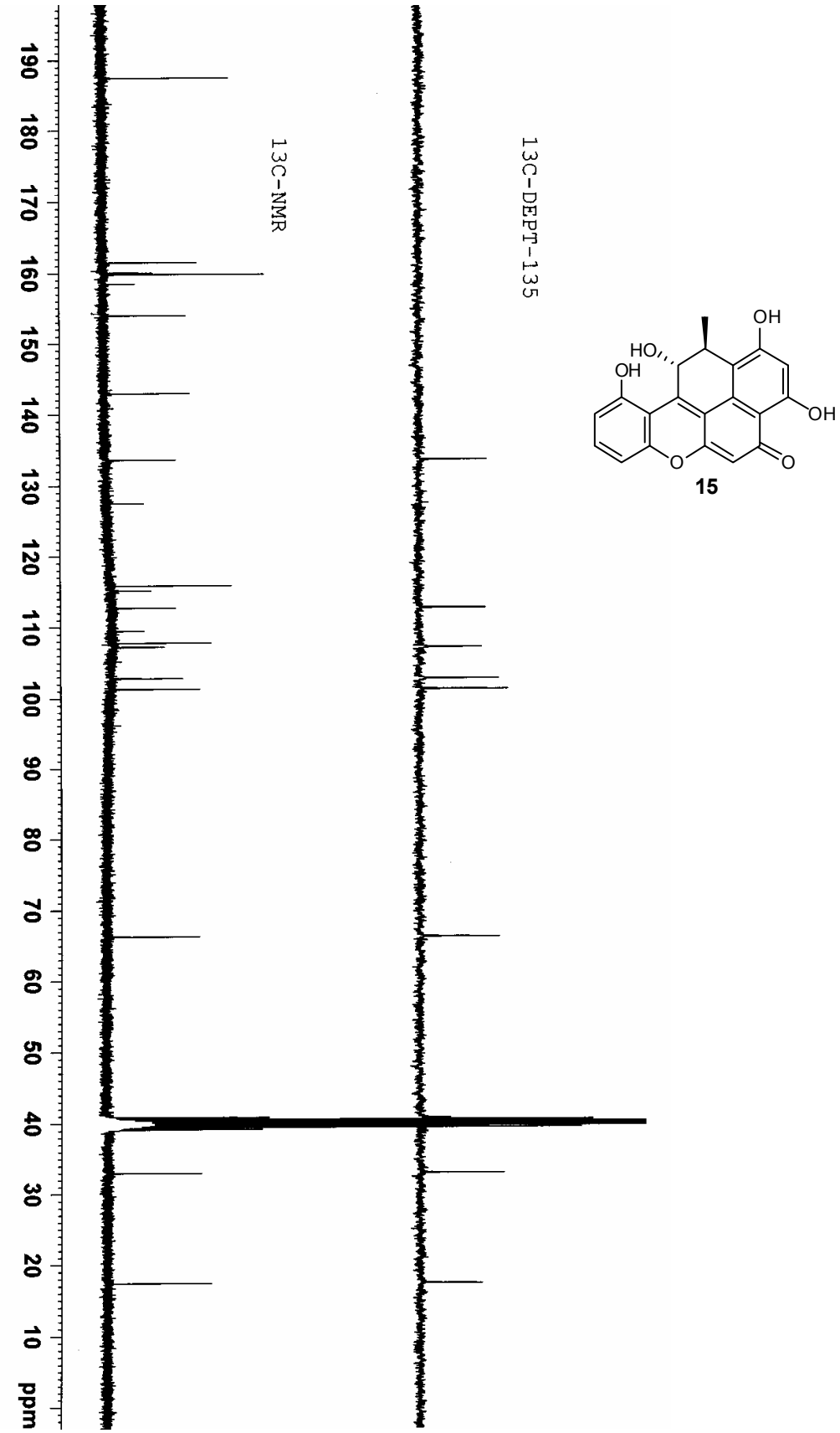

Figure S21. The DEPT spectrum of **15** in DMSO-d_6 (75 MHz).

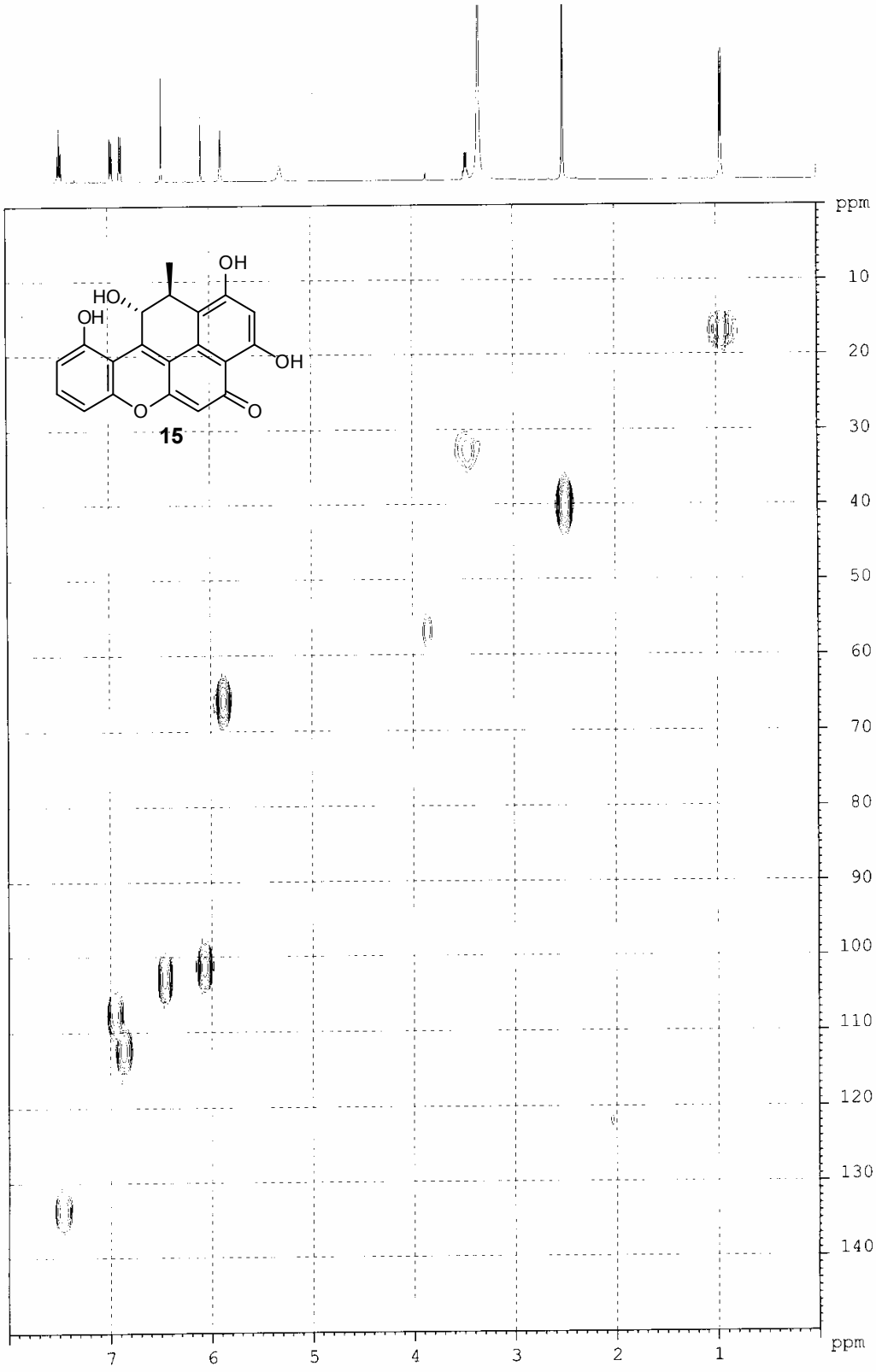

Figure S22. The HMQC spectrum of **15** in DMSO-d_6 (500 MHz).

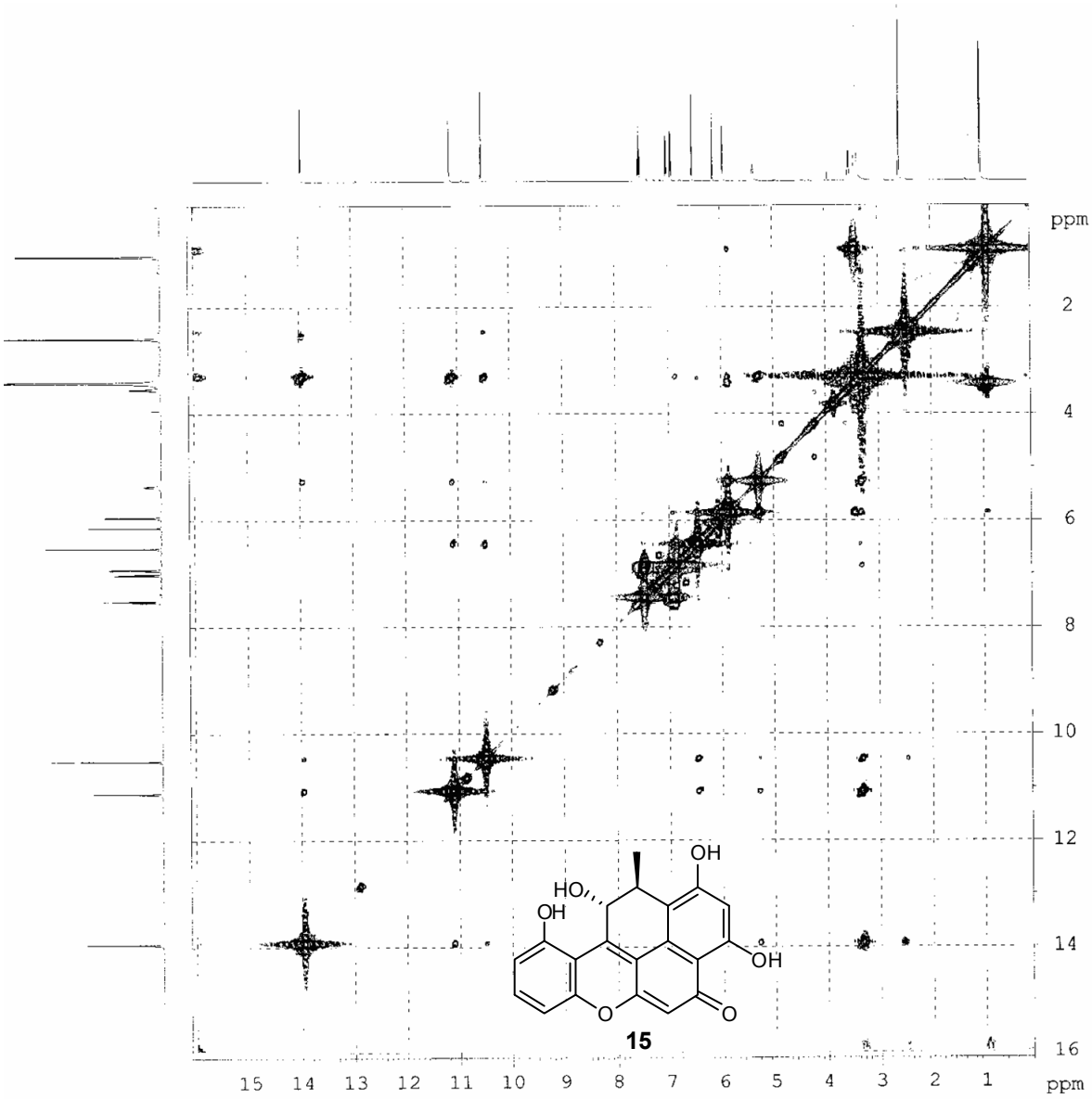

Figure S23. The ^{1}H-^{1}H COSY spectrum of **15** in DMSO-d_6 (500 MHz).

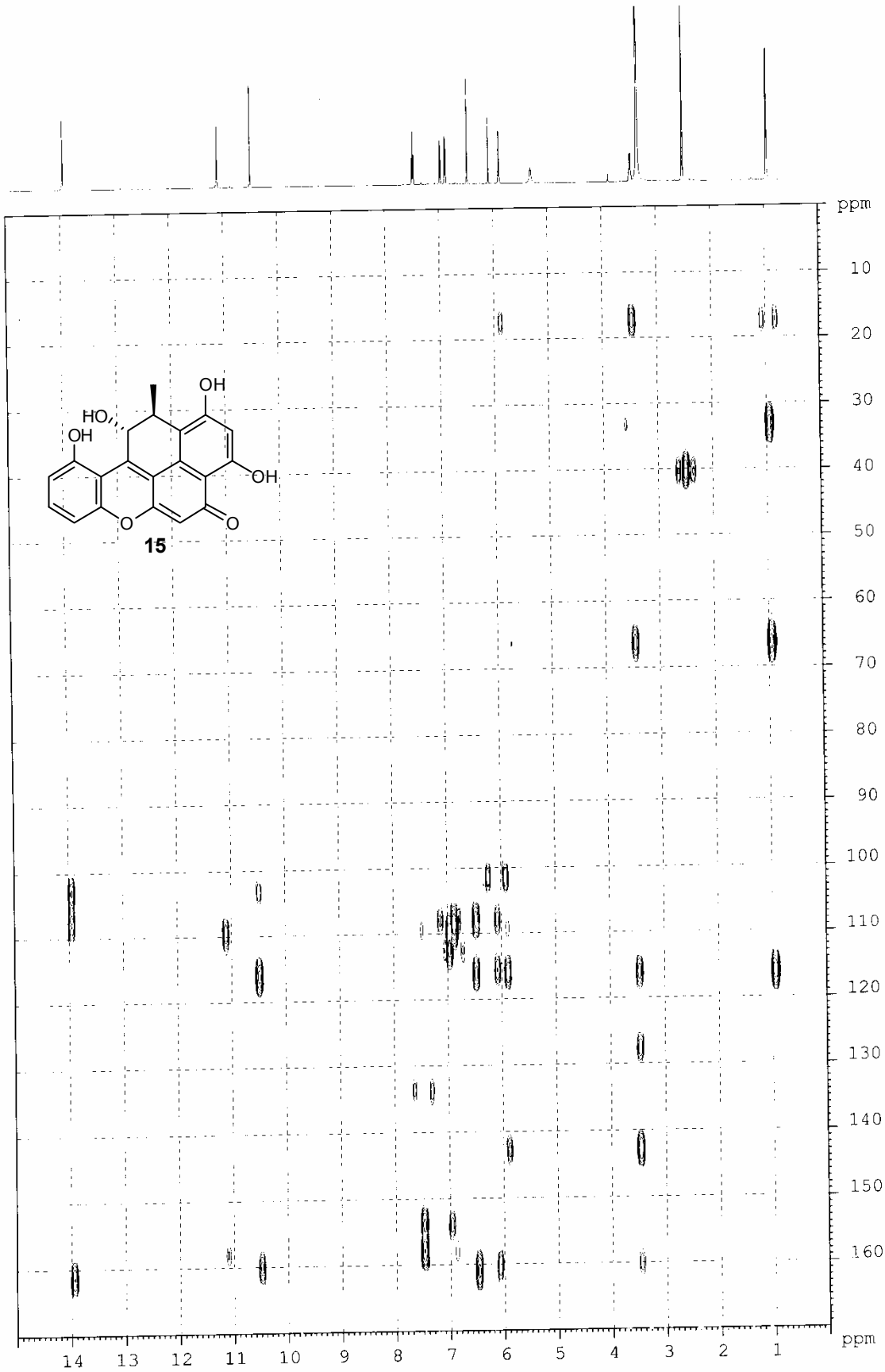

Figure S24. The HMBC spectrum of **15** in DMSO-d_6 (500 MHz).

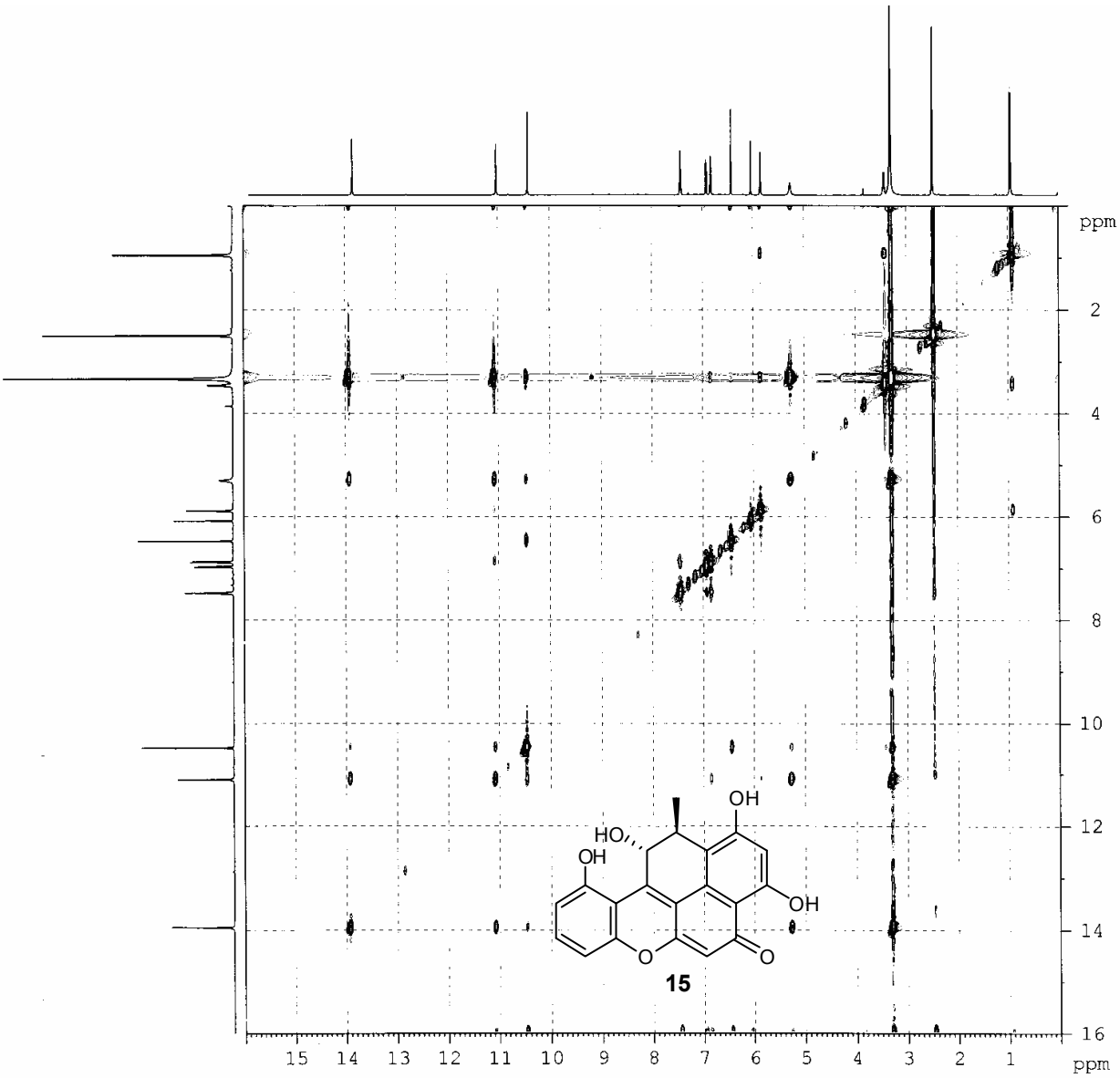

Figure S25. The NOESY spectrum of **15** in DMSO-d_6 (500 MHz).

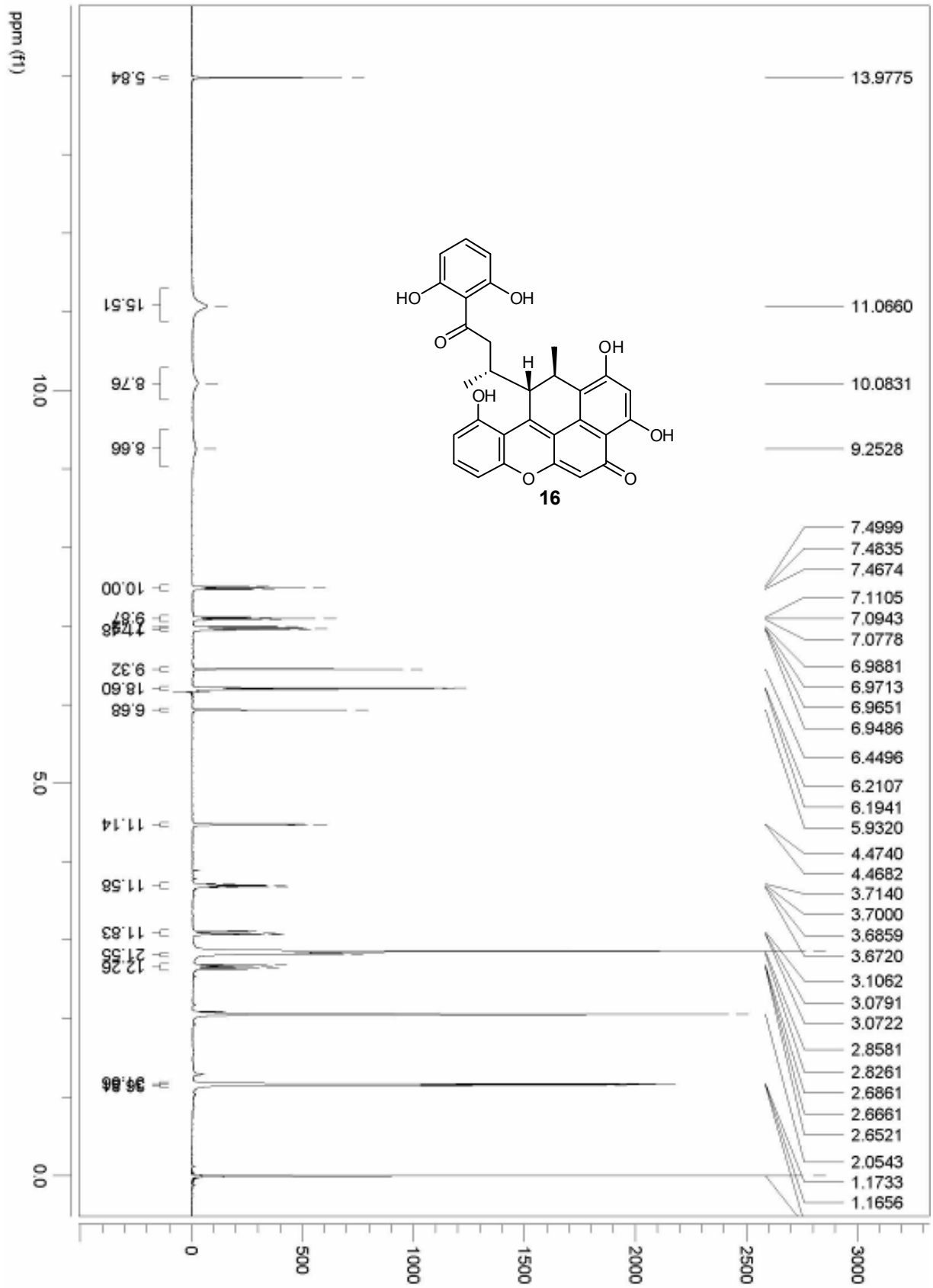

Figure S26. The ^{1}H NMR spectrum of **16** in acetone-d_6 (500 MHz).

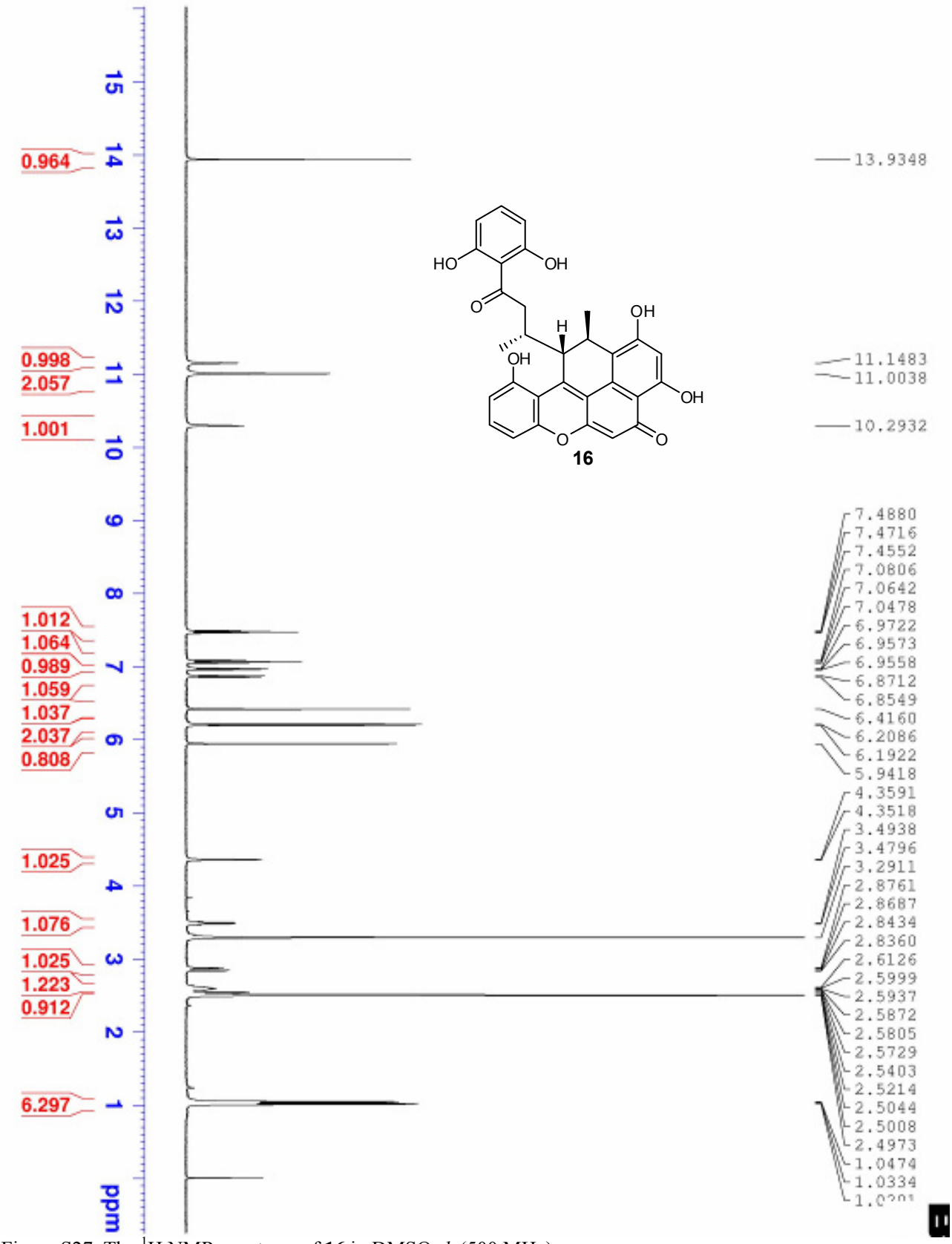

Figure S27. The ^{1}H NMR spectrum of **16** in DMSO-d_6 (500 MHz).

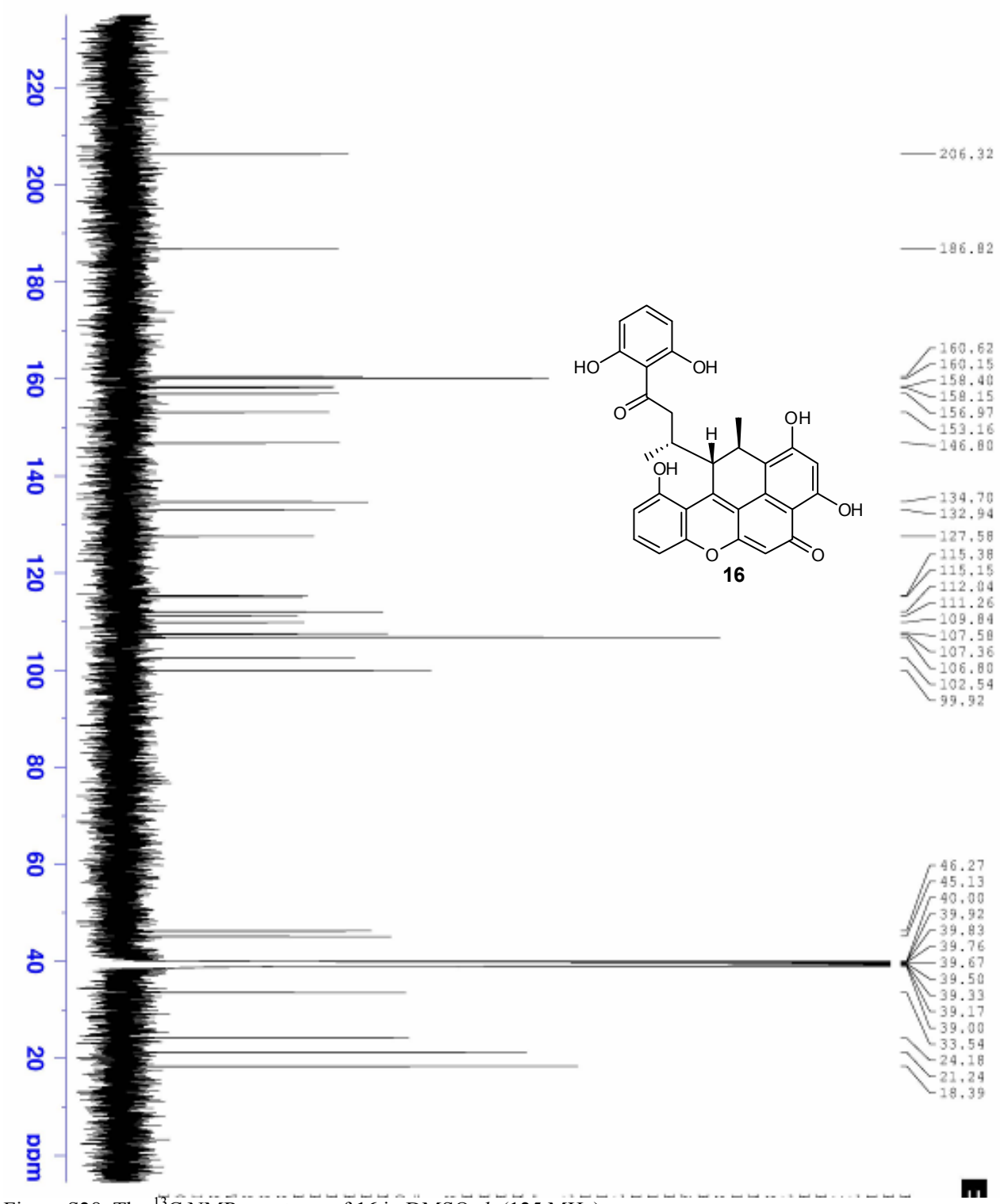

Figure S28. The ^{13}C NMR spectrum of **16** in DMSO-d_6 (125 MHz).

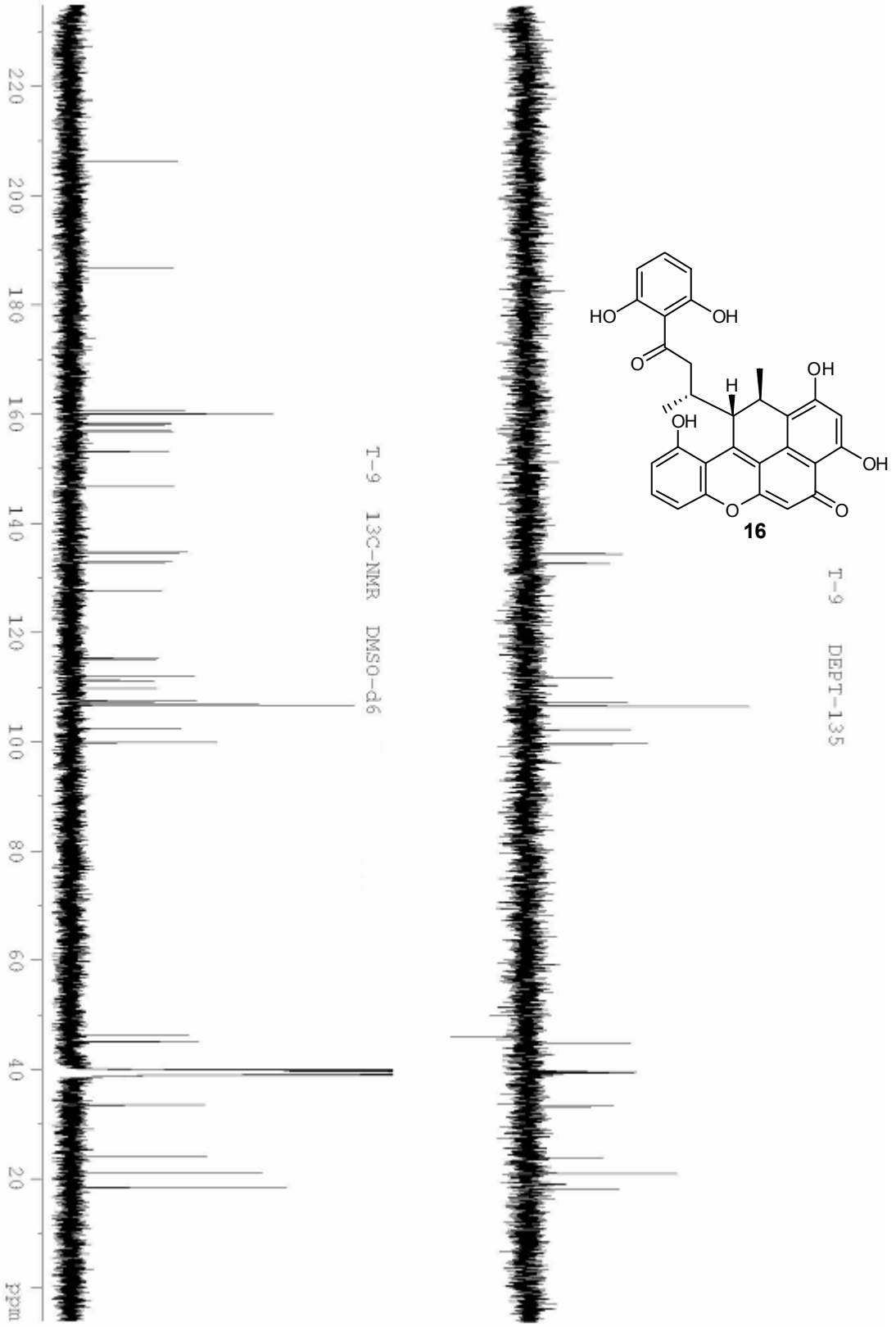

Figure S29. The DEPT135 spectrum of **16** in DMSO-d_6 (125 MHz).

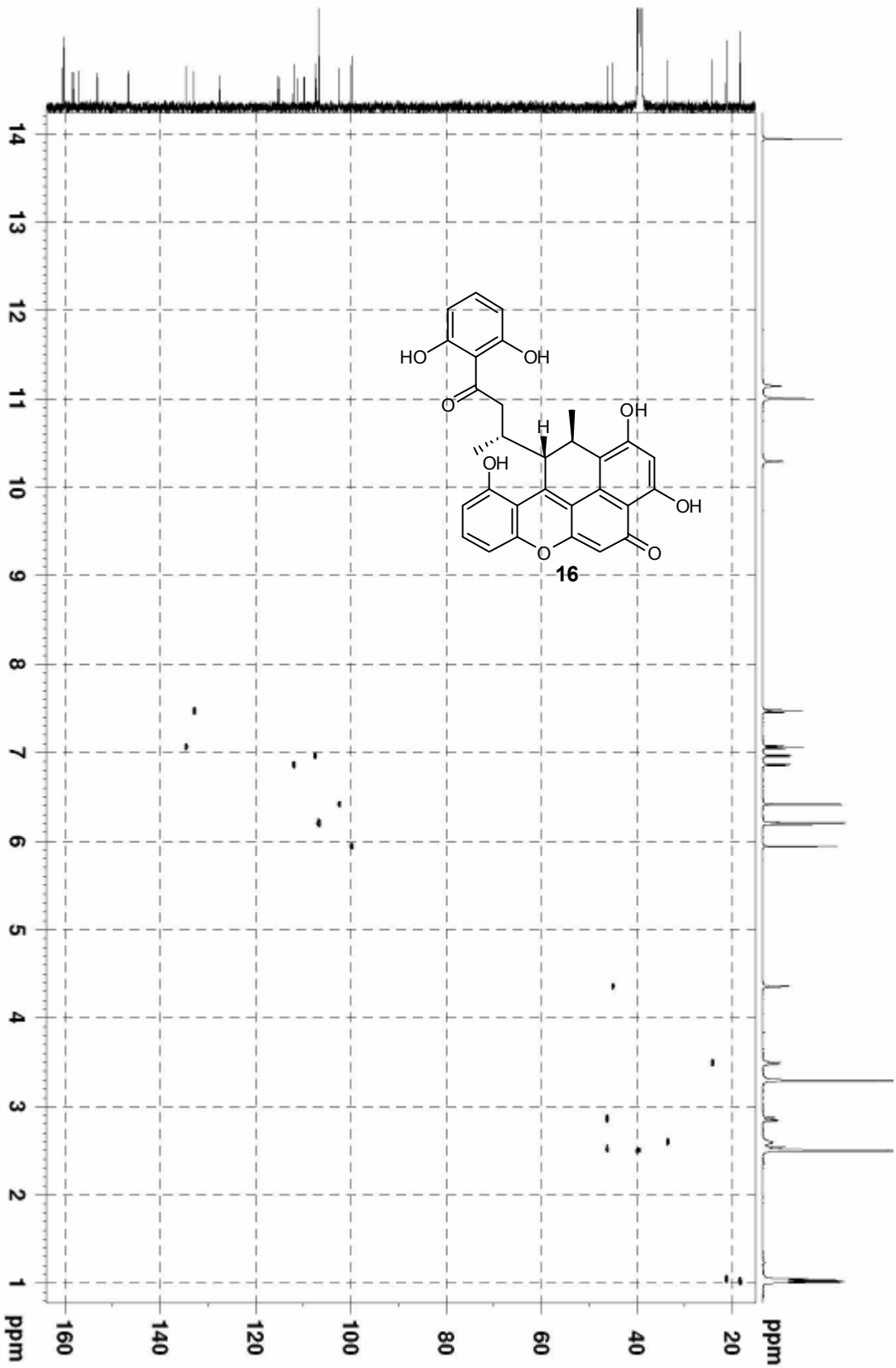

Figure S30. The HMQC spectrum of **16** in DMSO-d_6 (500 MHz).

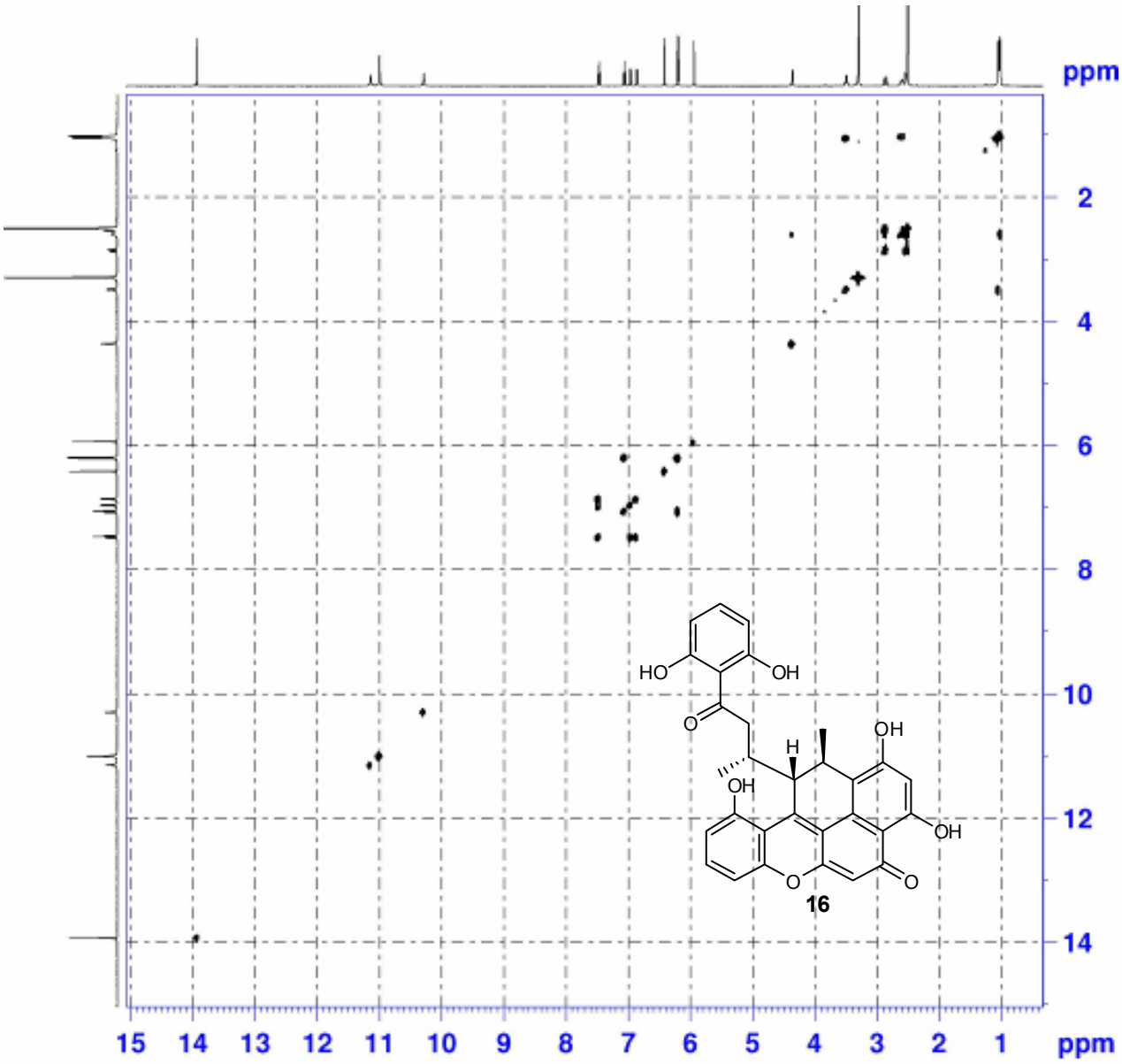

Figure S31. The ^{1}H-^{1}H COSY spectrum of **16** in DMSO-d_6 (500 MHz).

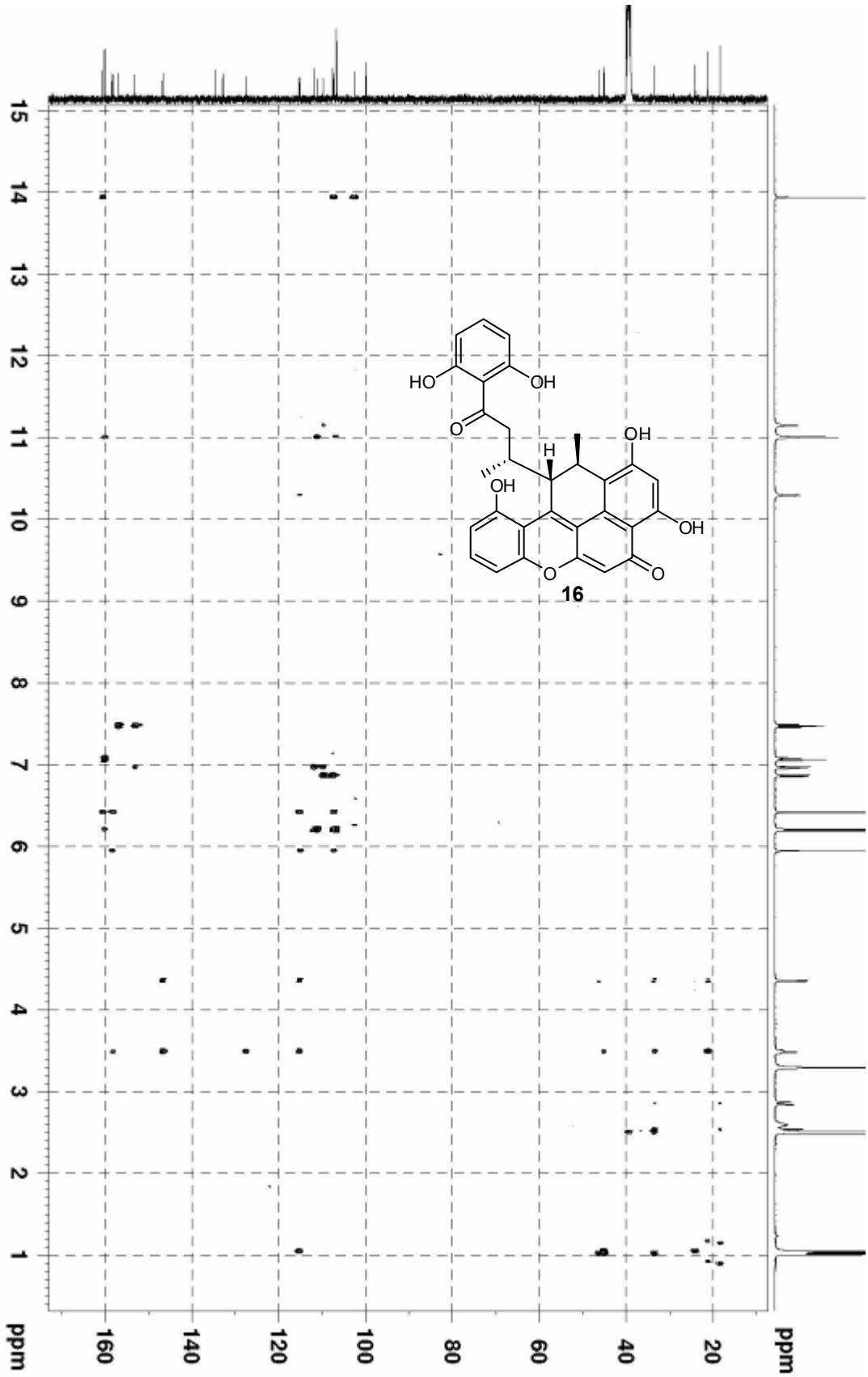

Figure S32. The HMBC spectrum of **16** in DMSO-d_6 (500 MHz).

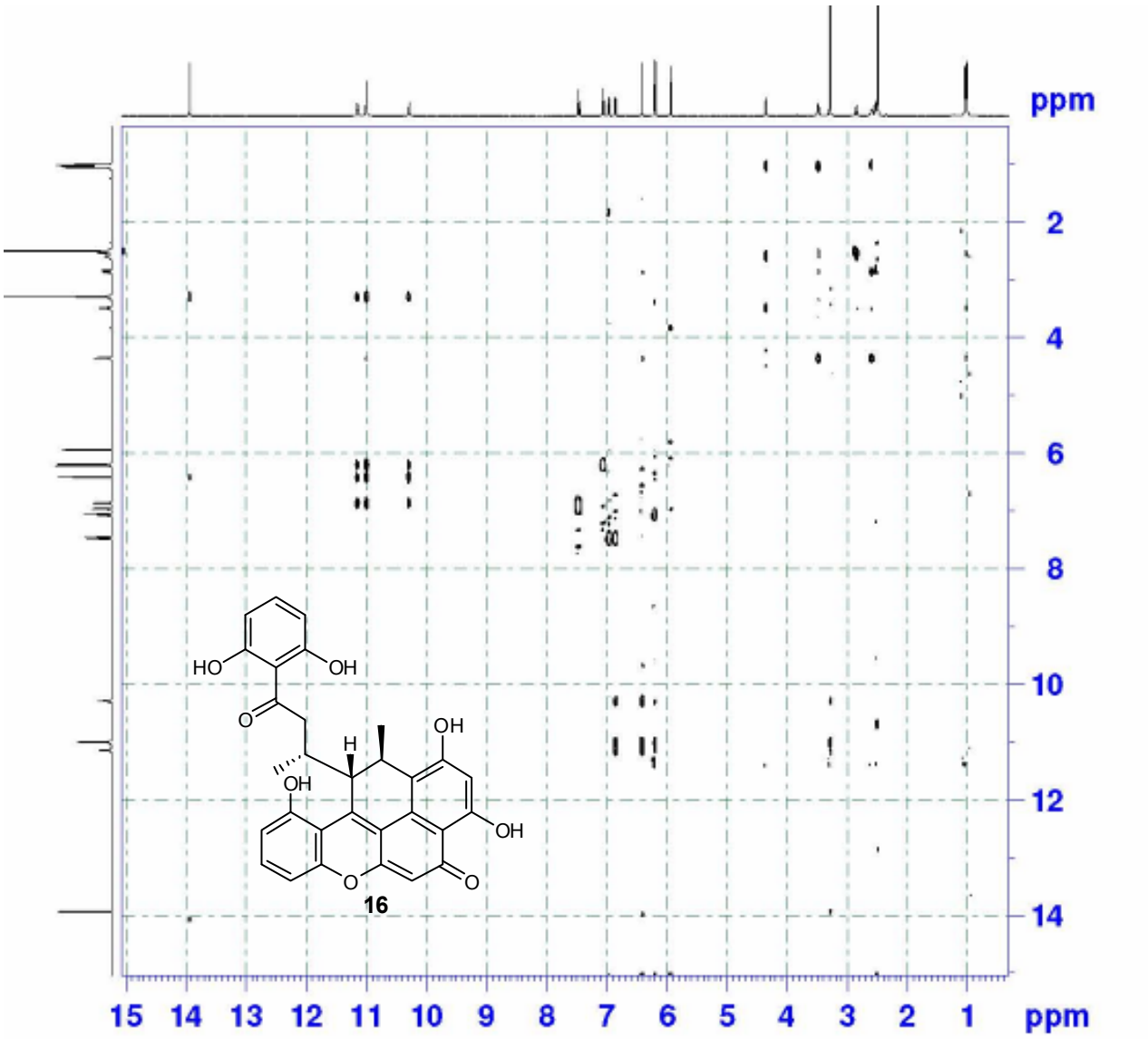

Figure S33. The ROESY spectrum of **16** in DMSO-d_6 (500 MHz).

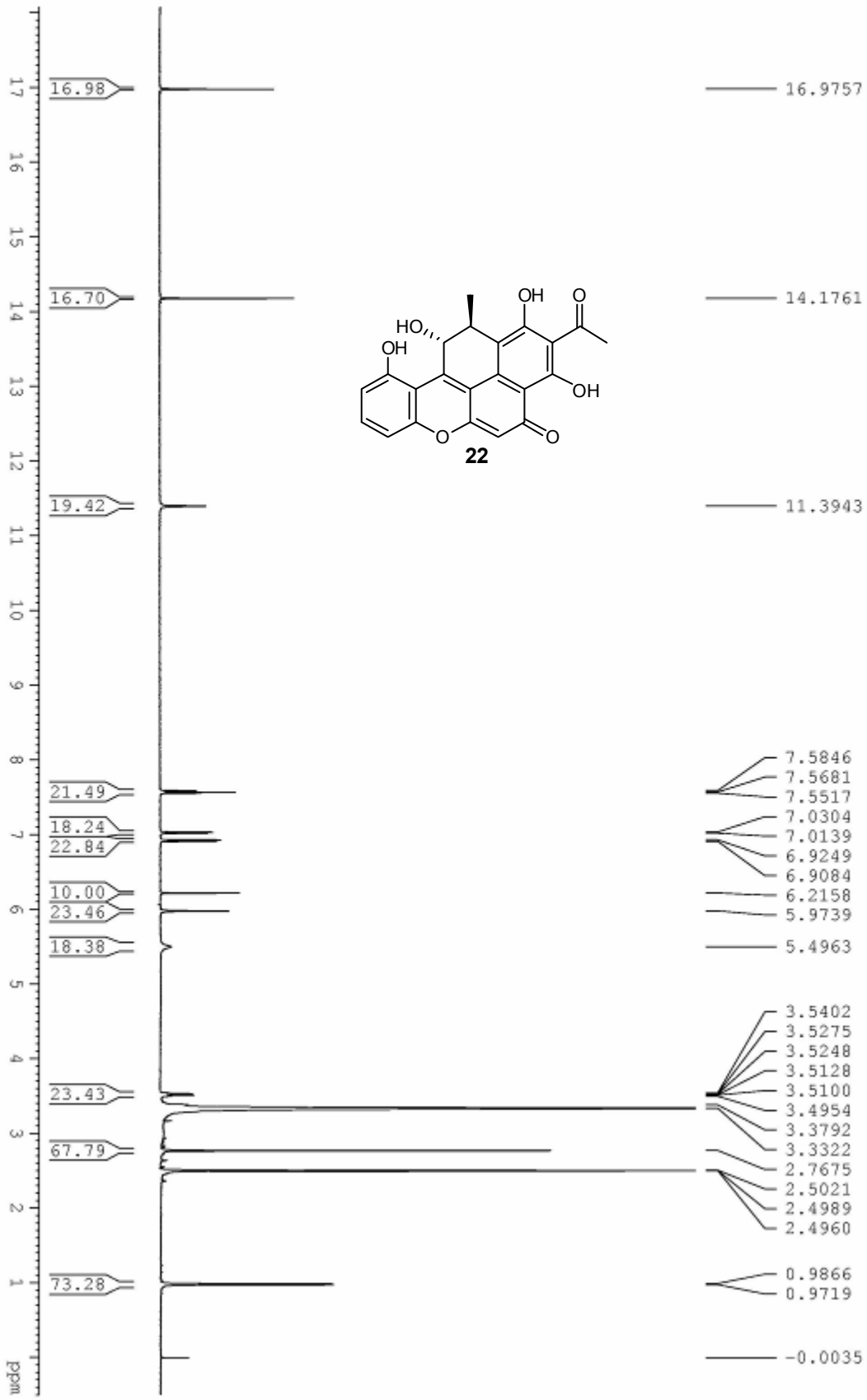

Figure S34. The ^{1}H NMR spectrum of **22** in DMSO-d_6 (500 MHz).

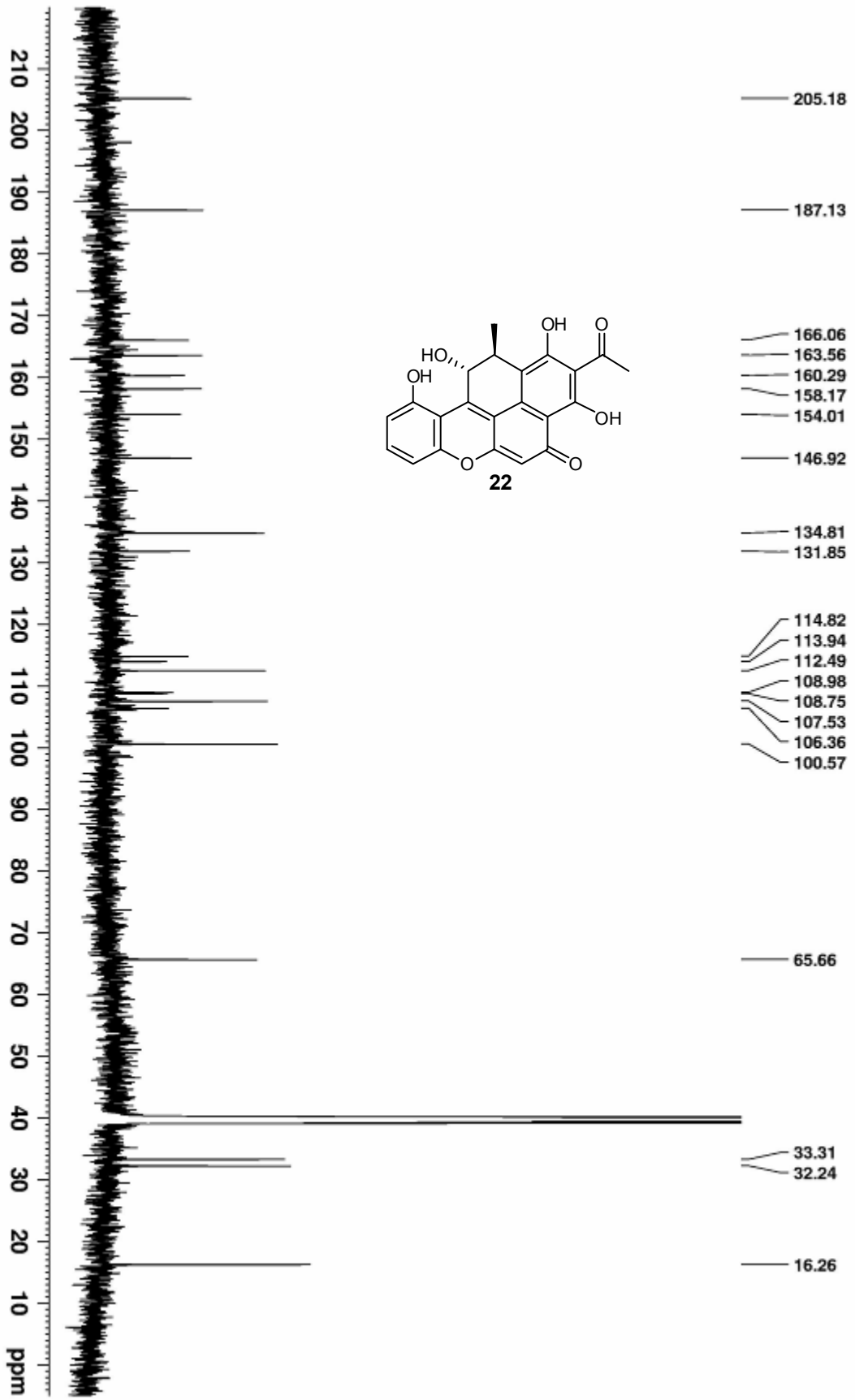

Figure S35. The ^{13}C NMR spectrum of **22** in DMSO-d_6 (125 MHz).

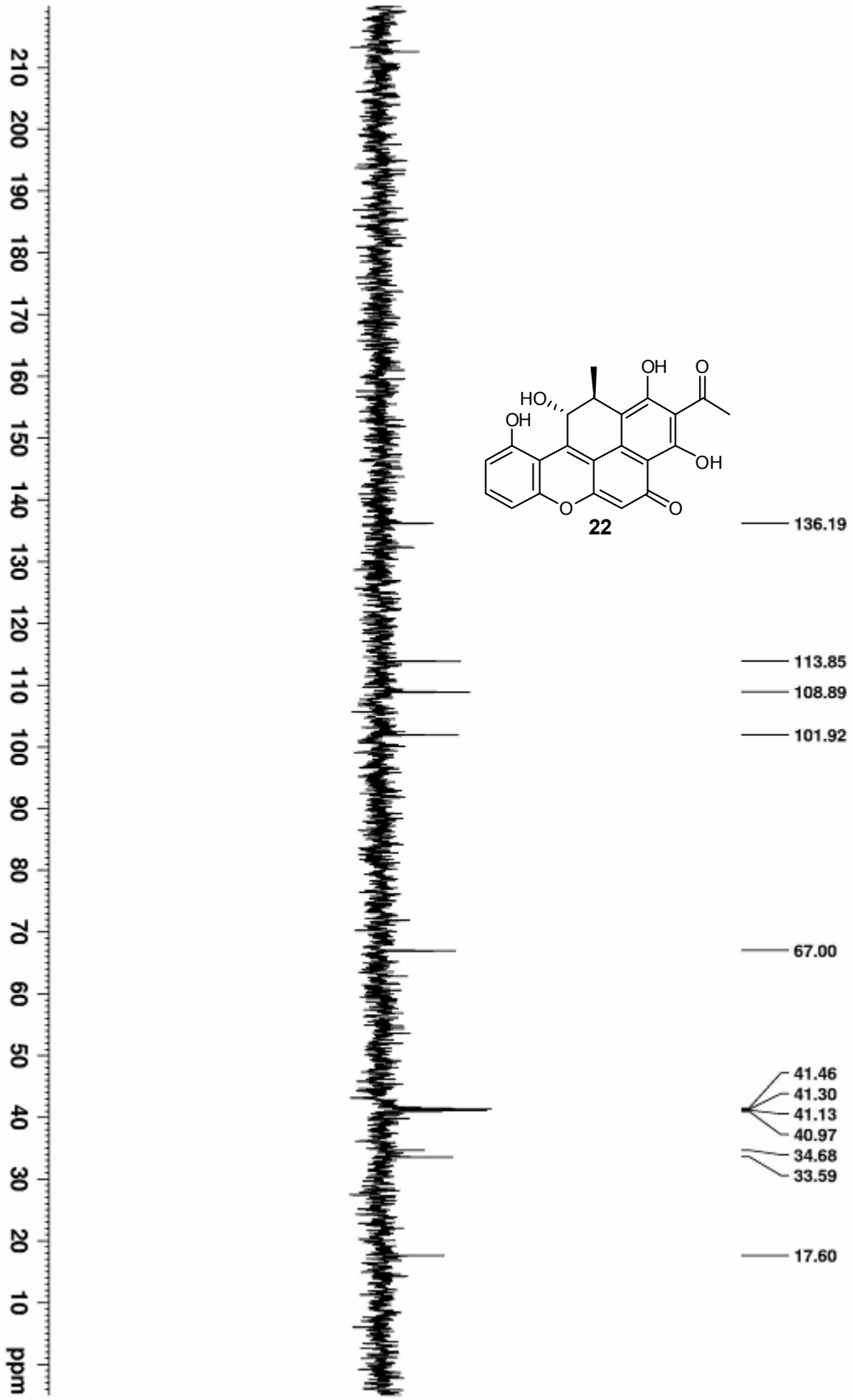

Figure S36. The DEPT135 spectrum of **22** in DMSO-d_6 (125 MHz).

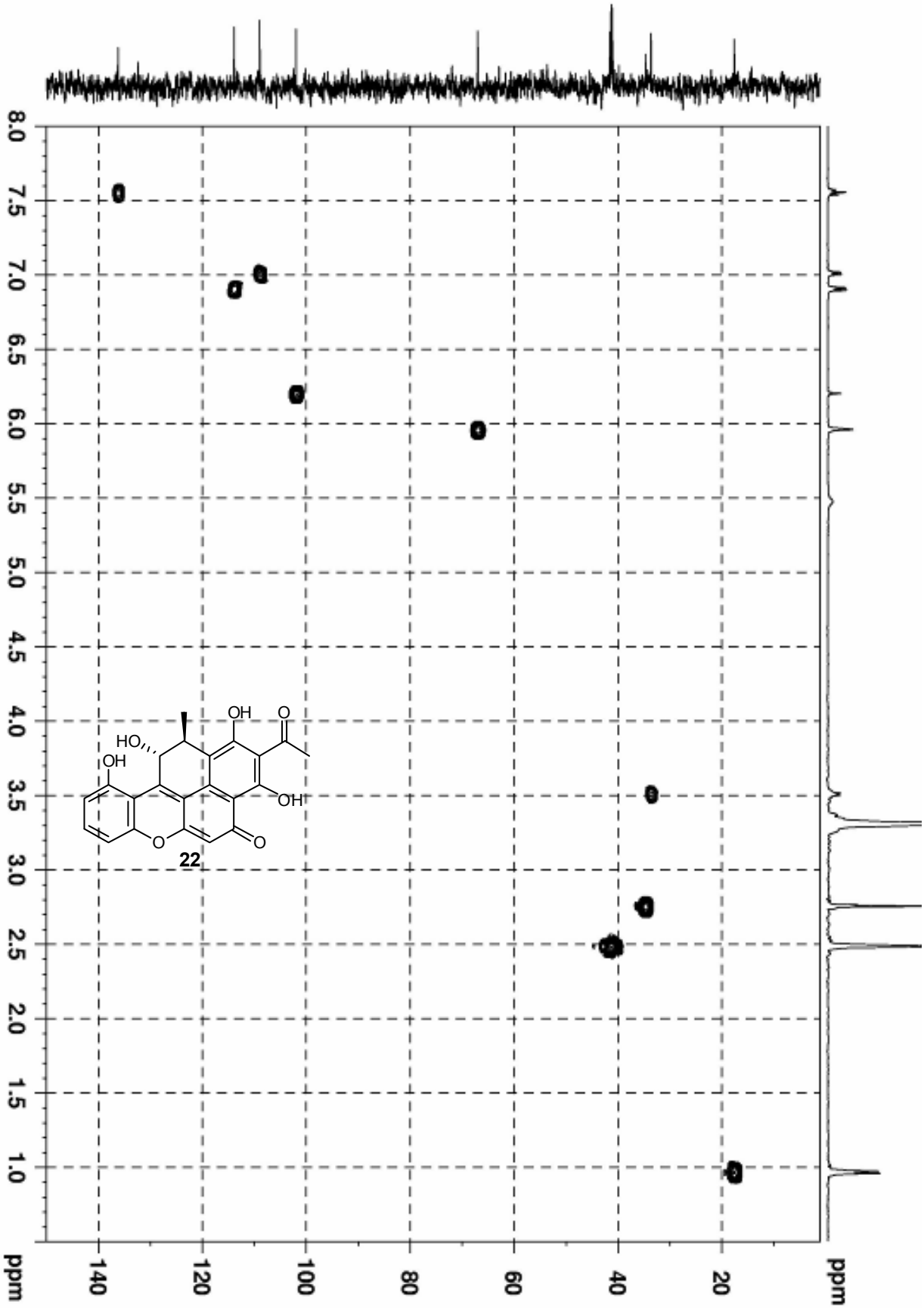

Figure S37. The HMQC spectrum of **22** in DMSO-d_6 (500 MHz).

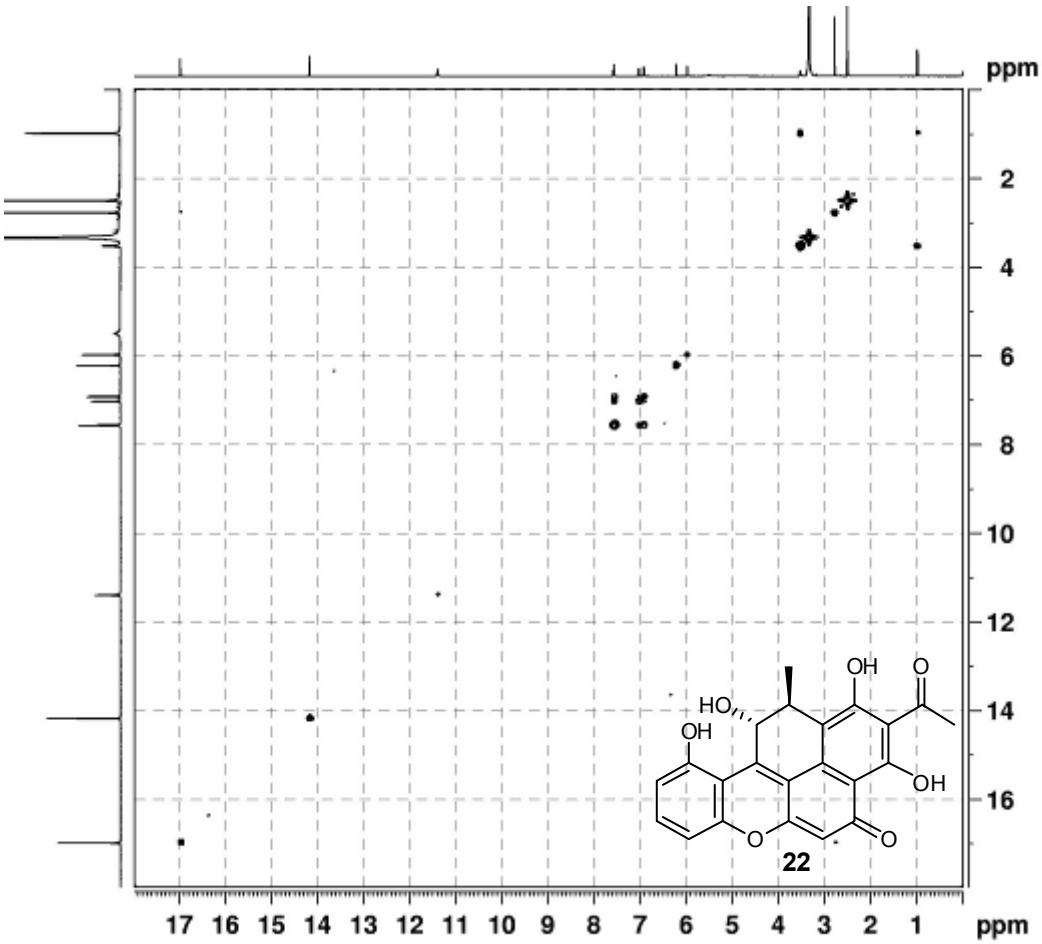

Figure S38. The ^{1}H-^{1}H COSY spectrum of **22** in DMSO-d_6 (500 MHz).

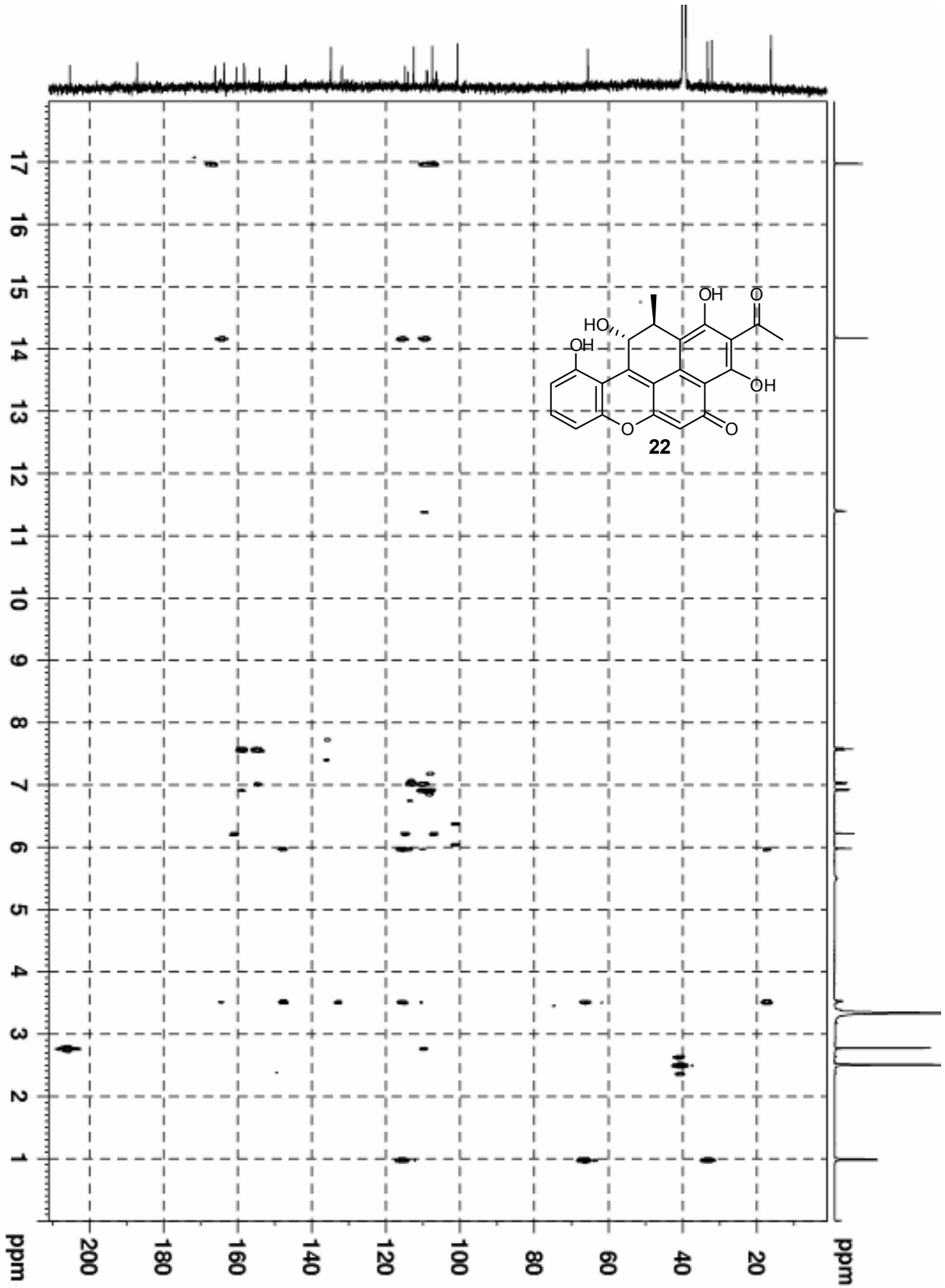

Figure S39. The HMBC spectrum of **22** in DMSO-d_6 (500MHz).

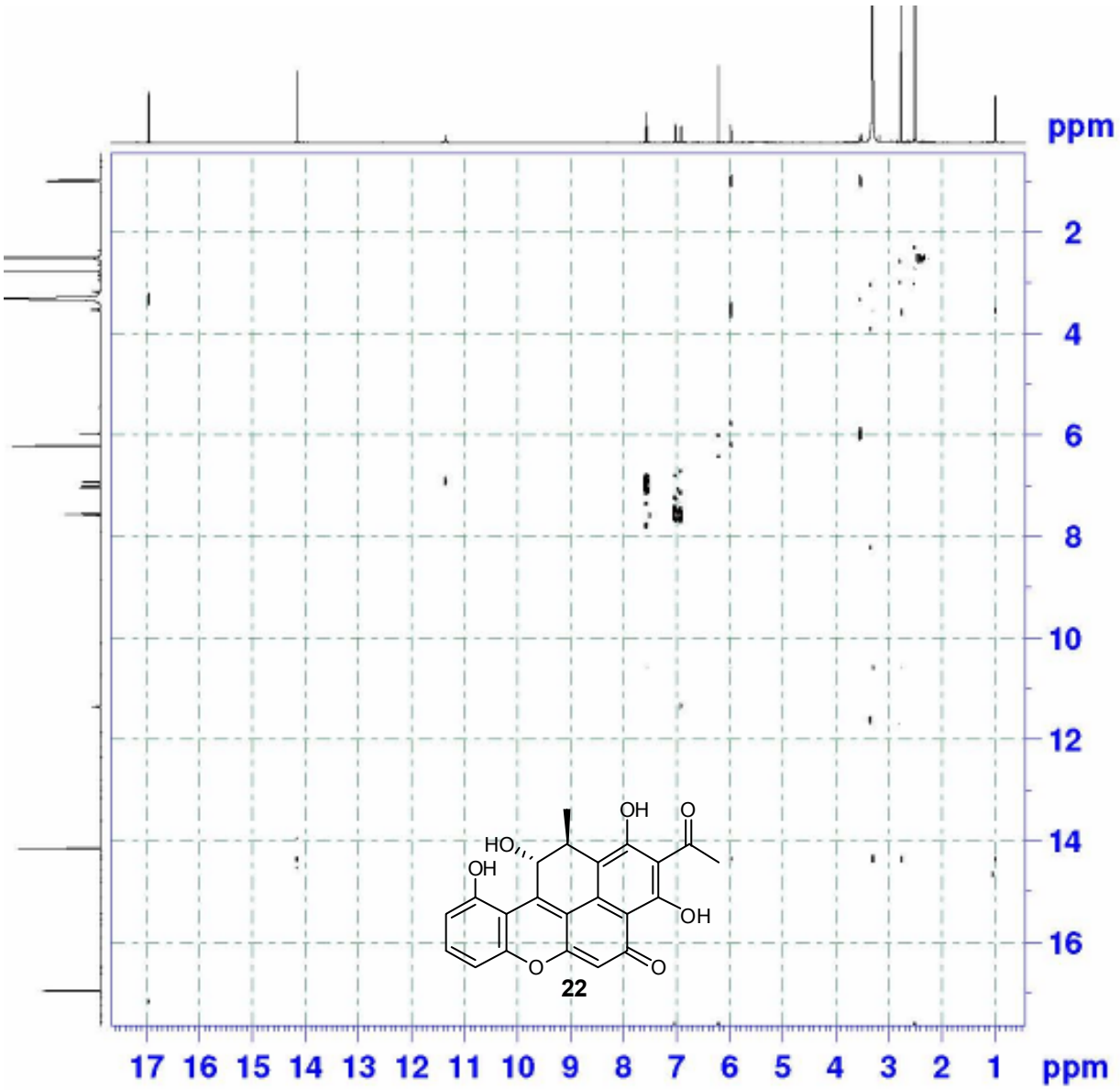

Figure S40. The ROESY spectrum of **22** in DMSO-d_6 (500MHz).

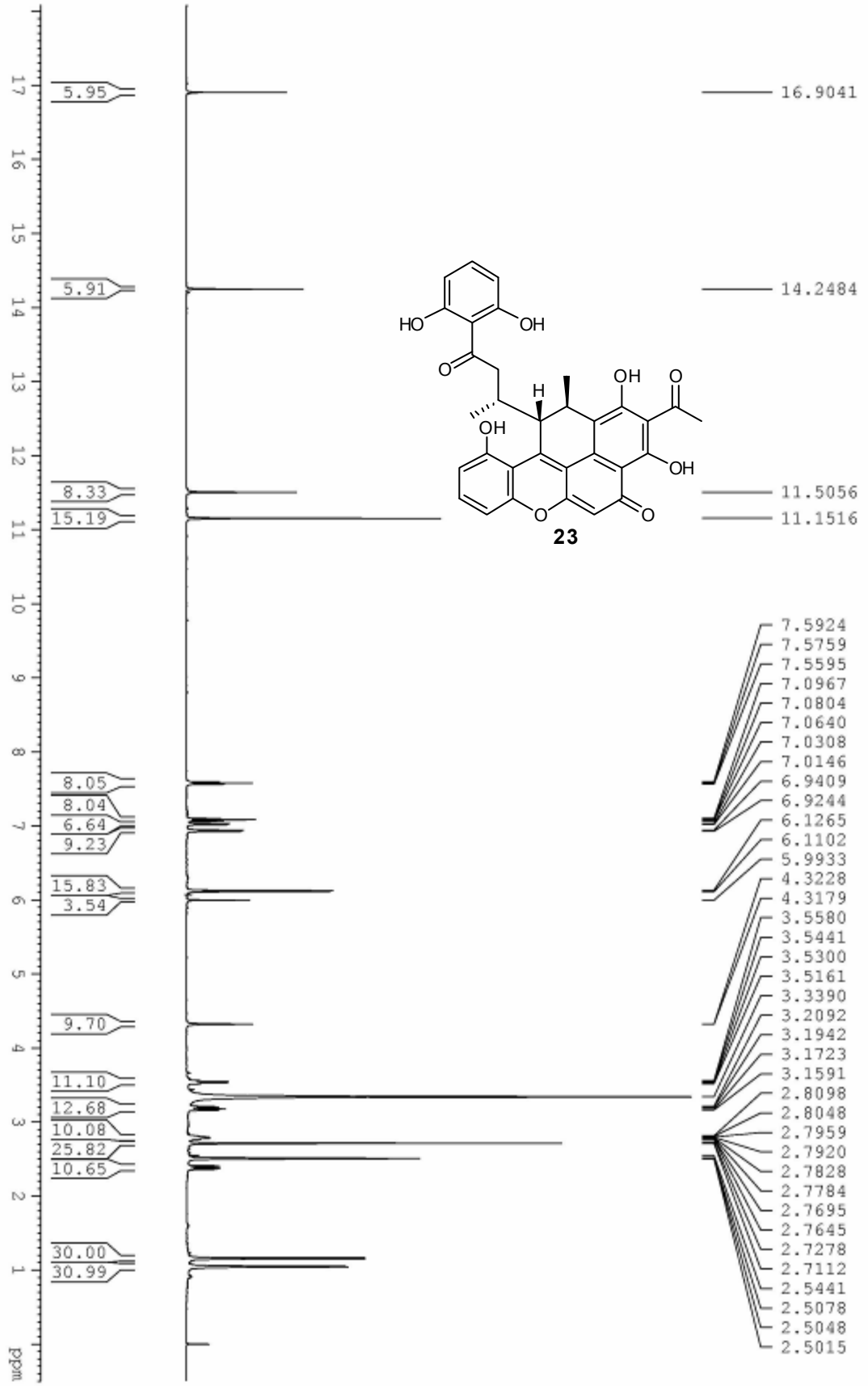

Figure S41. The ^{1}H NMR spectrum of **23** in DMSO-d_6 (500MHz).

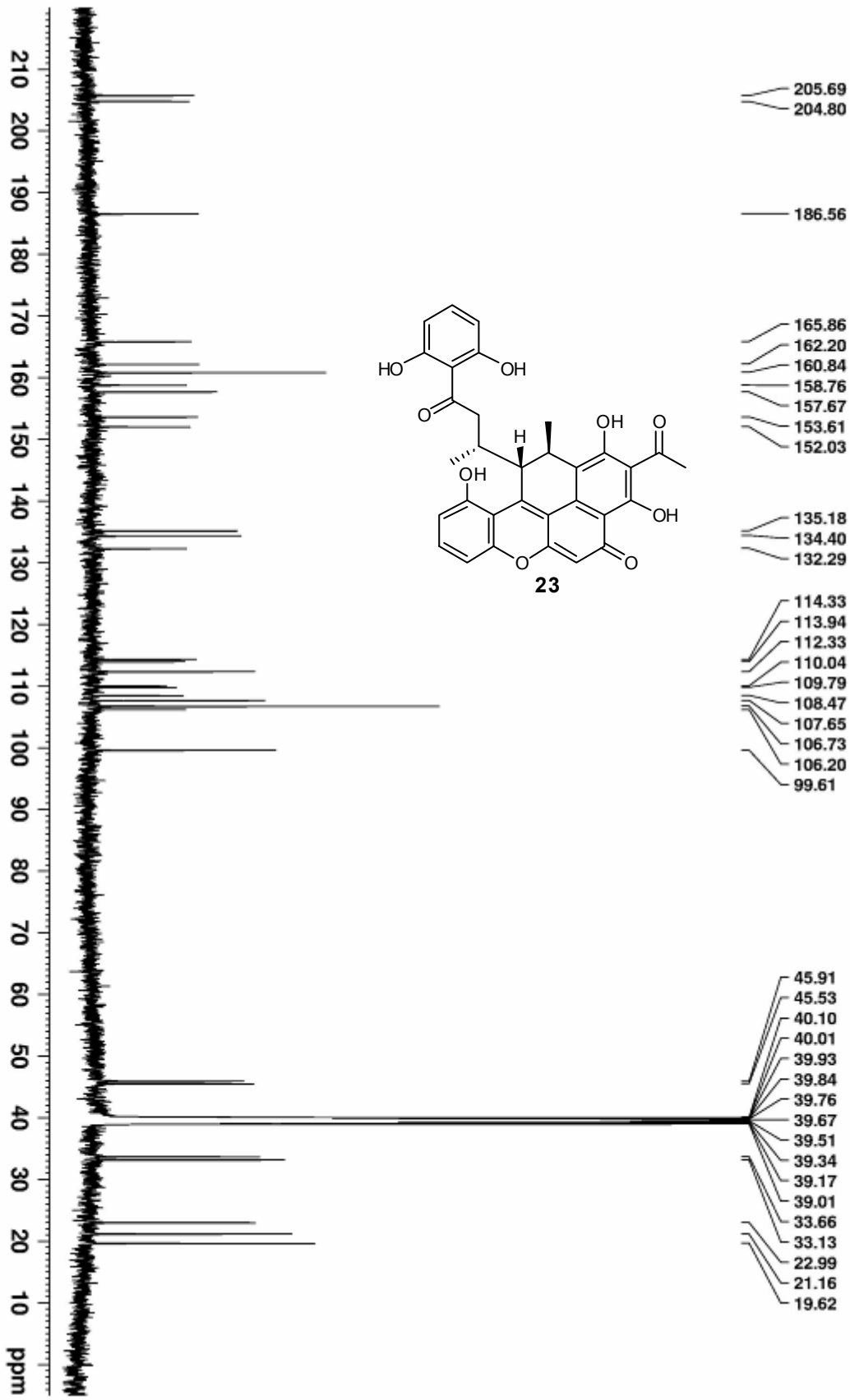

Figure S42. The ^{13}C NMR spectrum of **23** in DMSO-d_6 (125MHz).

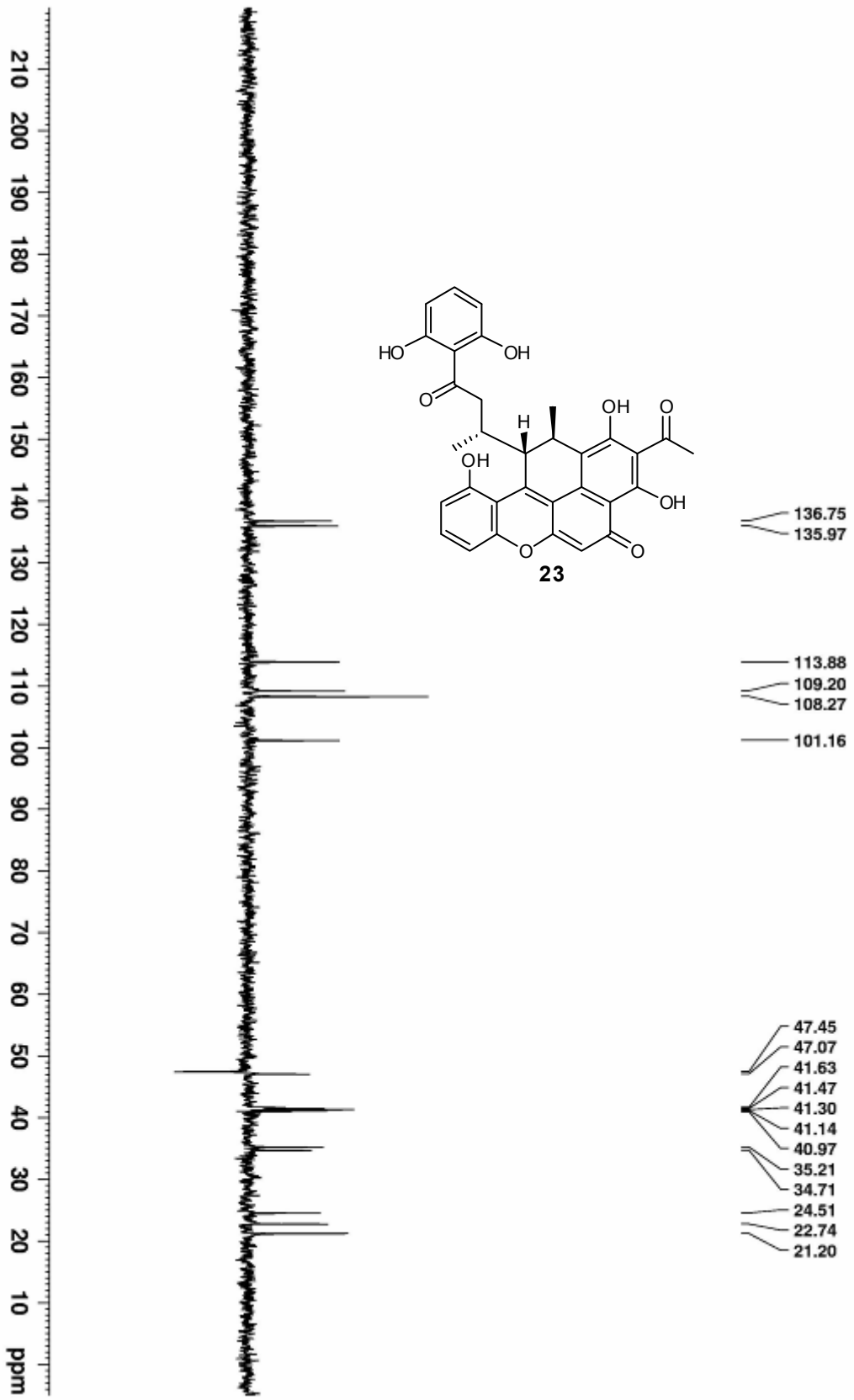

Figure S43. The DEPT135 spectrum of **23** in DMSO-d_6 (125 MHz).

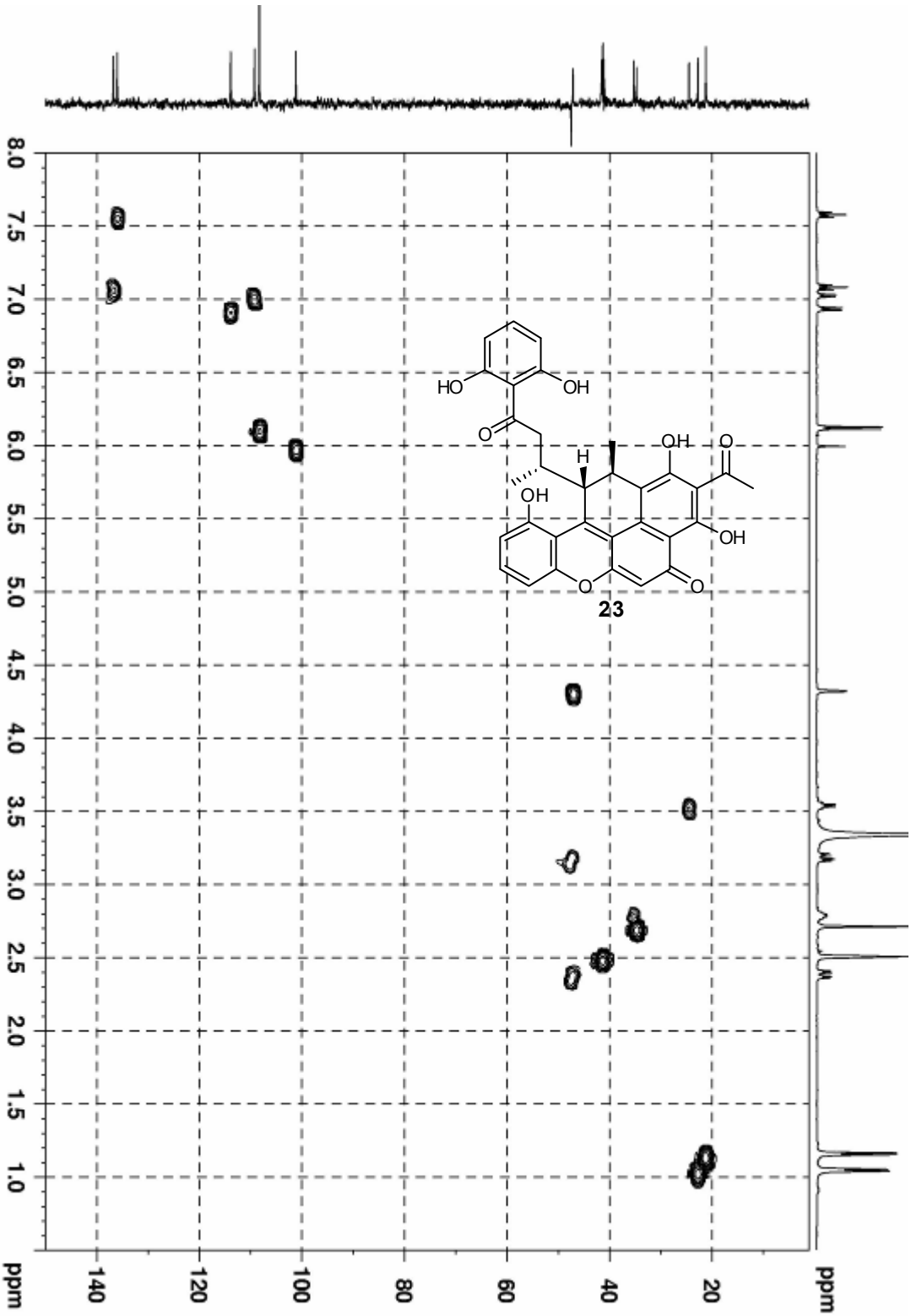

Figure S44. The HMQC spectrum of **23** in DMSO-d_6 (500MHz).

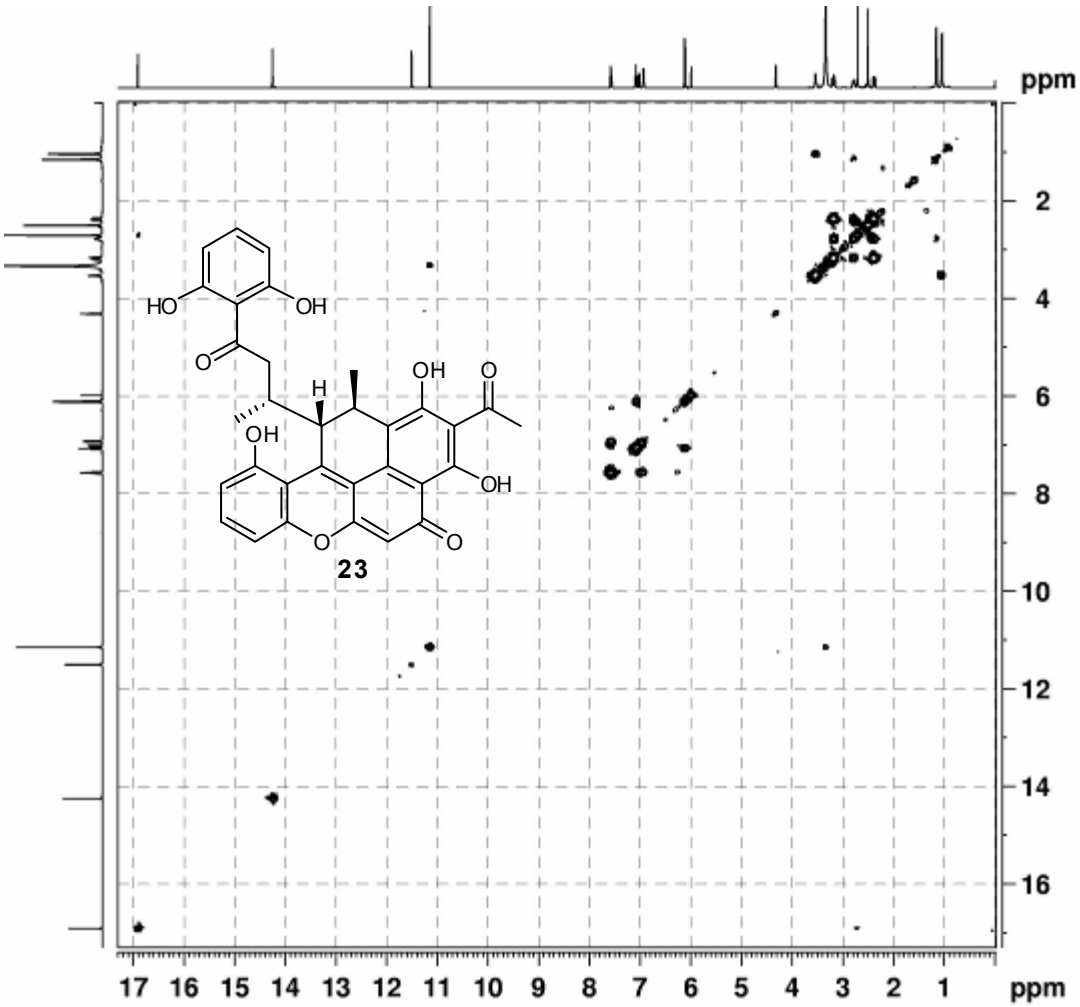

Figure S45. The ^{1}H-^{1}H COSY spectrum of **23** in DMSO-d_6 (500MHz).

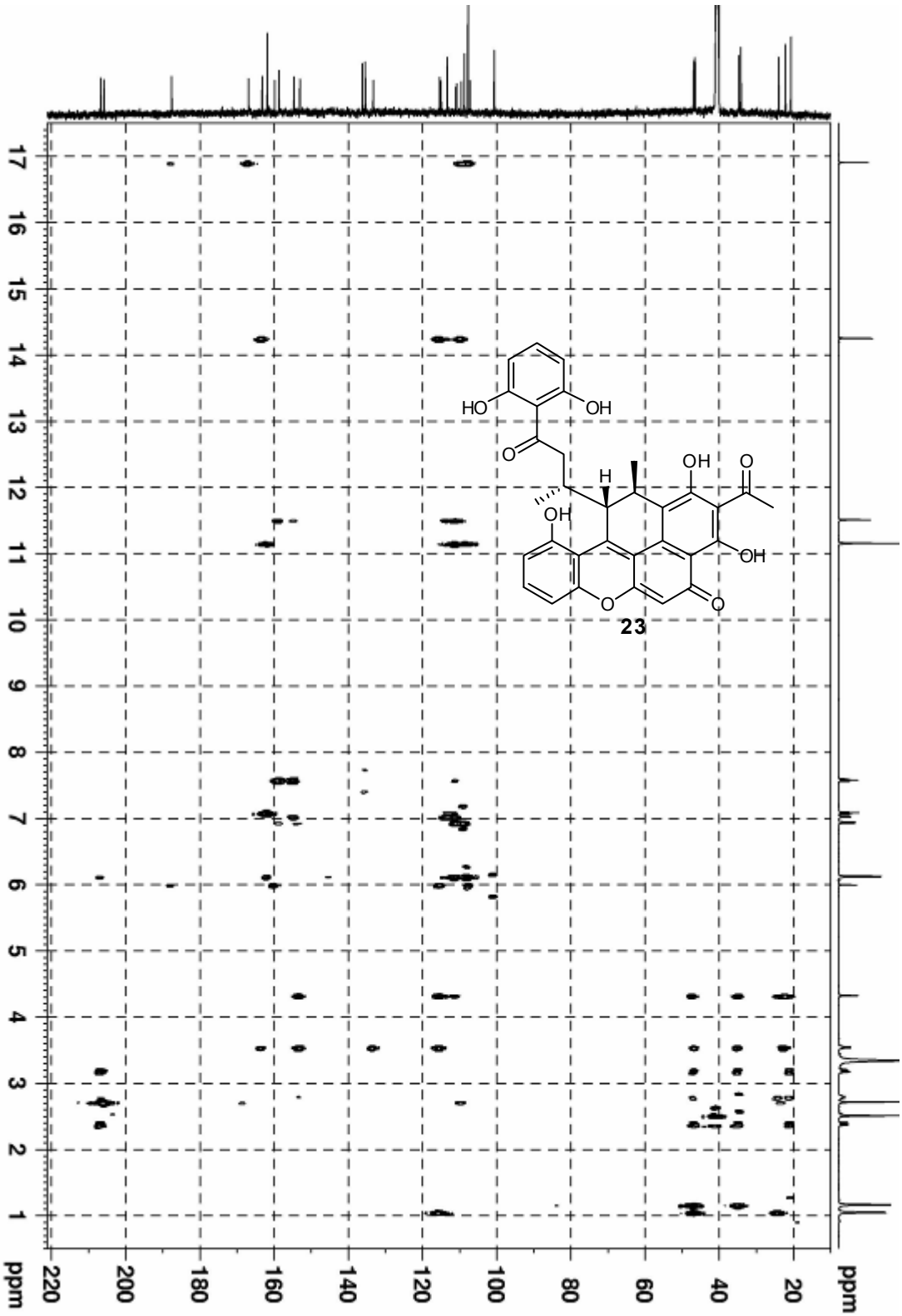

Figure S46. The HMBC spectrum of **23** in DMSO-d_6 (500MHz).

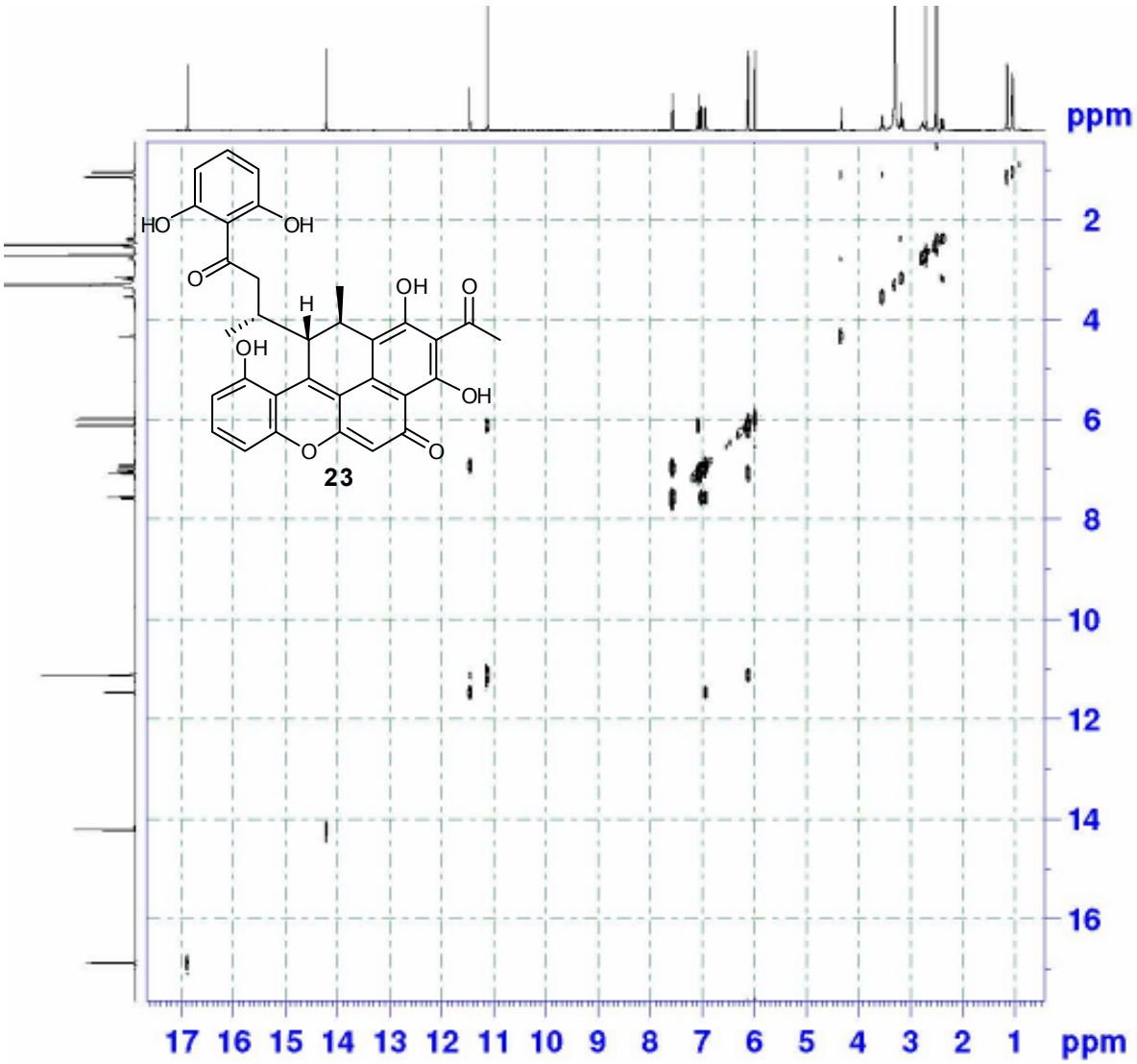

Figure S47. The ROESY spectrum of **23** in DMSO-d_6 (500MHz).

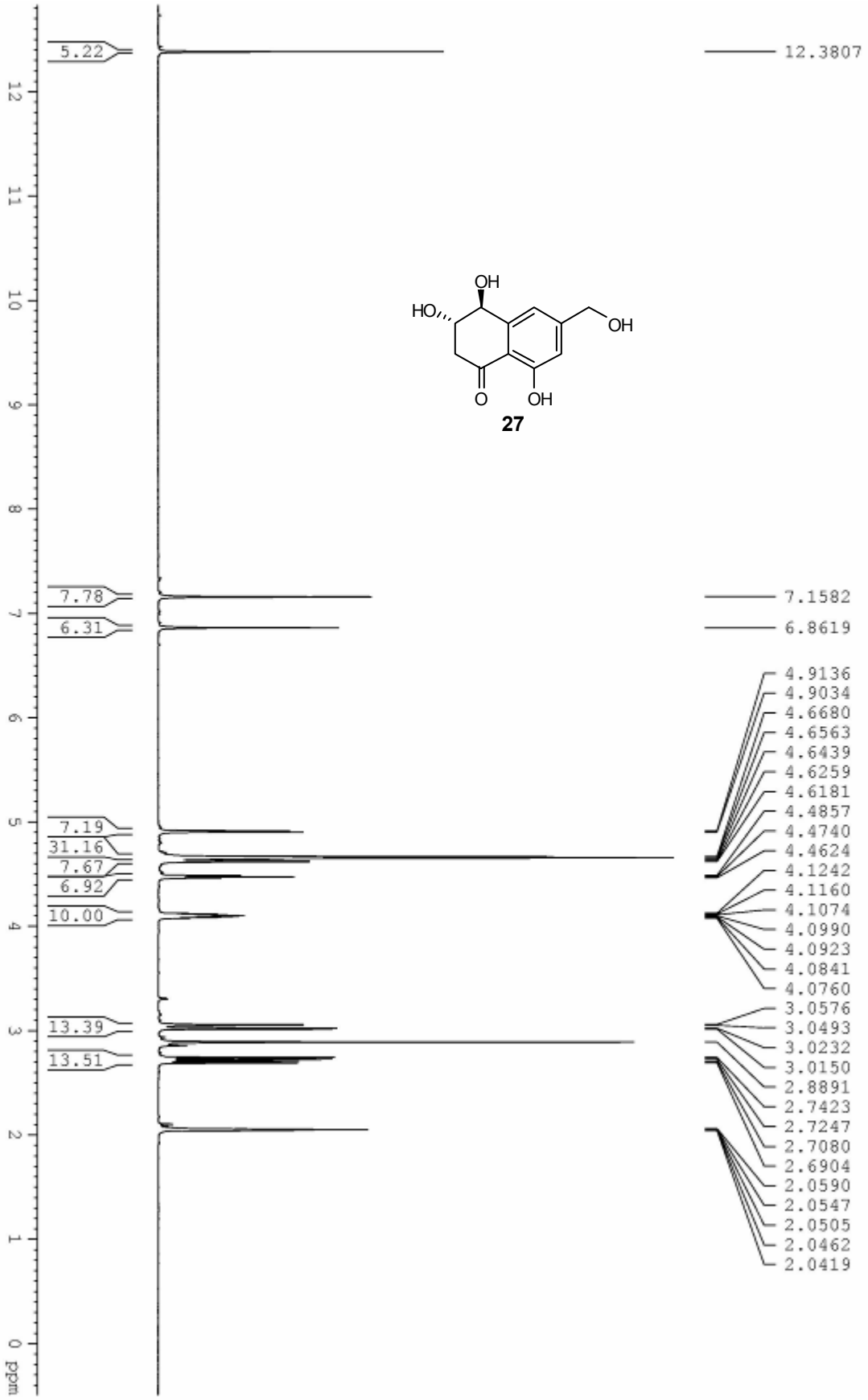

Figure S48. The ^{1}H NMR spectrum of **27** in acetone-d_6 (500 MHz).

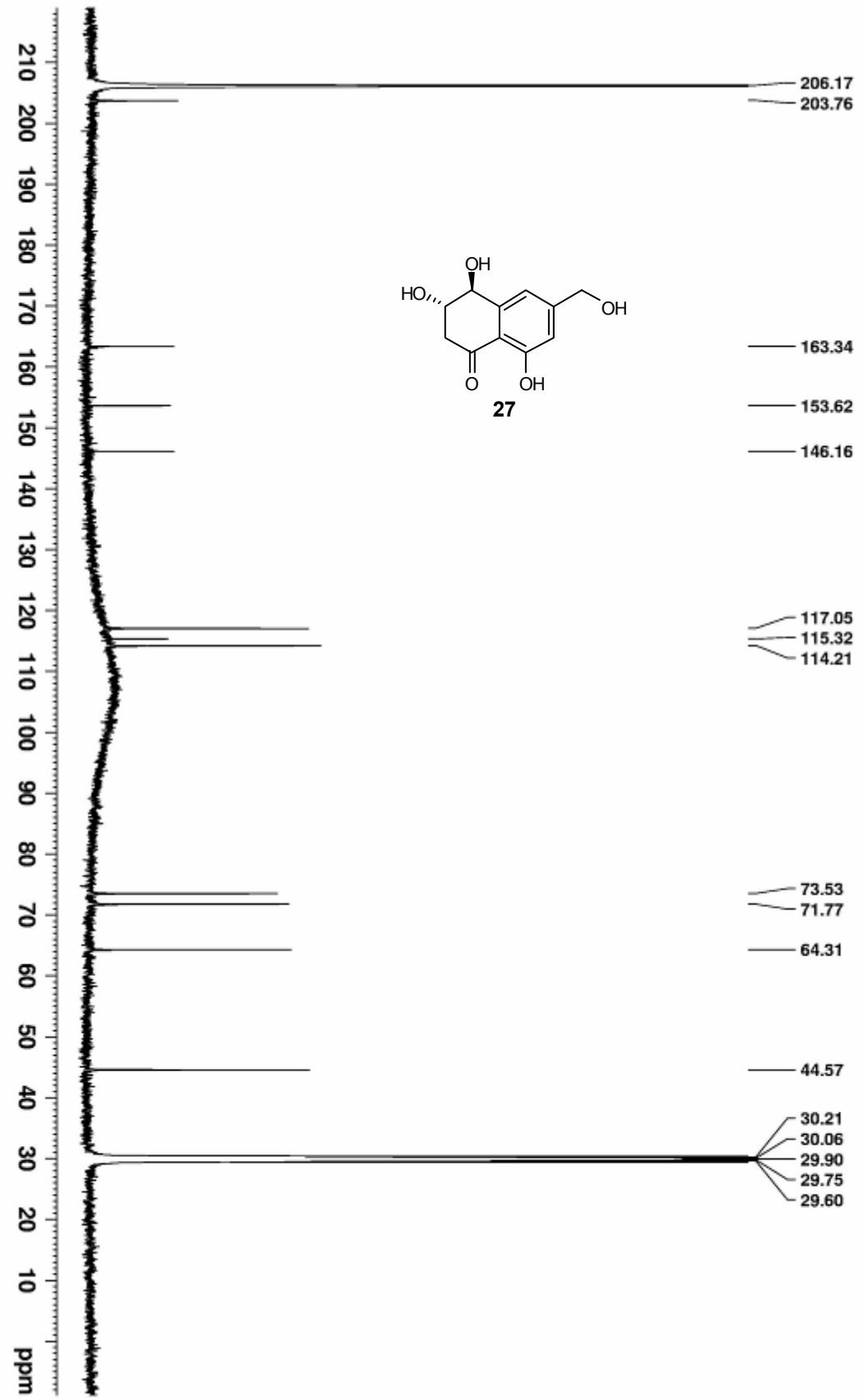

Figure S49. The ^{13}C NMR spectrum of **27** in acetone-d_6 (125 MHz).

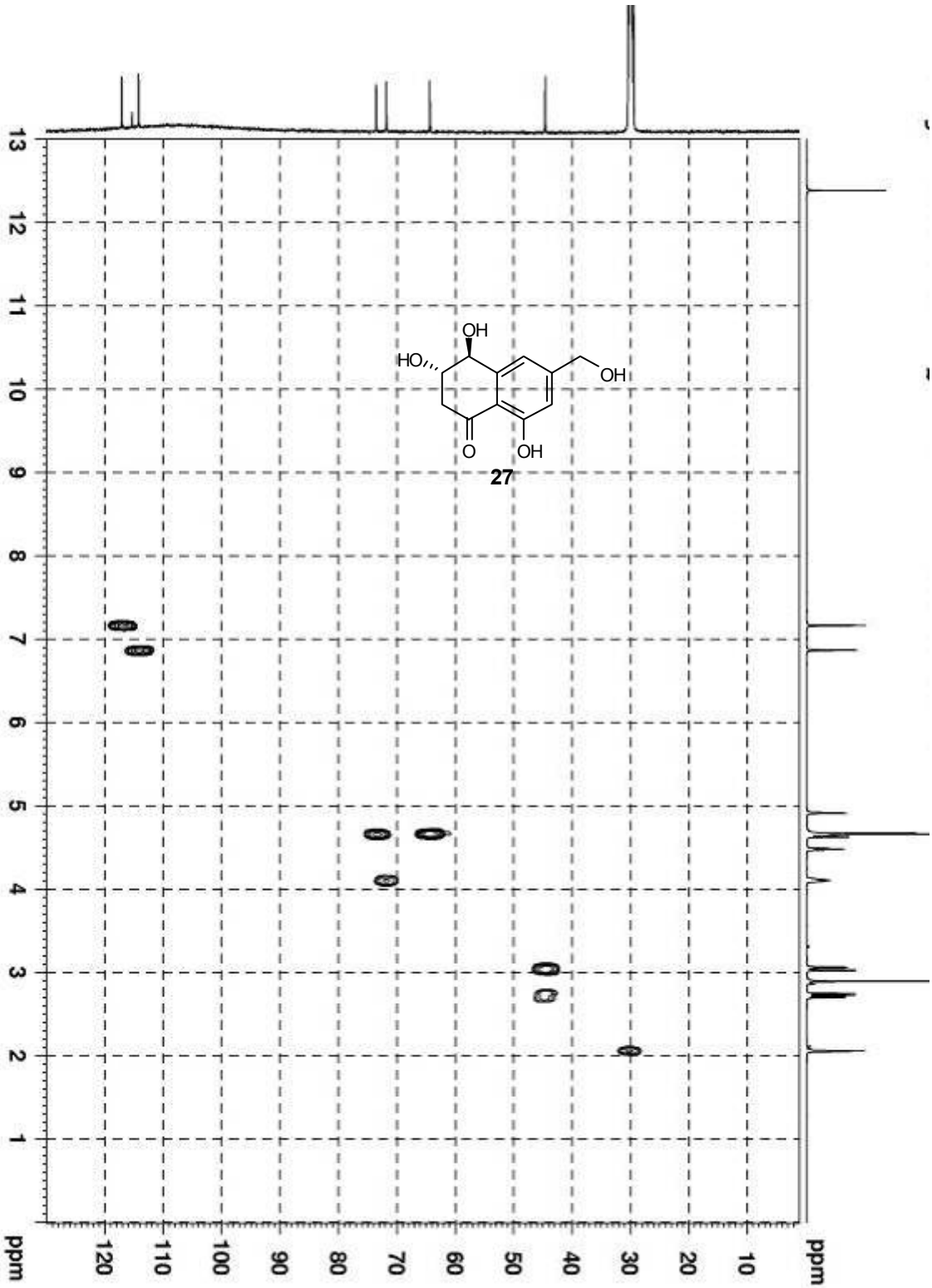

Figure S50. The HMQC spectrum of **27** in acetone-d_6 (500 MHz).

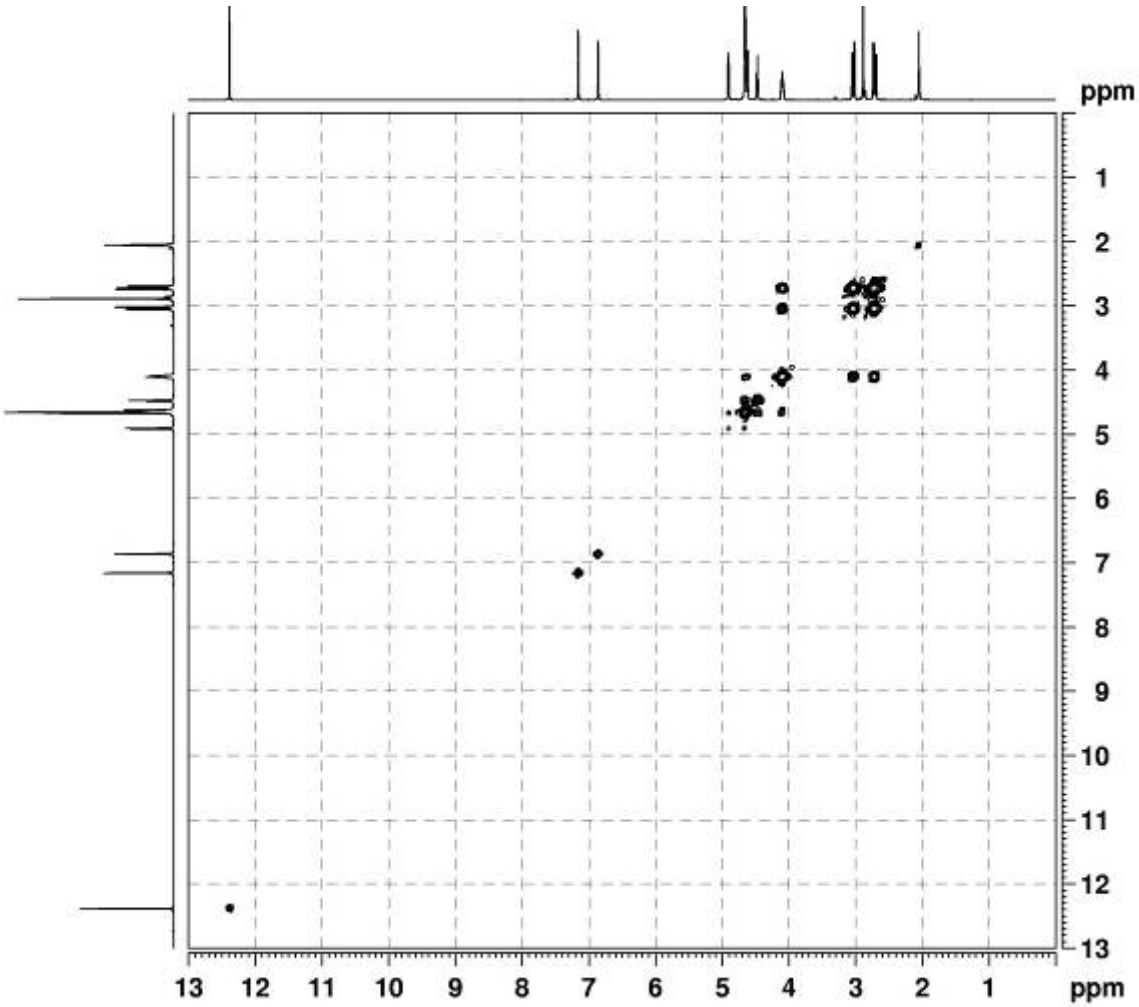

Figure S51. The ^{1}H-^{1}H COSY spectrum of **27** in acetone-d_6 (500 MHz).

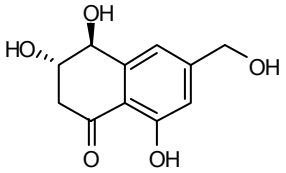

27

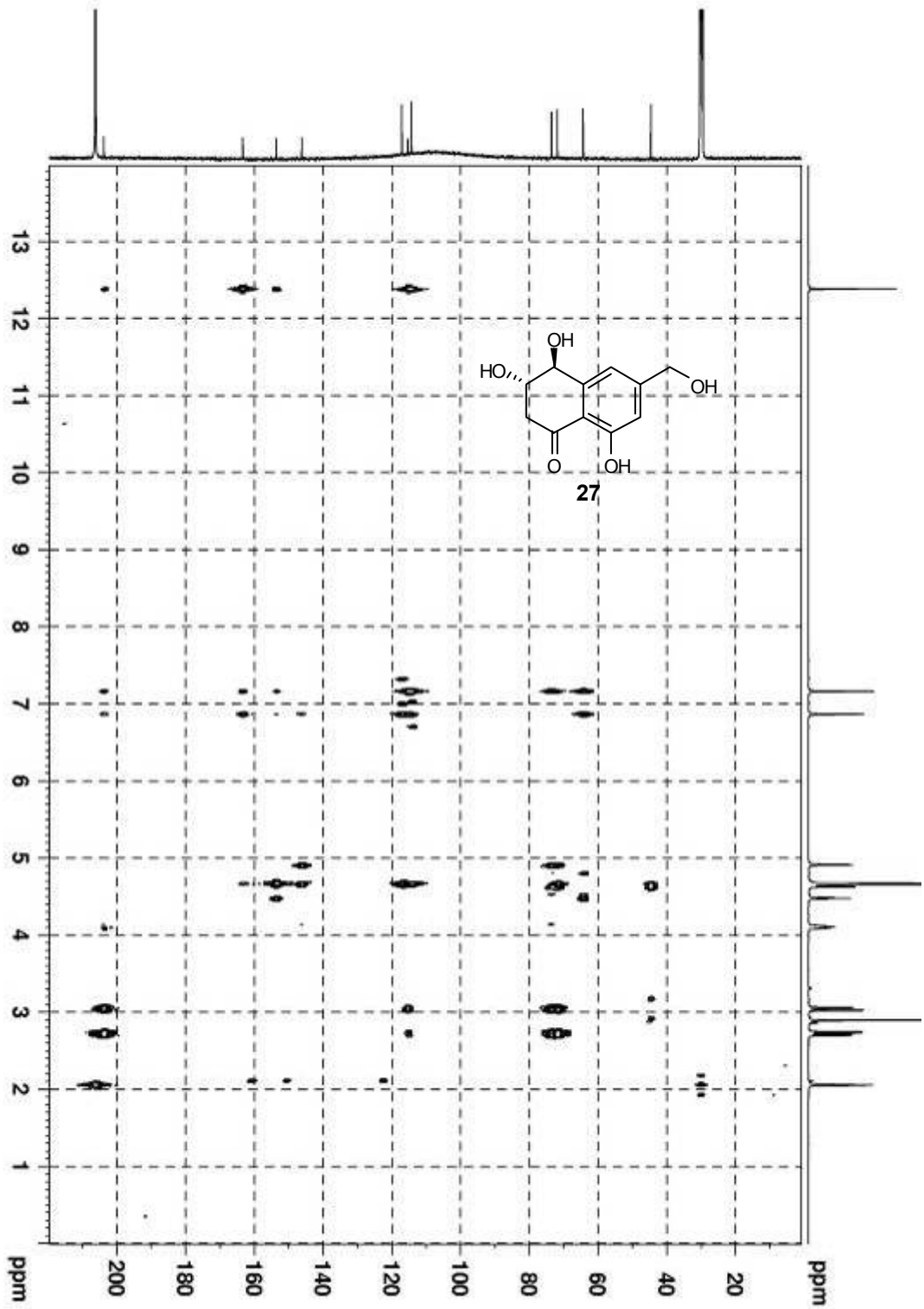

Figure S52. The HMBC spectrum of **27** in acetone-d_6 (500 MHz).

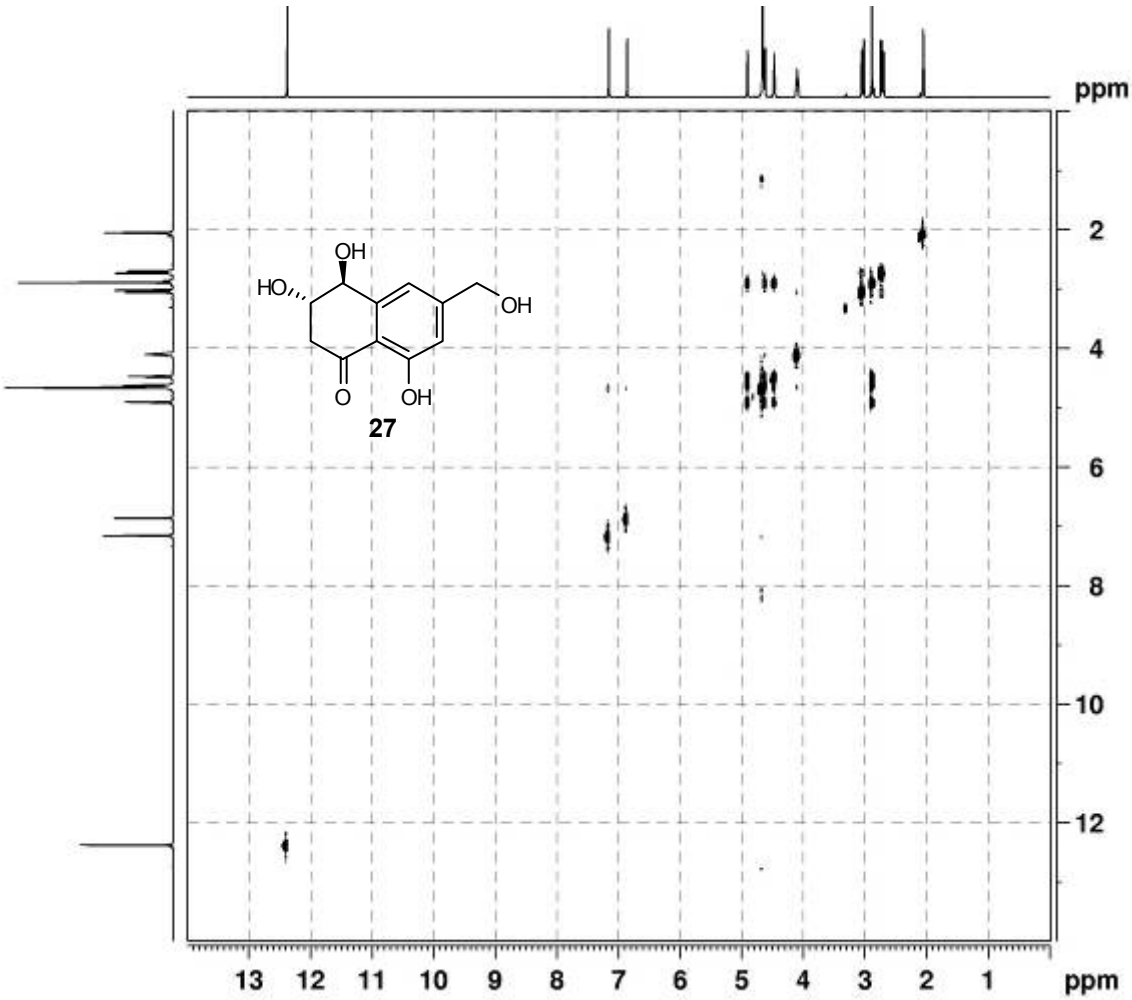

Figure S53. The NOESY spectrum of **27** in acetone-d_6 (500 MHz).

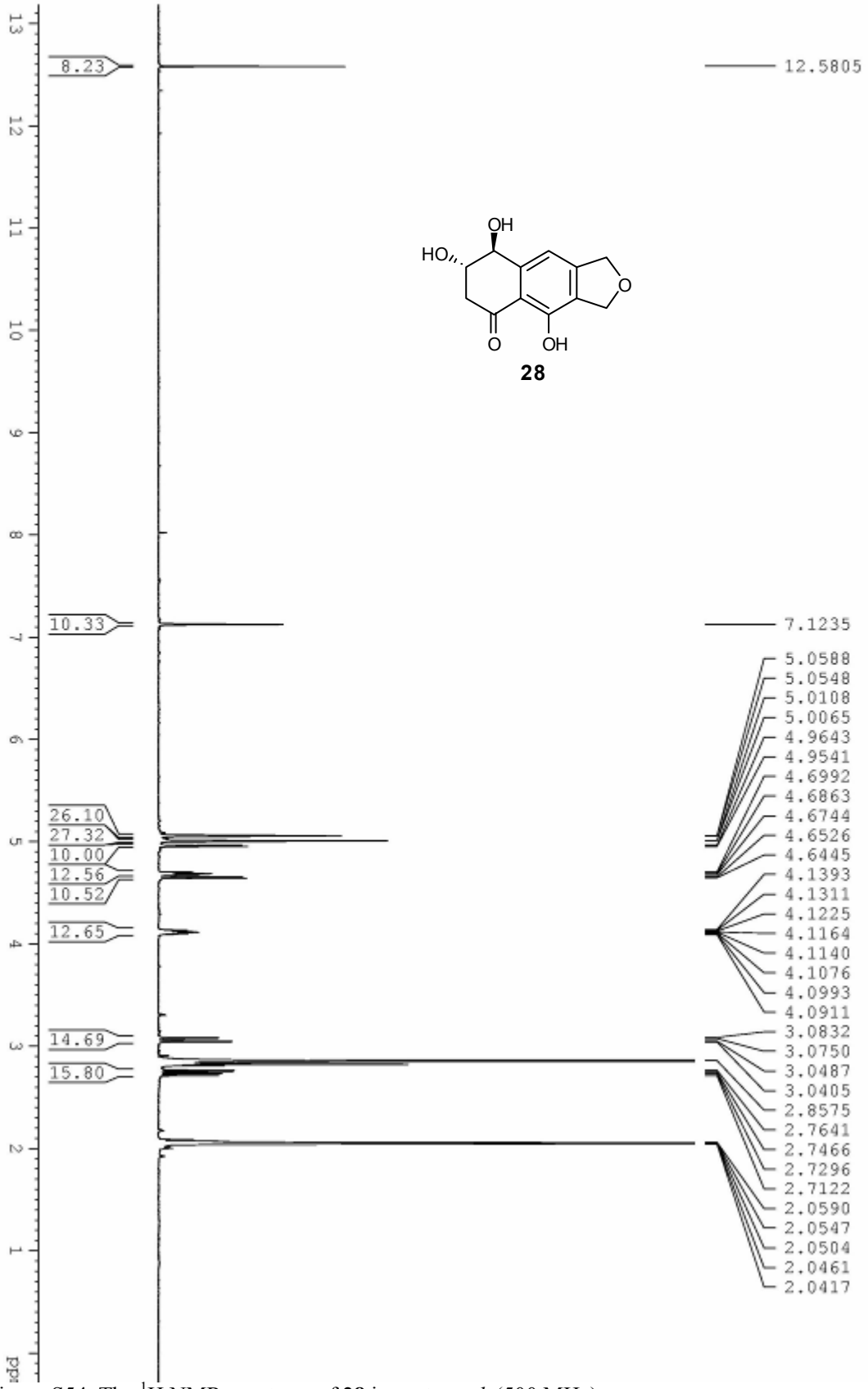

Figure S54. The ^{1}H NMR spectrum of **28** in acetone-d_6 (500 MHz).

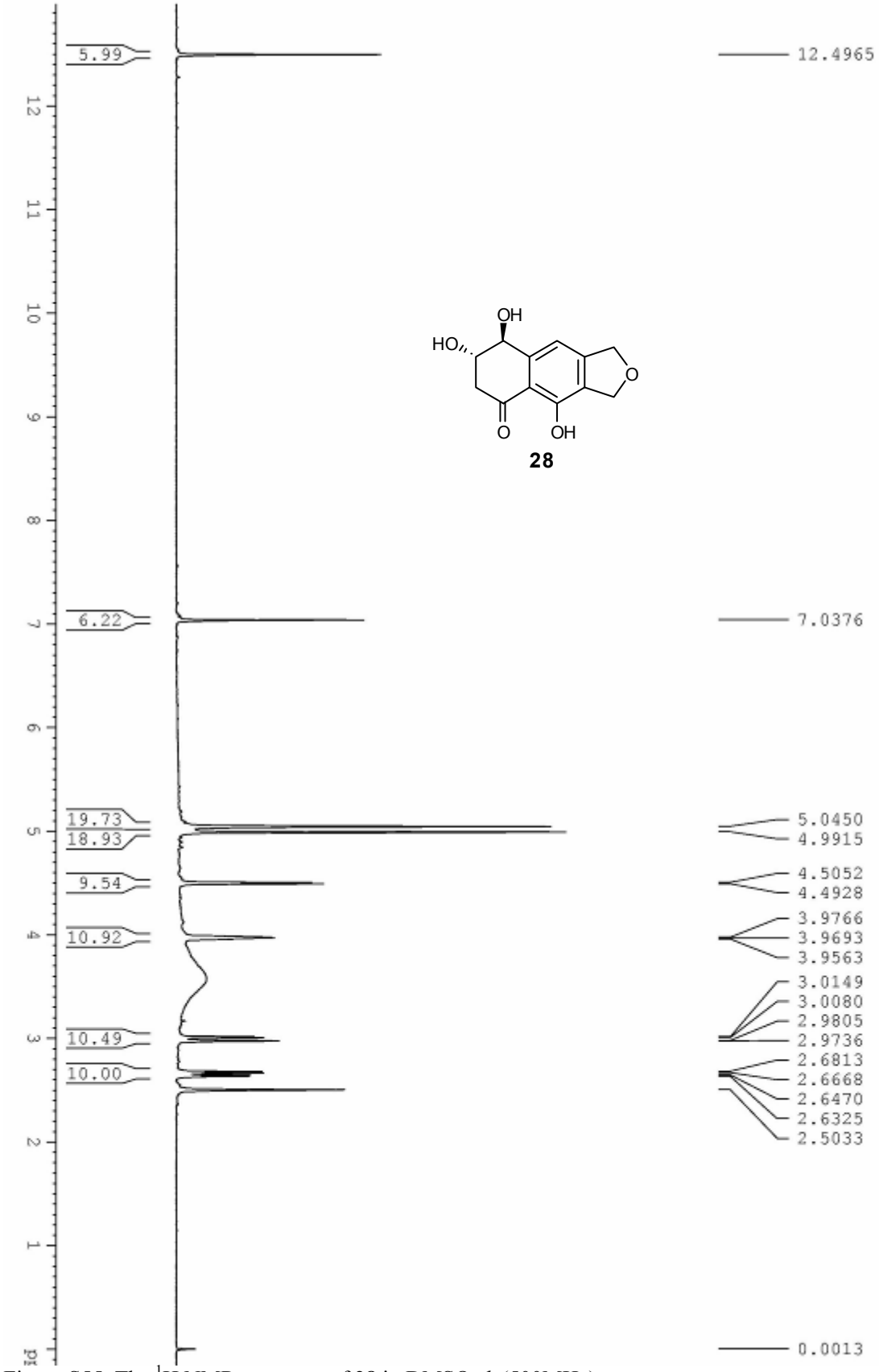

Figure S55. The ^{1}H NMR spectrum of **28** in DMSO-d_6 (500MHz).

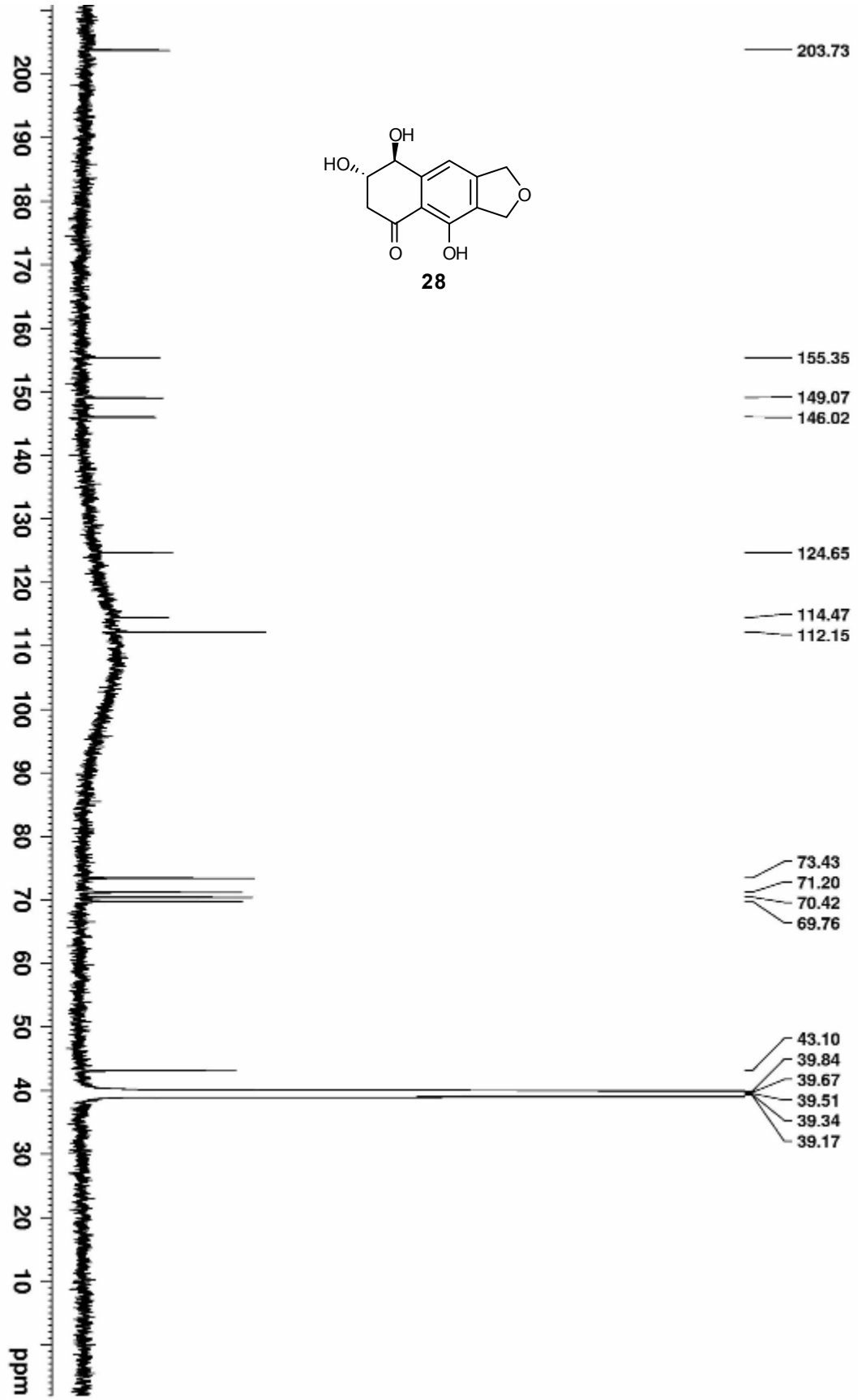

Figure S56. The ^{13}C NMR spectrum of **28** in DMSO-d_6 (125 MHz).

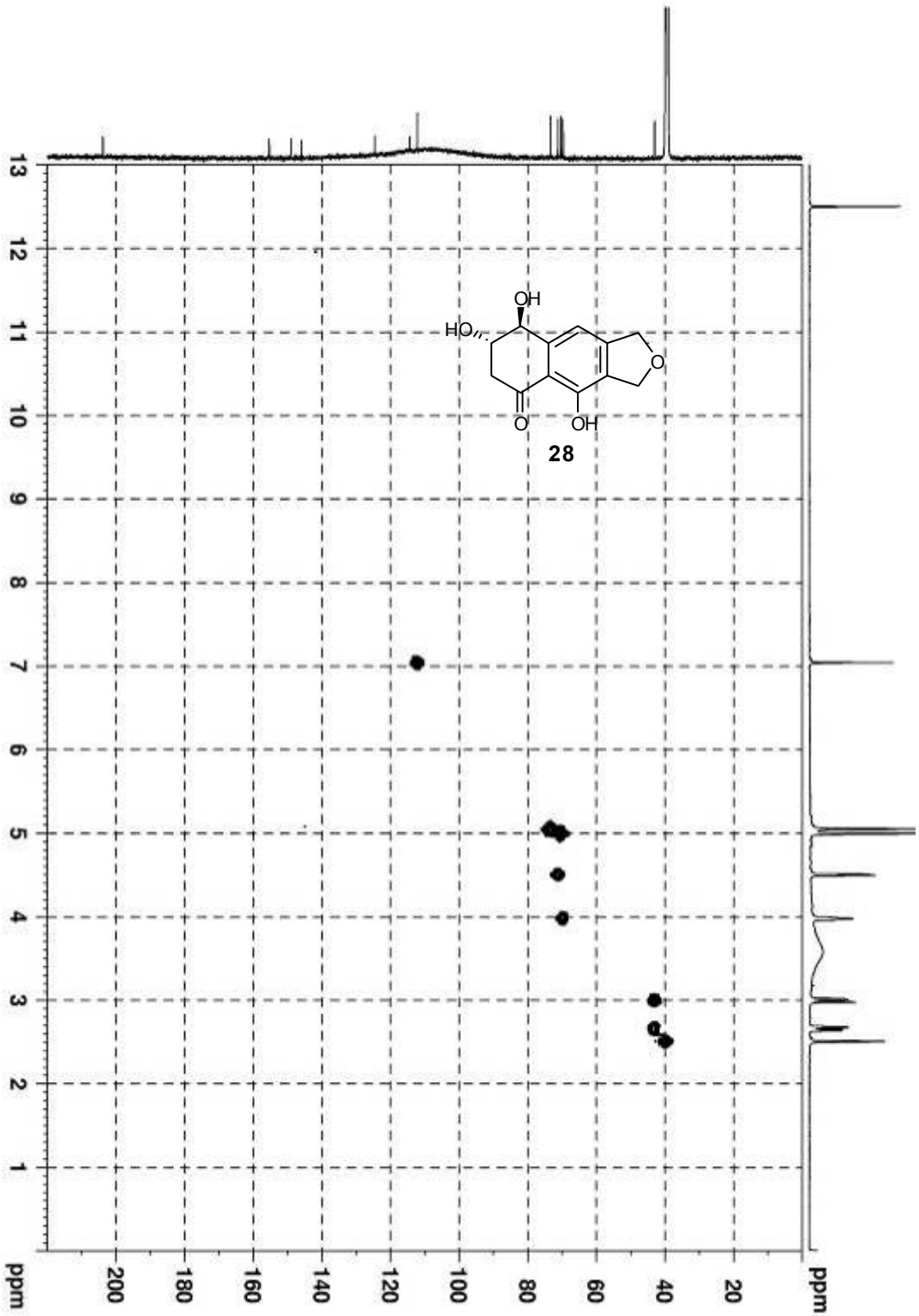

Figure S57. The HMQC spectrum of **28** in DMSO-d_6 (500 MHz).

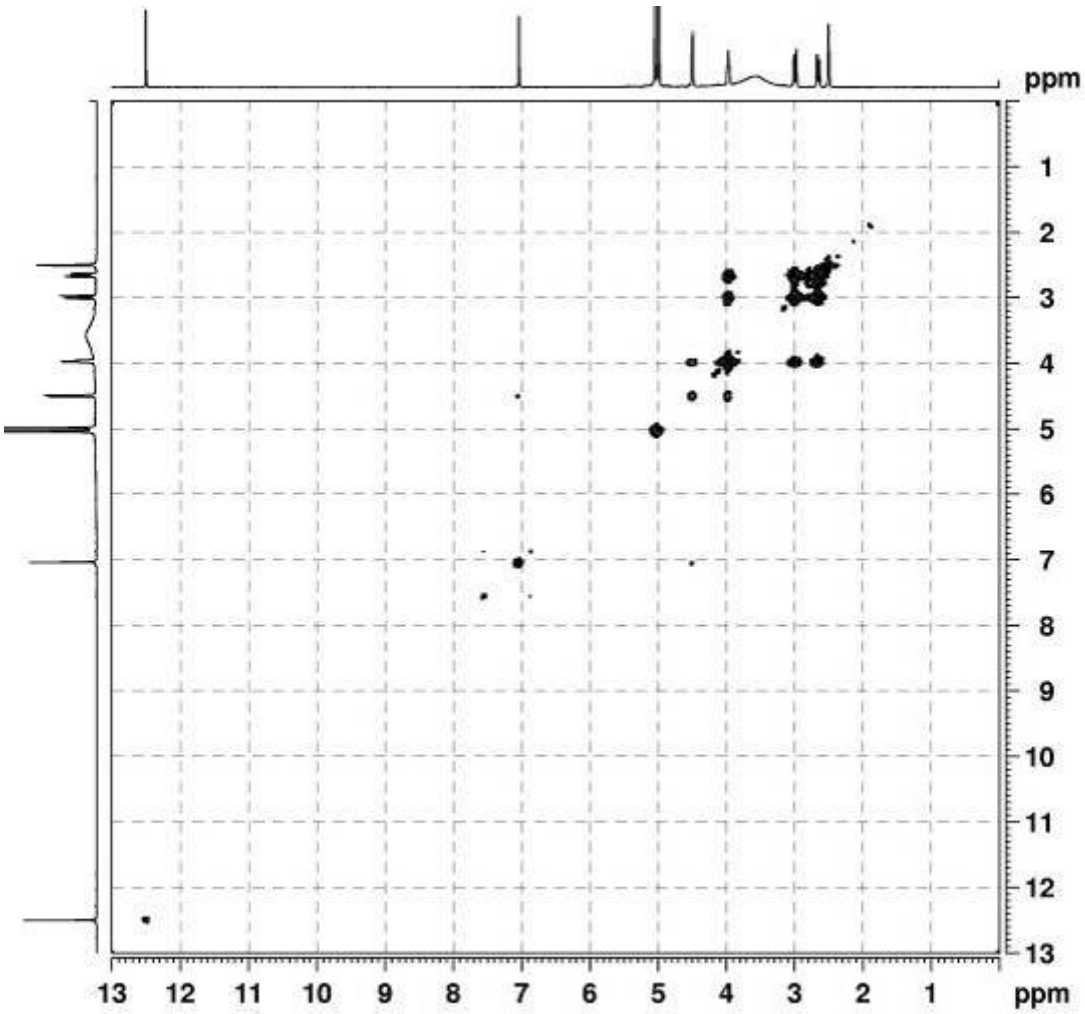

Figure S58. The ^{1}H-^{1}H COSY spectrum of **28** in DMSO-d_6 (500 MHz).

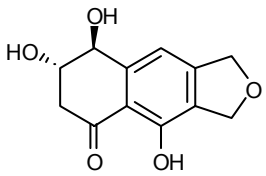

28

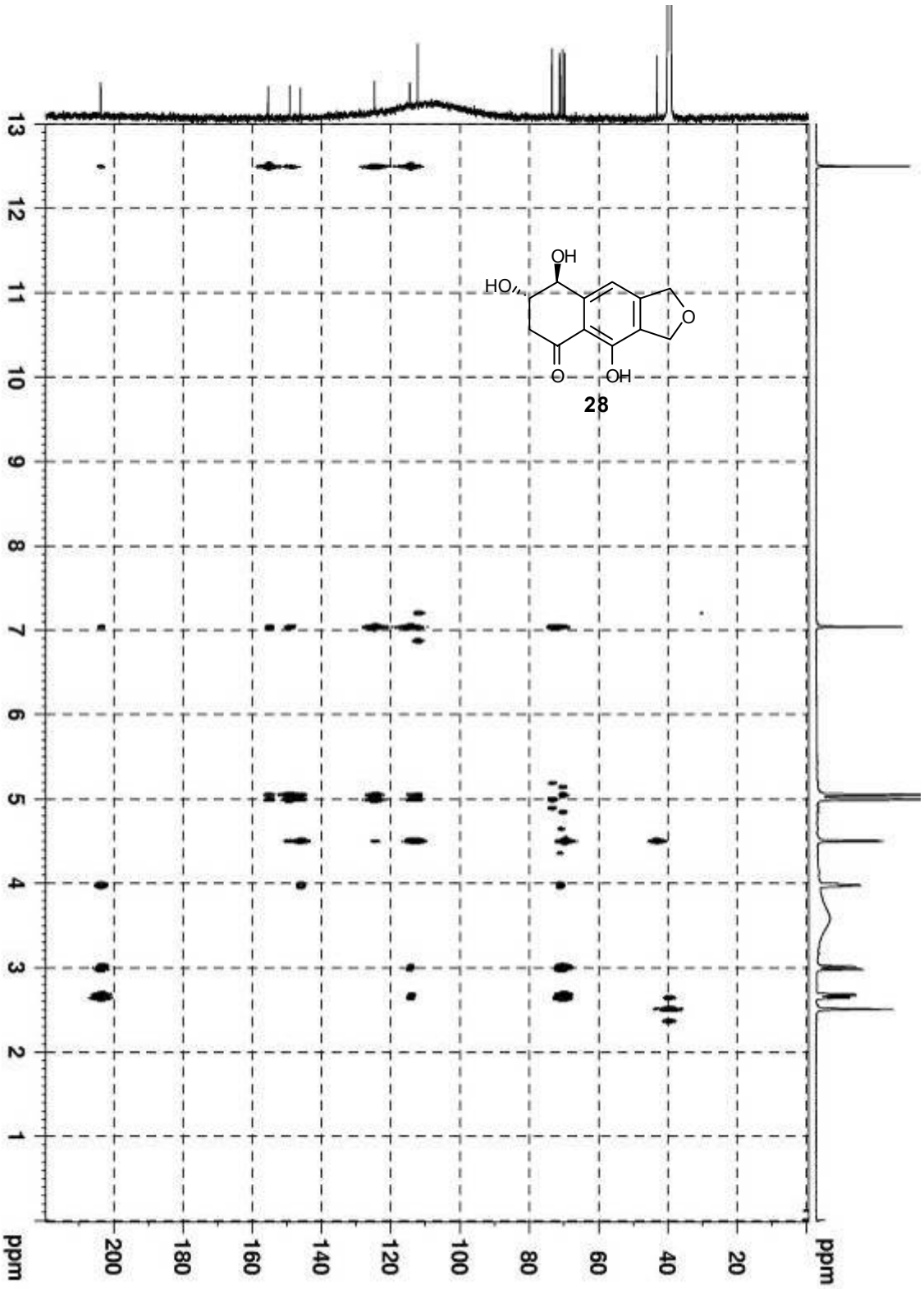

Figure S59. The HMBC spectrum of **28** in DMSO-d_6 (500 MHz).

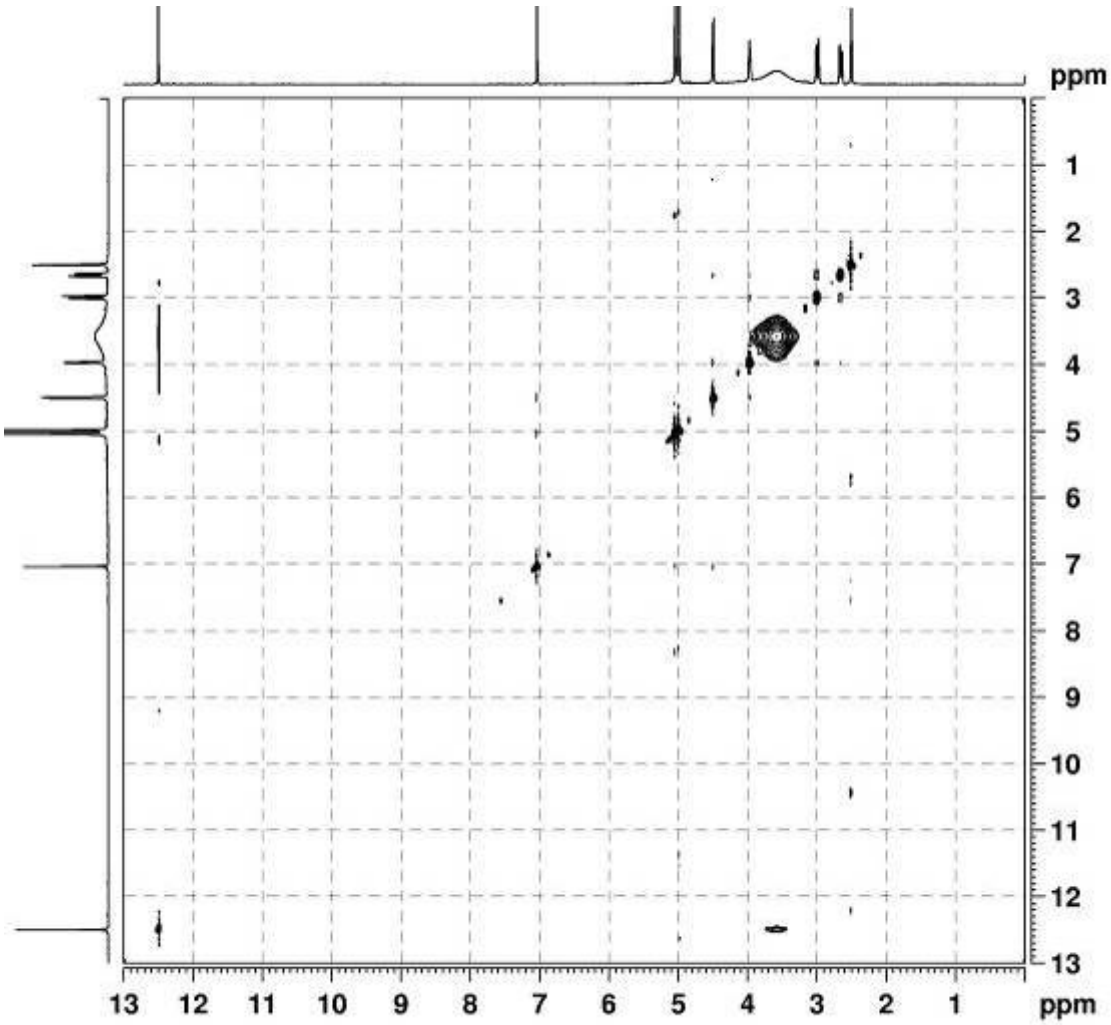

Figure S60. The NOESY spectrum of **28** in DMSO-d_6 (500 MHz).

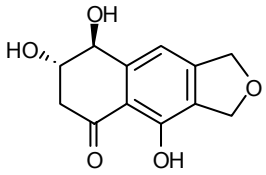

28

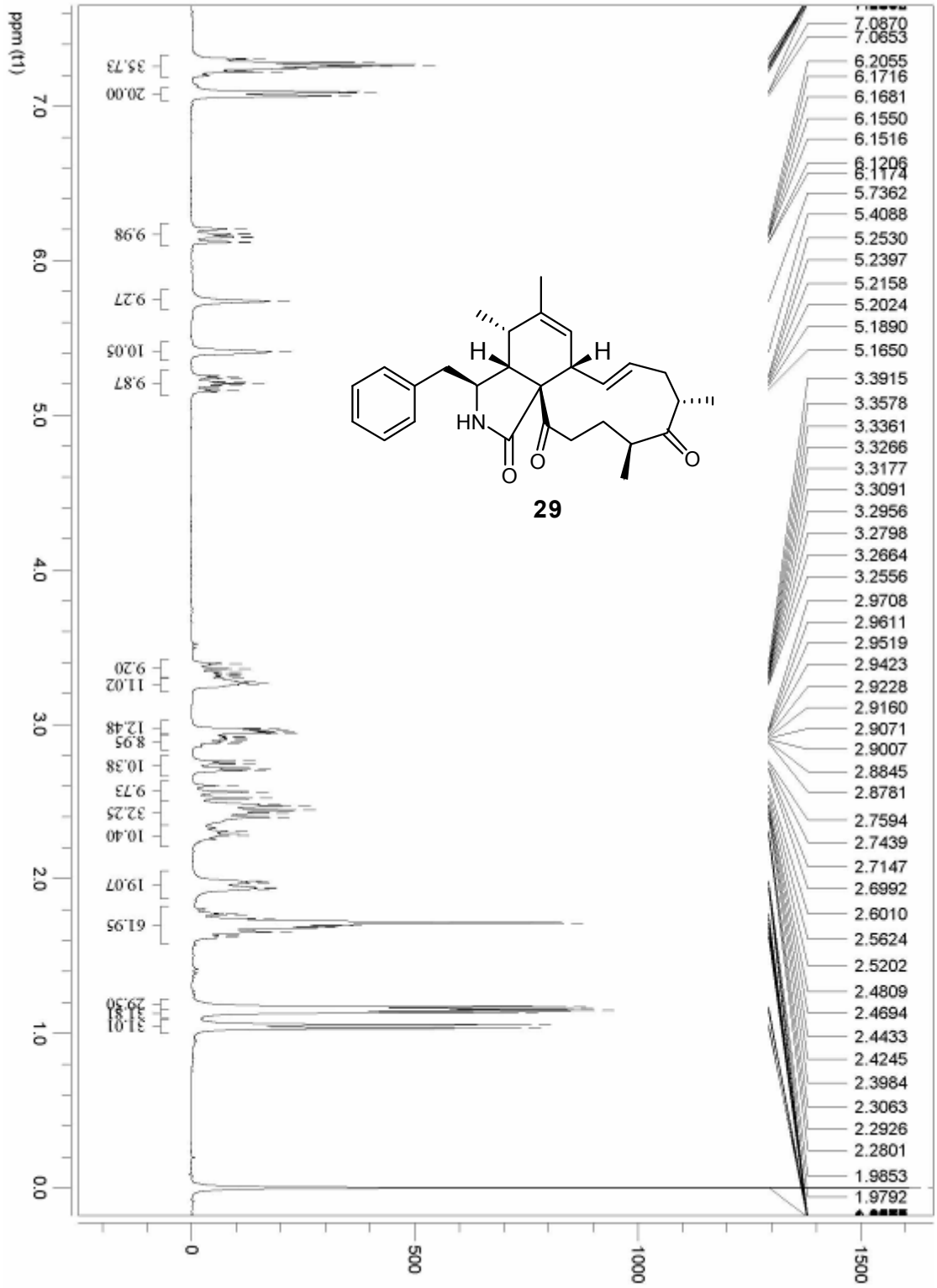

Figure S61. The ^{1}H NMR spectrum of **29** in $CDCl_3$ (300 MHz).

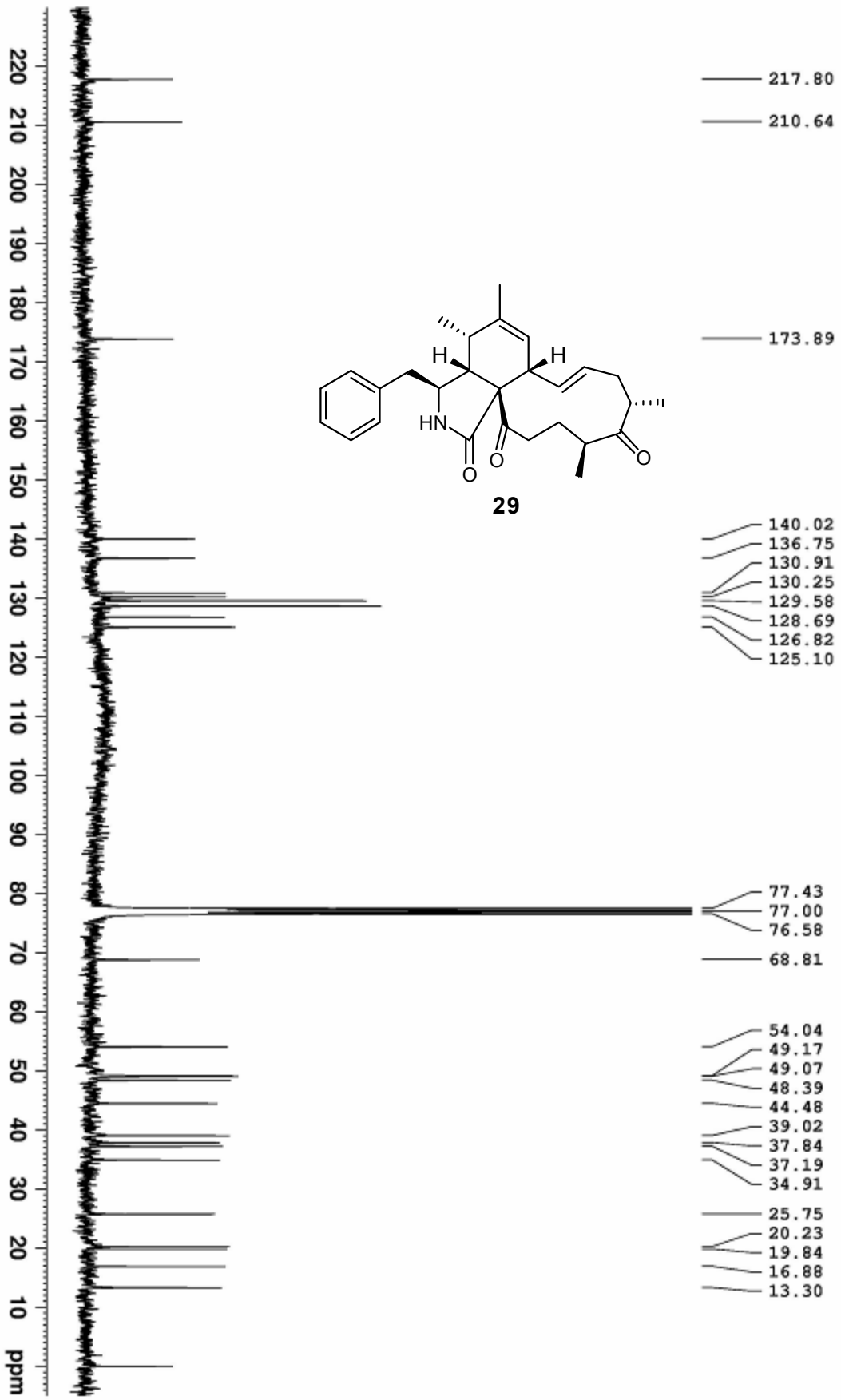

Figure S62. The ^{13}C NMR spectrum of **29** in $CDCl_3$ (75 MHz).

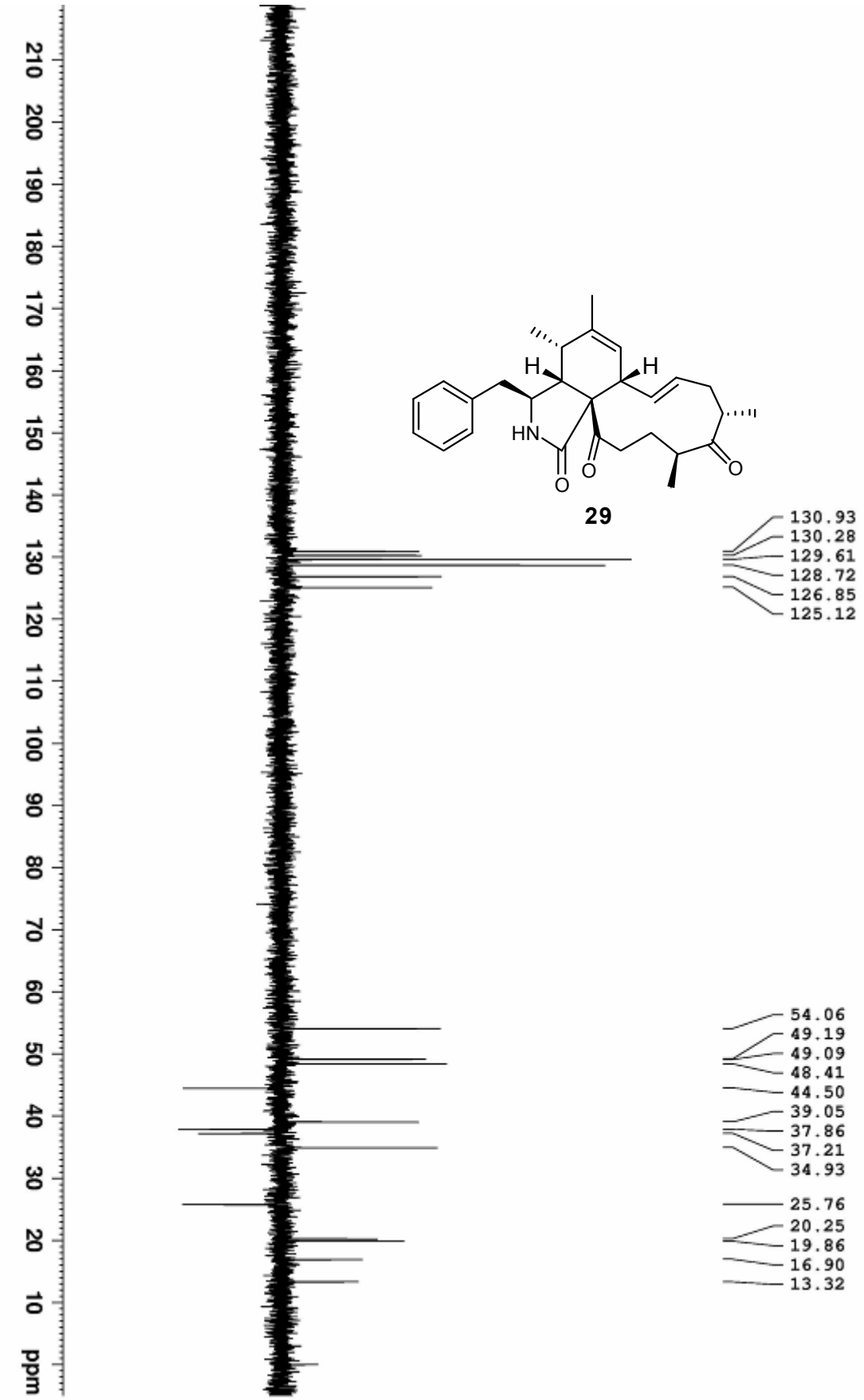

Figure S63. The DEPT135 spectrum of **29** in $CDCl_3$ (75 MHz).

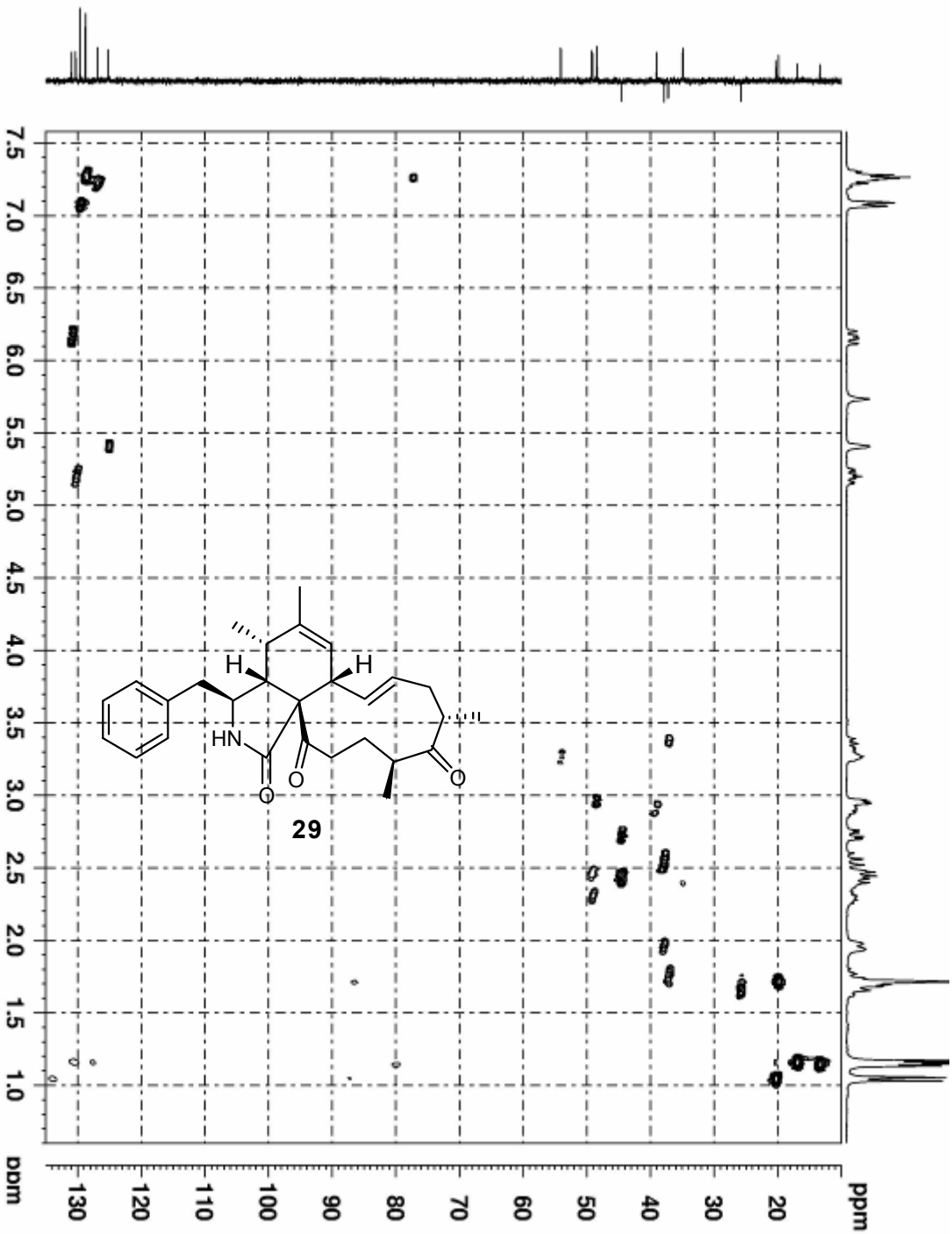

Figure S64. The HMQC spectrum of **29** in $CDCl_3$ (300 MHz).

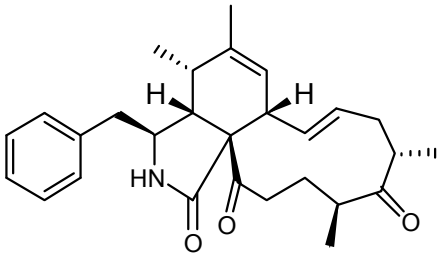

29

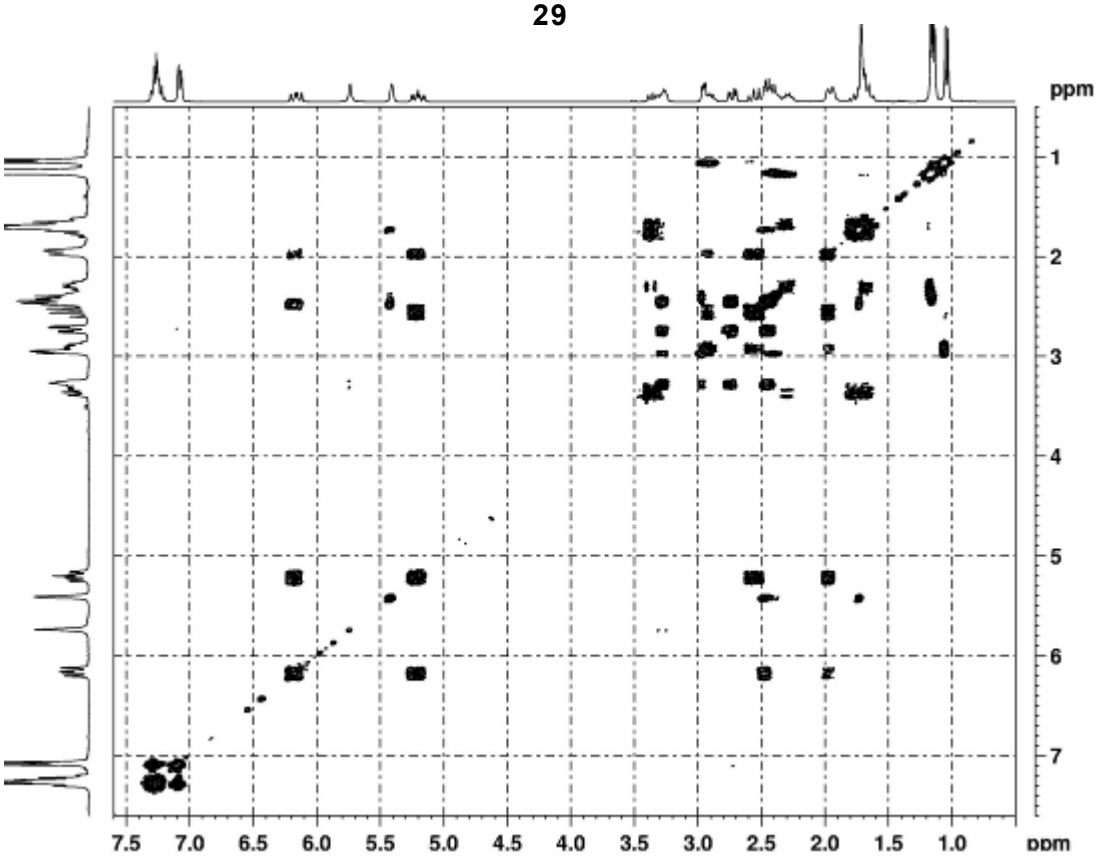

Figure S65. The ^{1}H-^{1}H COSY spectrum of **29** in $CDCl_3$ (300 MHz).

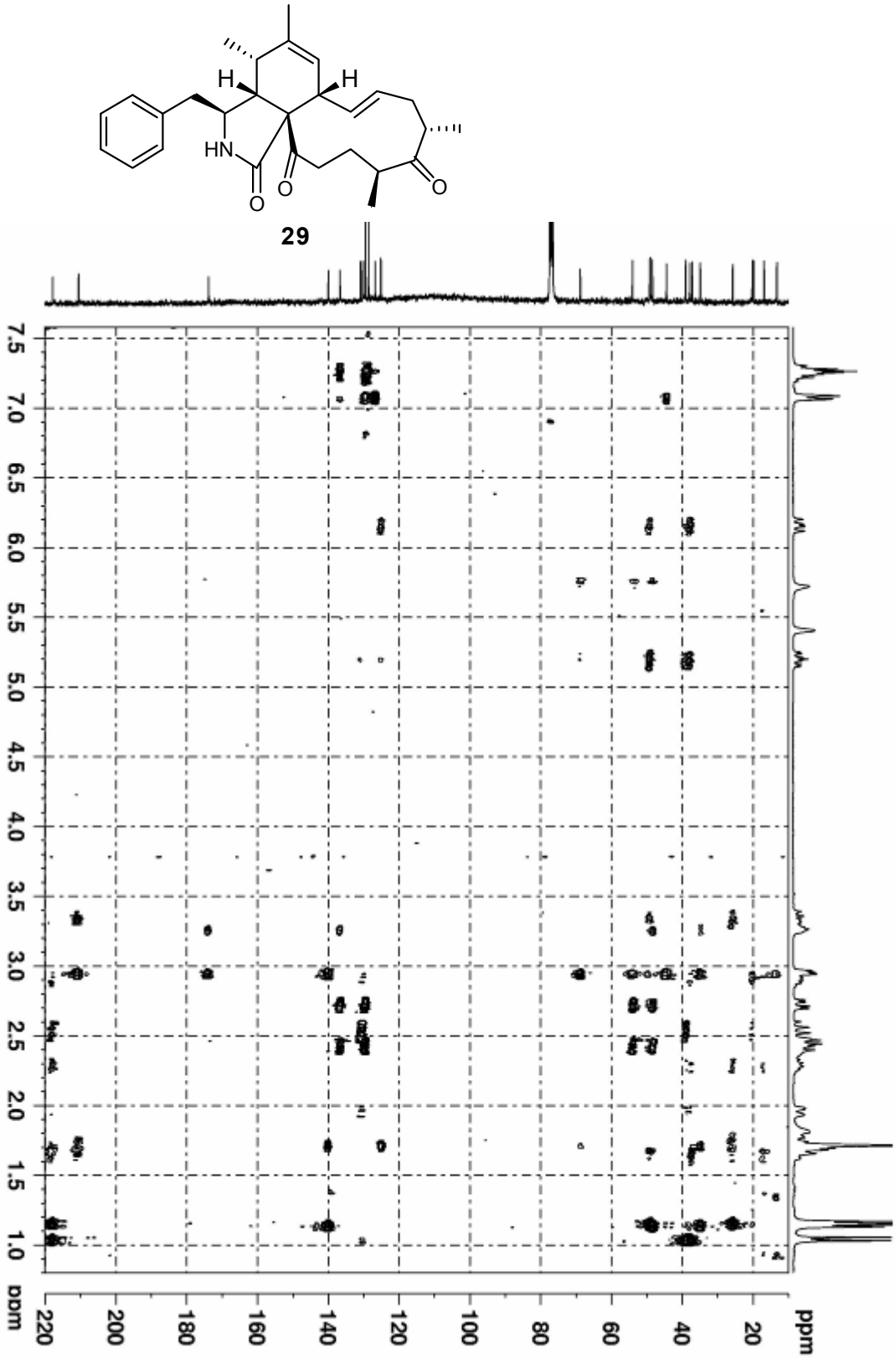

Figure S66. The HMBC spectrum of **29** in $CDCl_3$ (300 MHz).

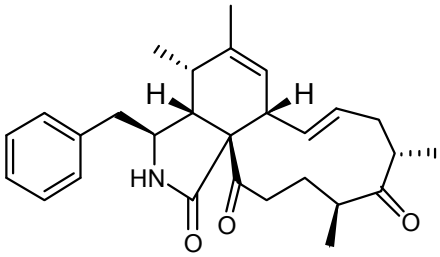

29

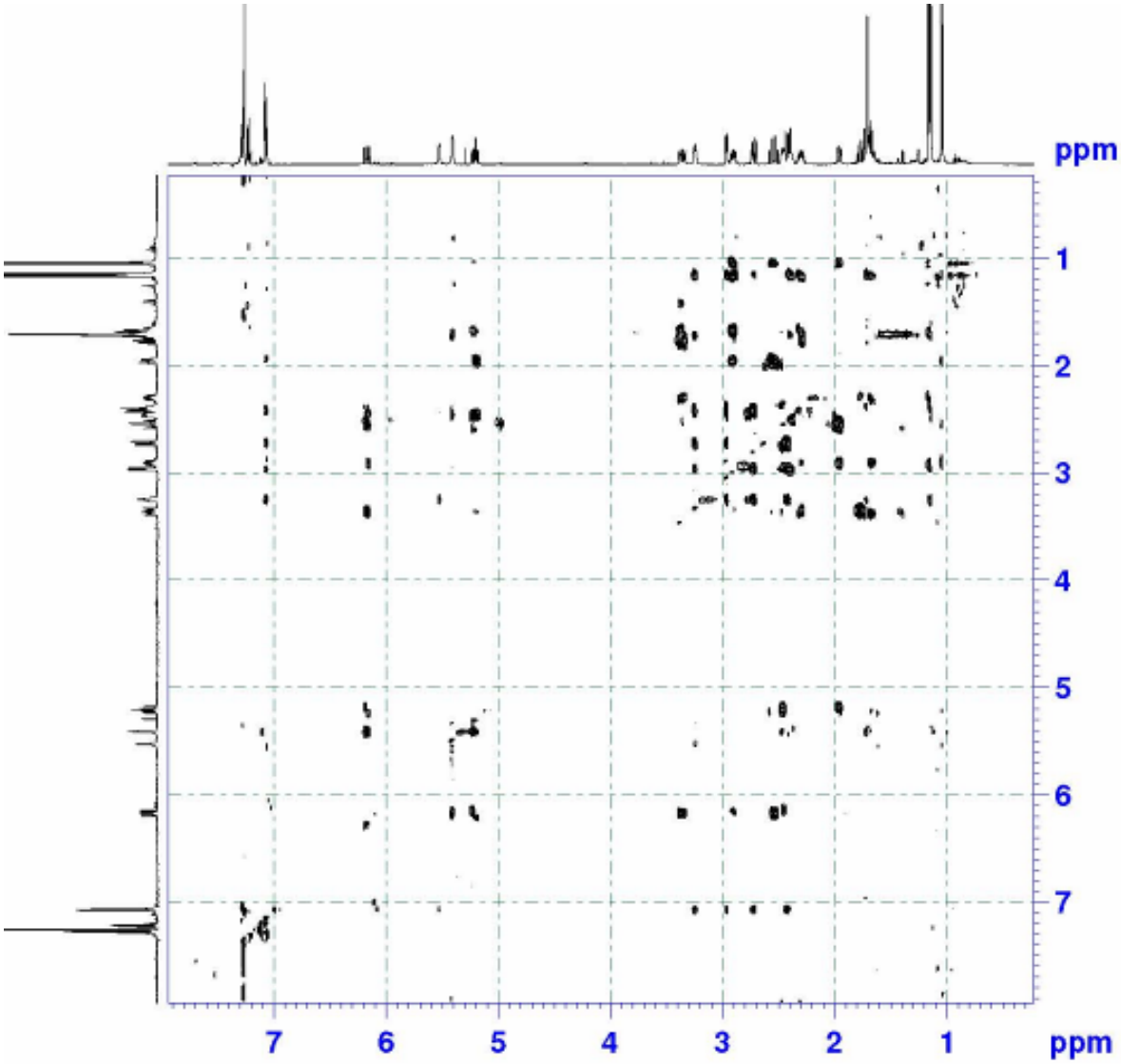

Figure S67. The ROESY spectrum of **29** in $CDCl_3$ (500 MHz).

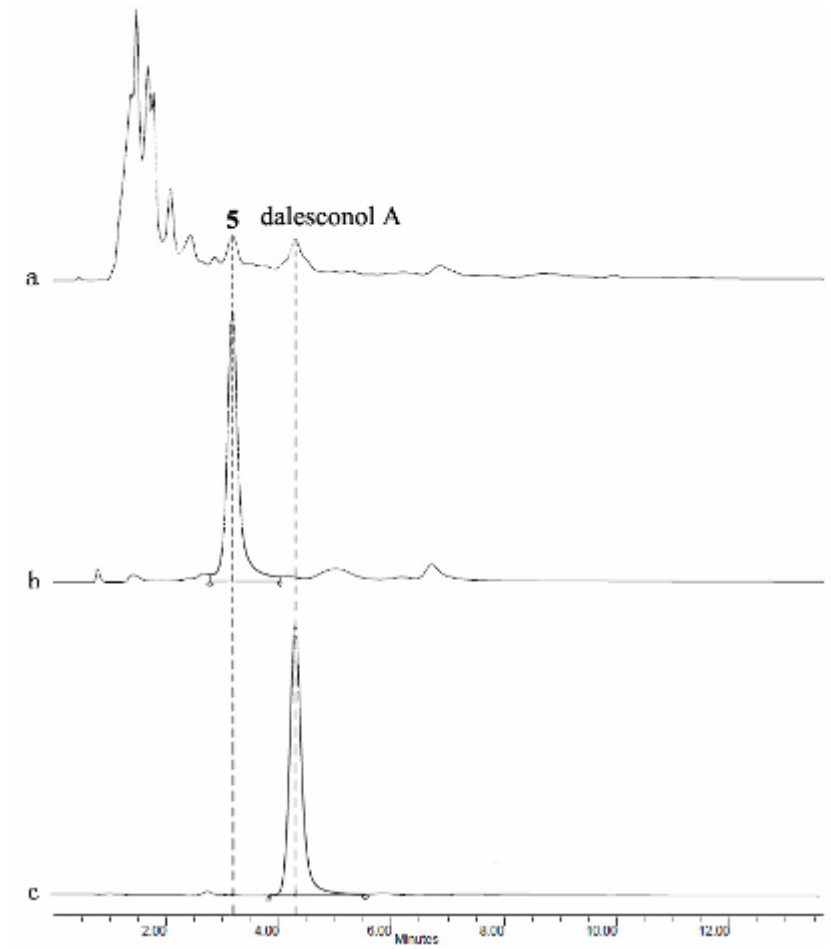

Figure S68. The reverse-phase HPLC analysis of the extract (column: Allsphere ODS-2.5 mm (250×4.6 mm), Waters 2487, Dual λ absorbance detector; mobile phase: MeOH/H_2O=80/20 (v/v); flow rate: 1.0 mL/min). (a) MeCN-soluble extracts of the fungus, which was cultured on liquid medium until 22 day. (b) daeschol A (**5**). (c) dalesconol A.

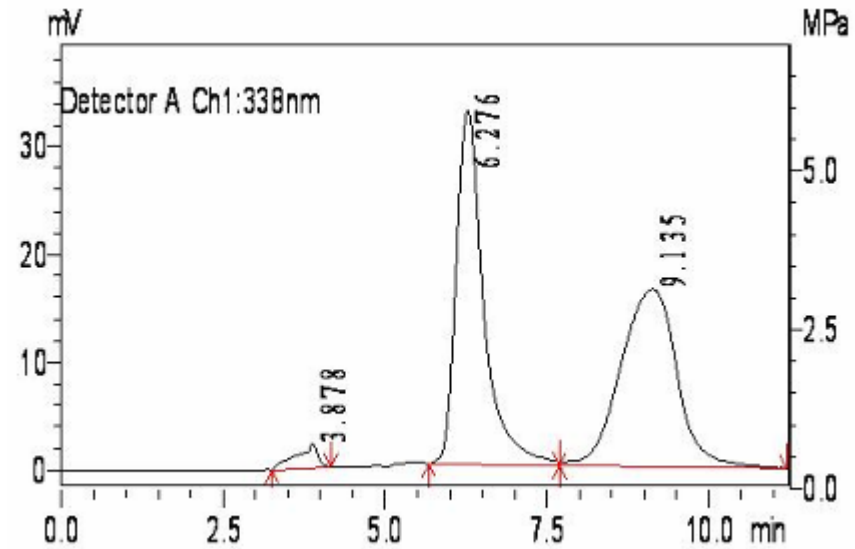

<Column Performance Report>

Peak No.	Time	Area	Area %	Plate number	Tailing	Resolution
1	6.276	975931	48.2591	1276.837	1.608	2.871
2	9.135	993573	49.1315	601.911	0.979	2.609

Figure S69. The chiral HPLC chromatograms of **16**.

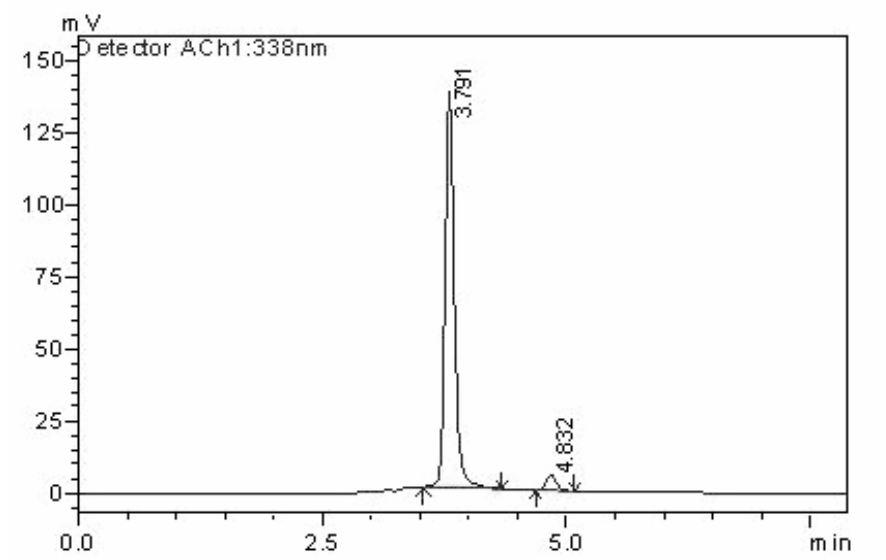

<Column Performance Report>

Peak No.	Time	Area	Area %	Plate number	Tailing	Resolution
1	3.791	901865	95.5878	6390.668	1.319	--
2	4.832	41629	4.4122	6938.245	1.242	4.940

Figure S70. The chiral HPLC chromatograms of **22**.

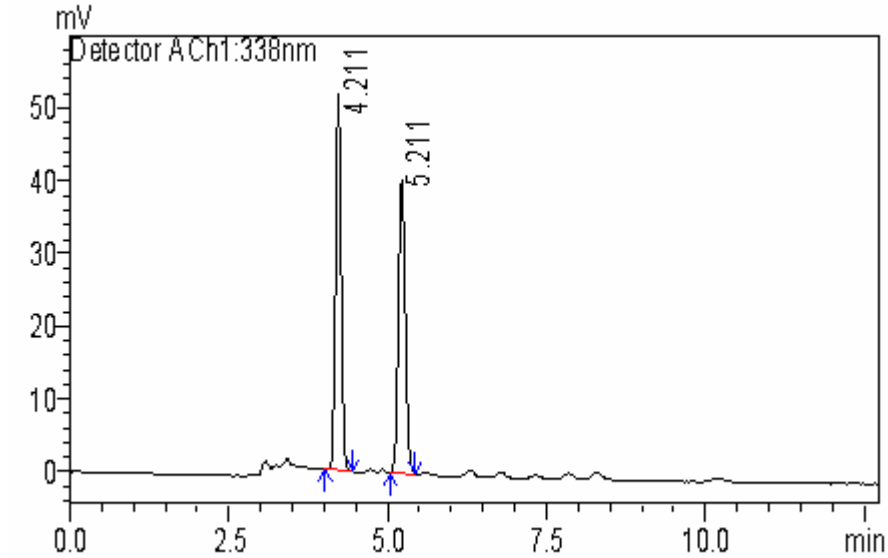

<Column Performance Report>

Peak No.	Time	Area	Area %	Plate number	Tailing	Resolution
1	4.211	320249	50.7	7859	1.20	--
2	5.211	311286	49.3	7726	1.15	4.68

Figure S71. The chiral HPLC chromatograms of **23**.

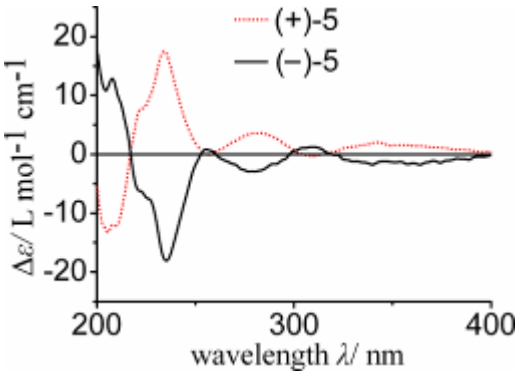

Figure S72. The CD spectra of (+)-**5** and (–)-**5** in MeOH.

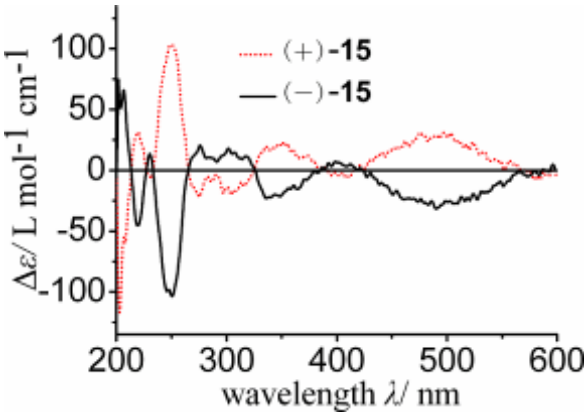

Figure S73. The CD spectra of (+)-**15** and (–)-**15** in MeOH.

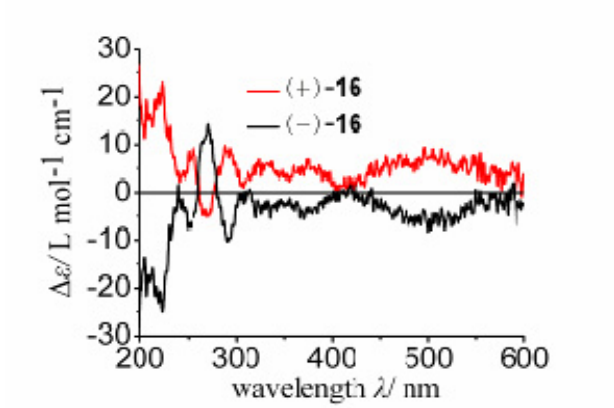

Figure S74. The CD spectra of (+)-**16** and (–)-**16** in MeOH.

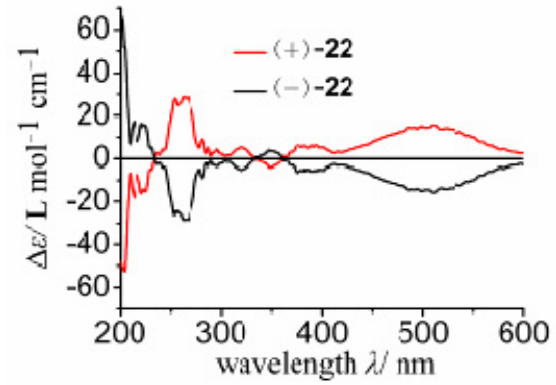

Figure S75. The CD spectra of (+)-**22** and (–)-**22** in MeOH.

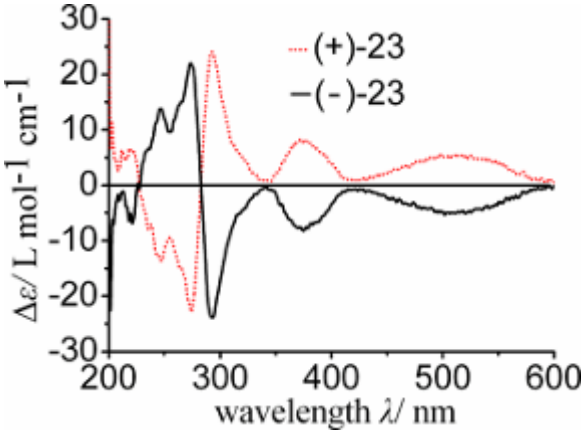

Figure S76. The CD spectra of (+)-**23** and (–)-**23** in MeOH.

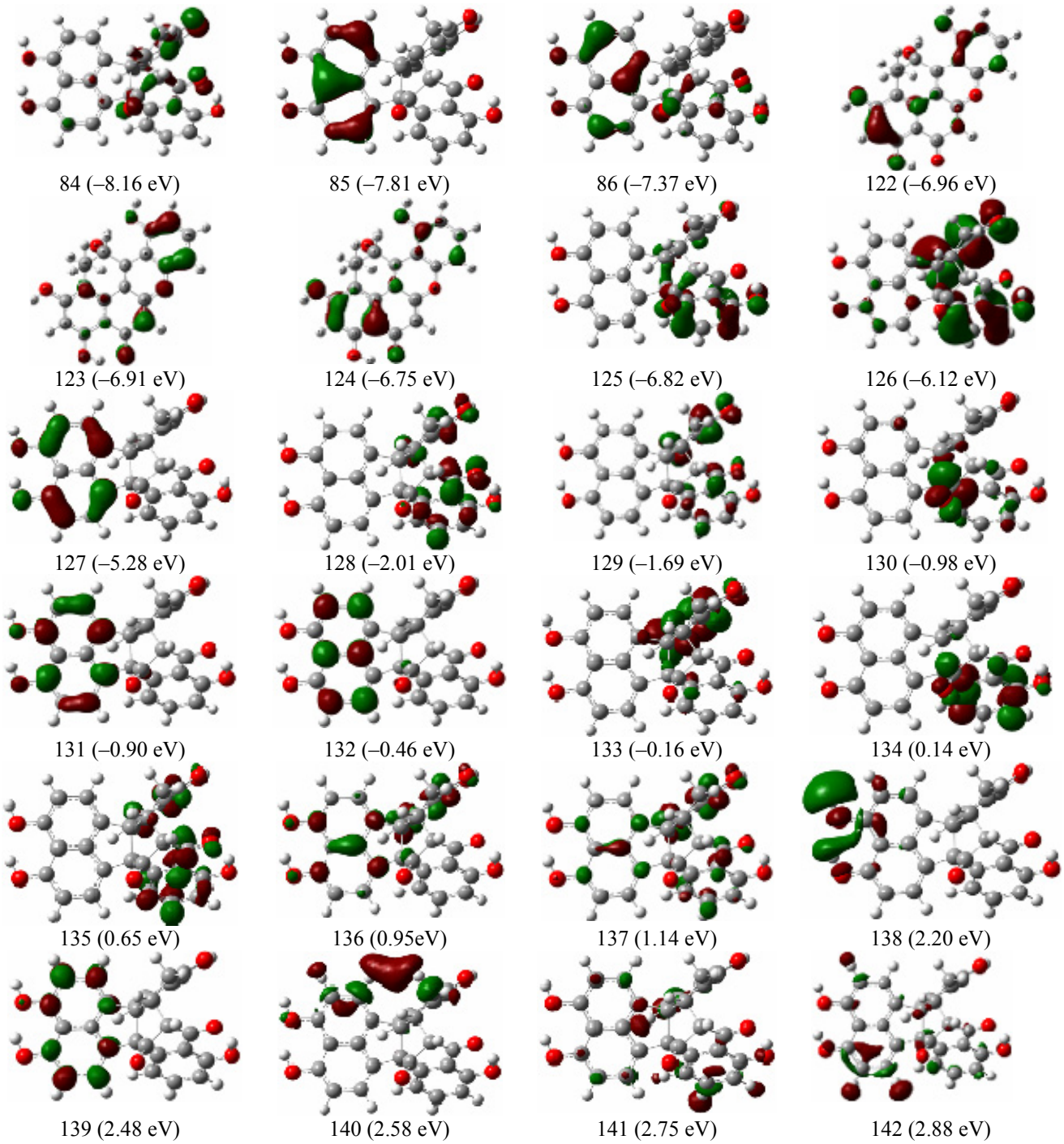

Figure S77. The most important molecular orbitals of the optimized conformer of (8*R*,19*R*,28*R*,29*S*)-**5** at B3LYP/6–31G(d) level in the PCM model (CH_3OH solvent, ε=32.63).

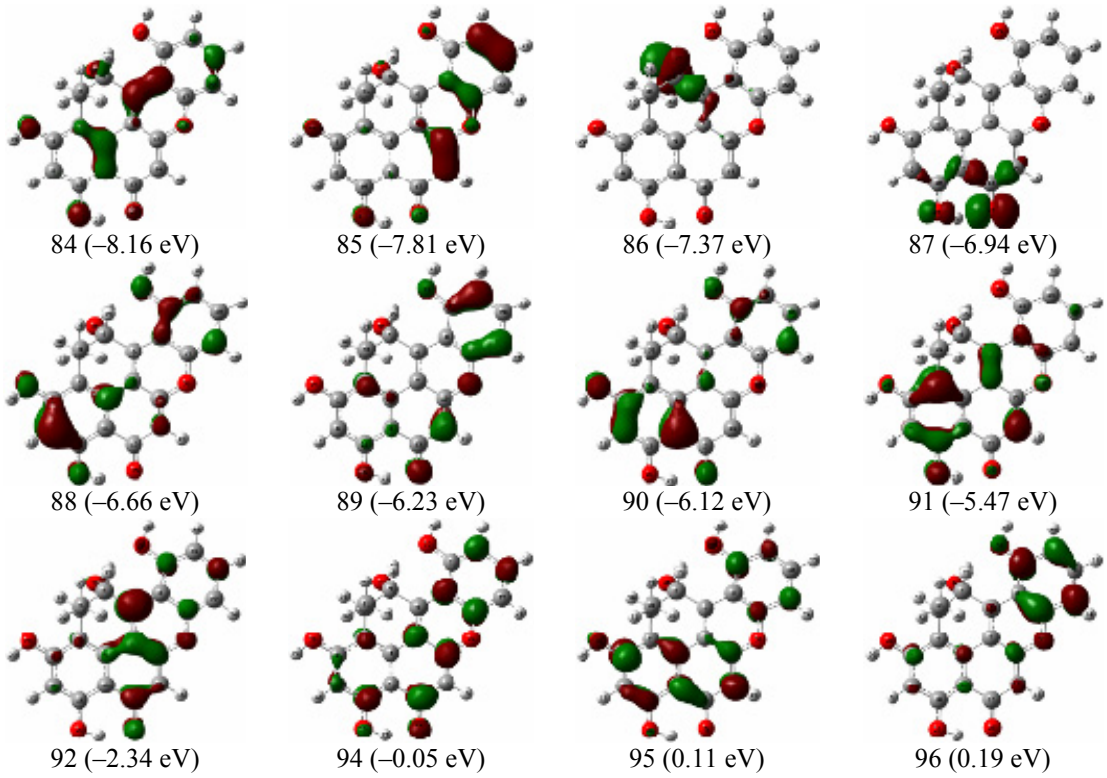

Figure S78. The most important molecular orbitals of the optimized conformer of (2*R*,3*S*)-**15** at B3LYP/6–31G(d) level in the PCM model (CH_3OH solvent, ε=32.63).

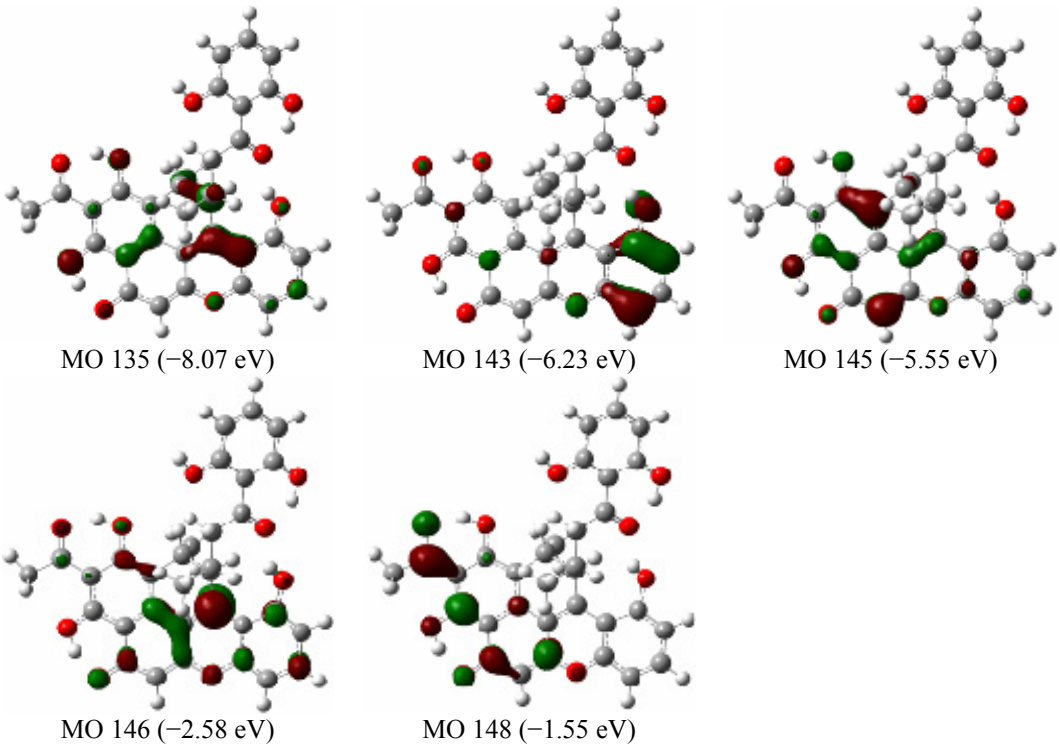

Figure S79. Plot of the most important molecular orbitals of the optimized conformer of (2*R*,3*R*,2′*R*)-**23** at B3LYP/6–31G(d) level in the PCM model (CH_3OH solvent, ε=32.63).

Supplementary References

(1) Zhang,Y. L.; Ge, H. M.; Zhao,W.; Dong, H.; Xu, Q.; Li, S. H.; Li, J.; Zhang, J.; Song, Y. C.; Tan, R. X. *Angew. Chem.* **2008**, *120*, 5907–5910; *Angew. Chem. Int. Ed.* **2008**, *47*, 5823–5826.

(2) Patra, A.; Ghosh, G. P.; Sengupta, K.; Nath, S. *Magn. Reson. Chem.* **1987**, *25*, 734-736.

(3) Lin, C. M.; Huang, S. T.; Lee, F. W.; Kuo, H. S.; Lin, M. H. *Bioorgan. Med. Chem.* **2006**, *14*, 4402–4409.

(4) Liu, Z. B.; Sun, Y. S.; Wang, J. H.; Zhu, H. F.; Zhou, H. Y.; Hu, J. N. Wang, J. *Sep. Purif. Technol.* **2008**, *64*, 247–252.

(5) Islam, M. S.; Ishigami, K.; Watanabe, H. *Tetrahedron* **2007**, *63* 1074–1079.

(6) Bode, H. B.; Zeeck, A. *Phytochemistry* **2000**, *54*, 597-601.

(7) Gu, W.; Ge, H. M.; Song, Y. C.; Ding, H.; Zhu, H. L.; Zhao, X. A.; Tan, R. X. *J. Nat. Prod.* **2007**, *70*, 114-117.

(8) Bell, A. A.; Stipanovic, R. D.; Puhalla, J. E. *Tetrahedron* **1976**, *32*, 1353-1356.

(9) Gremaud, G.; Tabacchi,R. *Phytochemistry* **1996**, *42*, 1547-1549.

(10) Iwasaki, S.; Muro, H.; Sasaki, K.; Nozoe, S.; Okuda, S.; Sato, Z. *Tetrahedron Lett.* **1973**, 37, 3537-3542.

(11) Venkatasubbaiah, P.; Chilton, W. S. *J. Nat. Prod.* **1991**, *54*, 1293-1297.

(12) Dai, J. Q.; Krohn, K.; Flörke, U.; Draeger, S.; Schulz, B.; Szikszai, A. K.; Antus, S.; Kurtán, T.; Ree, T. V. *Eur. J. Org. Chem.* **2006**, *15*, 3498–3506.

(13) Dai, J. Q.; Krohn, K.; Draeger, S.; Schulz, B. *Eur. J. Org. Chem.* **2009**, *10*, 1564-1569.

(14) Nicolet, B.; Tabacchi, R. International Reinhardsbrunn Symposium, 12th, Friedrichroda, Germany, May 24-29, 1998 (1999), Meeting Date **1998**, 469-476.

(15) Wen, L.; Du, D. S.; She, Z. G.; Guo, Z. Y.; Lin,Y. C.; Vrijmoed, L. L. P. *Nat. Prod. Res. Dev.* **2007**, *19*, 952-955.

(16) Ichihara, A.; Hashimoto, M.; Hirai, T.; Takeda, I.; Sasamura,Y.; Sakamura, S.; Sato, R.; Tajimi, A. *Chem. Lett.* **1989**, *8*, 1495-1498.

(17) Wu, Z. C.; Li, D. L.; Chen, Y. C.; Zhang, W. M. *Hel. Chim. Acta* **2010**, *93*, 920-924.

Complete reference 16:

Frisch, M. J.; Trucks, G. W.; Schlegel, H. B.; Scuseria, G. E.; Robb, M. A.; Cheeseman, J. R.; Montgomery Jr, J. A.; Vreven, T.; Kudin, K. N.; Burant, J. C.; Millam, J. M.; Iyengar, S. S.; Tomasi, J.; Barone, V.; Mennucci, B.; Cossi, M.; Scalmani, G.; Rega, N.; Petersson, G. A.; Nakatsuji, H.; Hada, M.; Ehara, M.; Toyota, K.; Fukuda, R.; Hasegawa, J.; Ishida, M.; Nakajima, T.; Honda, Y.; Kitao, O.; Nakai, H.; Klene, M.; Li, X.; Knox, J. E.; Hratchian, H. P.; Cross, J. B.; Bakken, V.; Adamo, C.; Jaramillo, J.; Gomperts, R.; Raghavachari, K.; Foresman, J. B.; Ortiz, J. V.; Cui, Q.; Baboul, A. G.; Clifford, S.; Cioslowski, J.; Stefanov, B. B.; Liu, G.; Liashenko, A.; Piskorz, P.; Komaromi, I.; Martin, R. L.; Fox, D. J.; Keith, T.; Al-Laham, M. A.; Peng, C. Y.; Nanayakkara, A.; Challacombe, M.; Gill, P. M. W.; Johnson, B.; Chen, W.; Wong, M. W. Gonzalez, C.; Pople, J. A.. Gaussian 03, Revision E.01, Gaussian, Inc., Wallingford CT, **2004**.